

Disentangling a dynamical Higgs

I. Brivio ^{a)}, T. Corbett ^{b)}, O. J. P. Éboli ^{c)}, M.B. Gavela ^{a)},
J. Gonzalez–Fraile ^{d)}, M. C. Gonzalez–Garcia ^{e,d,b)}, L. Merlo ^{a)}, S. Rigolin ^{f)}

^{a)} Departamento de Física Teórica and Instituto de Física Teórica, IFT-UAM/CSIC,
Universidad Autónoma de Madrid, Cantoblanco, 28049, Madrid, Spain

^{b)} C.N. Yang Institute for Theoretical Physics and Department of Physics and Astronomy, SUNY at
Stony Brook, Stony Brook, NY 11794-3840, USA

^{c)} Instituto de Física, Universidade de São Paulo, C.P. 66318, 05315-970, São Paulo SP, Brazil

^{d)} Departament d'Estructura i Constituents de la Matèria and ICC-UB, Universitat de Barcelona, 647
Diagonal, E-08028 Barcelona, Spain

^{e)} Institució Catalana de Recerca i Estudis Avançats (ICREA)

^{f)} Dipartimento di Fisica e Astronomia “G. Galilei”, Università di Padova and
INFN, Sezione di Padova, Via Marzolo 8, I-35131 Padua, Italy

E-mail: ilaria.brivio@uam.es, corbett.ts@gmail.com, eboli@fma.if.usp.br,
belen.gavela@uam.es, fraile@ecm.ub.edu, concha@insti.physics.sunysb.edu,
luca.merlo@uam.es, stefano.rigolin@pd.infn.it

Abstract

The pattern of deviations from Standard Model predictions and couplings is different for theories of new physics based on a non-linear realization of the $SU(2)_L \times U(1)_Y$ gauge symmetry breaking and those assuming a linear realization. We clarify this issue in a model-independent way via its effective Lagrangian formulation in the presence of a light Higgs particle, up to first order in the expansions: dimension-six operators for the linear expansion and four derivatives for the non-linear one. Complete sets of gauge and gauge-Higgs operators are considered, implementing the renormalization procedure and deriving the Feynman rules for the non-linear expansion. We establish the theoretical relation and the differences in physics impact between the two expansions. Promising discriminating signals include the decorrelation in the non-linear case of signals correlated in the linear one: some pure gauge versus gauge-Higgs couplings and also between couplings with the same number of Higgs legs. Furthermore, anomalous signals expected at first order in the non-linear realization may appear only at higher orders of the linear one, and vice versa. We analyze in detail the impact of both type of discriminating signals on LHC physics.

Contents

1	Introduction	1
2	The effective Lagrangian	5
3	Comparison with the linear regime	10
3.1	The effective Lagrangian in the linear regime	10
3.2	Decorrelation of signals with respect to the linear analysis	13
3.3	Signals specific to the linear expansion	15
3.4	New signals specific to the non-linear expansion	15
4	Phenomenology	16
4.1	Renormalization Procedure	16
4.2	Present bounds on operators weighted by ξ	24
4.3	ξ^2 -weighted couplings: LHC potential to study g_5^Z	28
4.4	Anomalous quartic couplings	34
5	Conclusions	35
A	EOM and fermion operators	37
B	Equivalence of the $d = 6$ basis with the SILH Lagrangian	42
C	Relations between chiral and linear operators	43
D	Feynman rules	43

1 Introduction

The present ensemble of data does not show evidence for new exotic resonances and points to a scenario compatible with the Standard Model (SM) scalar boson (so-called “Higgs” for short) [1–3]. Either the SM is all there is even at energies well above the TeV scale, which would raise a number of questions about its theoretical consistency (electroweak hierarchy problem, triviality, stability), or new physics (NP) should still be expected around or not far from the TeV scale.

This putative NP could be either detected directly or studied indirectly, analysing the modifications of the SM couplings. To this aim, a rather model-independent approach is that of Lorentz and gauge-invariant effective Lagrangians, which respect a given set of symmetries including the low-energy established ones. These effective Lagrangians respect symmetries in addition to $U(1)_{\text{em}}$ and Lorentz invariance and as a consequence they relate and constrain phenomenological couplings [4] based only on the latter symmetries.

With a light Higgs observed, two main classes of effective Lagrangians are pertinent, depending on how the electroweak (EW) symmetry breaking is assumed to be realized: linearly for elementary Higgs particles or non-linearly for “dynamical” -composite- ones.

It is important to find signals which discriminate among those two categories and this will be one of the main focuses of this paper.

In elementary Higgs scenarios, the effective Lagrangian provides a basis for all possible Lorentz and $SU(3)_c \times SU(2)_L \times U(1)_Y$ gauge invariant operators built out of SM fields. The latter set includes a Higgs particle belonging to an $SU(2)_L$ doublet, and the operators are weighted by inverse powers of the unknown high-energy scale Λ characteristic of NP: the leading corrections to the SM Lagrangian have then canonical mass dimension (d) six [5, 6]. Many studies of the effective Lagrangian for the linear expansion have been carried out over the years, including its effects on Higgs production and decay [7, 8], with a revival of activity [9, 10] after the Higgs discovery [11, 12] (see also Refs. [13–40] for studies of Higgs couplings in alternative and related frameworks). Supersymmetric models are a typical example of the possible underlying physics.

In dynamical Higgs scenarios, the Higgs particle is instead a composite field which happens to be a pseudo-goldstone boson (GB) of a global symmetry exact at scales Λ_s , corresponding to the masses of the lightest strong resonances. The Higgs mass is protected by the global symmetry, thus avoiding the electroweak hierarchy problem. Explicit realizations include the revived and now popular models usually dubbed “composite Higgs” scenarios [41–50], for various strong groups and symmetry breaking patterns¹. To the extent that the light Higgs particle has a goldstone boson parenthood, the effective Lagrangian is non-linear [53] or “chiral”: a derivative expansion as befits goldstone boson dynamics. The explicit breaking of the strong group -necessary to allow a non-zero Higgs mass- introduces chiral-symmetry breaking terms. In this scenario, the characteristic scale f of the Goldstone bosons arising from the spontaneous breaking of the global symmetry at the scale Λ_s is different² from both the EW scale v defined by the EW gauge boson mass, e.g. the W mass $m_W = gv/2$, and the EW symmetry breaking (EWSB) scale $\langle h \rangle$, and respects $\Lambda_s < 4\pi f$. A model-dependent function g links the three scales, $v = g(f, \langle h \rangle)$, and a parameter measuring the degree of non-linearity of the Higgs dynamics is usually introduced:

$$\xi \equiv (v/f)^2. \quad (1.1)$$

The corresponding effective low-energy chiral Lagrangian is entirely written in terms of the SM fermions and gauge bosons and of the physical Higgs h . The longitudinal degrees of freedom of the EW gauge bosons can be effectively described at low energies by a dimensionless unitary matrix transforming as a bi-doublet of the global symmetry:

$$\mathbf{U}(x) = e^{i\sigma_a \pi^a(x)/v}, \quad \mathbf{U}(x) \rightarrow L \mathbf{U}(x) R^\dagger, \quad (1.2)$$

where here the scale associated with the eaten GBs is v , and not f , in order to provide canonically normalized kinetic terms, and L, R denotes $SU(2)_{L,R}$ global transformations, respectively. Because of EWSB, the $SU(2)_{L,R}$ symmetries are broken down to the diagonal $SU(2)_C$, which in turn is explicitly broken by the gauged $U(1)_Y$ and by the heterogeneity

¹ Also “little Higgs” [51] (see Ref. [52] for a review) models and some higher-dimensional scenarios can be cast in the category of constructions in which the Higgs is a goldstone boson.

²In the historical and simplest formulations of “technicolor” [54–56], the Higgs particle was completely removed from the low-energy spectrum, which only retained the three SM would-be-Goldstone bosons with a characteristic scale $f = v$.

of the fermion masses. On the other hand, while insertions of the Higgs particle are weighted down as h/f , as explained above, its couplings are now (model-dependent) general functions. In all generality, the $SU(2)_L$ structure is absent in them and, as often pointed out (e.g. Refs. [57, 58]), the resulting effective Lagrangian can describe many setups including that for a light SM singlet isoscalar.

To our knowledge, the first attempts to formulate a non-linear effective Lagrangian in the presence of a “non standard/singlet light Higgs boson” go back to the 90’s [59, 60], and later works [57, 61]. More recently, Ref. [62] introduced a relevant set of operators, while Ref. [63] derived a complete effective Lagrangian basis for pure gauge and gauge- h operators up to four derivatives. Later on, Ref. [64] added the pure Higgs operator in Ref. [65] as well as fermionic couplings, proposing a complete basis for all SM fields up to four derivatives, and trading some of the operators in Ref. [63] by fermionic ones³.

The effective linear and chiral Lagrangians with a light Higgs particle h are intrinsically different, in particular from the point of view of the transformation properties under the $SU(2)_L$ symmetry. There is not a one-to-one correspondence of the leading corrections of both expansions, and one expansion is not the limit of the other unless specific constraints are imposed by hand -as illustrated below- or follow from particular dynamics at high energies [68]. In the linear expansion, the physical Higgs h participates in the scalar $SU(2)_L$ doublet Φ ; having canonical mass dimension one, this field appears weighted by powers of the cut-off Λ in any non-renormalizable operator and, moreover, its presence in the Lagrangian must necessarily respect a pattern in powers of $(v + h)$. In the non-linear Lagrangian instead, the behavior of the h particle does not abide any more to that of an $SU(2)_L$ doublet, but h appears as a SM singlet. Less symmetry constraints means more possible invariant operators [69–71] at a given order, and in summary:

- In the non-linear realization, the chiral-symmetry breaking interactions of h are now generic/arbitrary functions $\mathcal{F}(h)$.
- Furthermore, a relative reshuffling of the order at which couplings appear in each expansion takes place [63, 72, 73]. As a consequence, a higher number of independent (uncorrelated) couplings are present in the leading corrections for a non-linear Lagrangian.

Both effects increase the relative freedom of the purely phenomenological Lorentz and $U(1)_{\text{em}}$ couplings required at a given order of the expansion, with respect to the linear analysis. Decorrelations induced by the first point have been recently stressed in Ref. [74] (analysing form factors for Higgs decays), while those resulting from the second point above lead to further discriminating signals and should be taken into account as well. Both types of effects will be explored below.

³The inferred criticisms in Ref. [64] to the results in Ref. [63] about missing and redundant operators are incorrect: Ref. [63] concentrated by definition in pure gauge and gauge- h couplings and those criticized as “missing” are not in this category; a similar comment applies to the redundancy issue, explained by the choice mentioned above of trading some gauge operators by fermionic ones in Ref. [64]. Finally, the ξ weights and the truncations defined for the first time in Ref. [63] lead to rules for operator weights consistent with those defined long ago in the Georgi-Manohar counting [66], and more recently in Ref. [67].

In what respects the analysis of present LHC and electroweak data, a first step in the direction of using a non-linear realization was the substitution of the functional dependence on $(v + h)$ for a doublet Higgs in the linear expansion by a generic function $\mathcal{F}(h)$ for a generic SM scalar singlet h , mentioned in the first point above. This has already led to a rich phenomenology [26, 62, 74, 75]. Nevertheless, the scope of the decorrelations that a generic $\mathcal{F}(h)$ induces between the pure gauge and the gauge- h part of a given operator is limited: whenever data set a strong constraint on the pure gauge part of the coupling, that is on the global operator coefficient, this constraint also affects the gauge- h part as it is also proportional to the global coefficient; only in appealing to strong and, in general, unnatural fine-tunings of the constants inside $\mathcal{F}(h)$ could that constraint be overcome.

As for the second consequence mentioned above, the point is that if higher orders in both expansions are considered, all possible Lorentz and $U(1)_{\text{em}}$ couplings would appear in both towers (as it is easily seen in the unitary gauge), but not necessarily at the same leading or sub-leading order. One technical key to understand this difference is the adimensionality of the field $\mathbf{U}(x)$. The induced tower of the leading low-energy operators is different for the linear and chiral regimes, a fact illustrated recently for the pure gauge and gauge- h effective non-linear Lagrangian [63, 72, 73]. More recently, and conversely, an example was pointed out [64] of a $d = 6$ operator of the linear expansion whose equivalent coupling does not appear among the leading derivative corrections in the non-linear expansion.

It will be shown below that, due to that reshuffling of the order at which certain leading corrections appear, correlations that are expected as leading corrections in one case may not hold in the other, unless specific constraints are imposed by hand or follow from high energy dynamics. Moreover, interactions that are strongly suppressed (subleading) in one regime may be leading order in the other.

In this paper we will first consider the basis of CP-even bosonic operators for the general non-linear effective Lagrangian and analyse in detail its complete and independent set of pure gauge and gauge-Higgs operators, implementing the tree-level renormalization procedure and deriving the corresponding Feynman rules. The similarities and differences with the couplings obtained in the linear regime will be carefully determined, considering in particular the Hagiwara-Ishihara-Szalapski-Zeppenfeld (HISZ) basis [76, 77]. Nevertheless, the physical results are checked to be independent of the specific linear basis used, as they should be. The comparison of the effects in both realizations will be performed in the context of complete bases of gauge and/or Higgs boson operators: all possible independent (and thus non-redundant) such operators will be contemplated for each expansion, and compared. For each non-linear operator we will identify linear ones which lead to the same gauge couplings, and it will be shown that up to $d = 12$ linear operators would be required to cover all the non-linear operators with at most four derivatives. We will then identify some of the most promising signals to discriminate experimentally among both expansions in hypothetical departures from the size and Lorentz structure of couplings predicted by the SM. This task is facilitated by the partial use of results obtained earlier on the physics impact of the linear regime on LHC physics from $d = 6$ operators in Refs. [9, 10, 78], and from previous analysis of 4-point phenomenological couplings carried out in Refs. [79–83]. In this paper we concentrate on the tree-level effects of operators, as a necessary first step before loop effects are considered [84].

The structure of the paper can be easily inferred from the Table of Contents.

2 The effective Lagrangian

We describe below the effective Lagrangian for a light dynamical Higgs [63] (see also Ref. [64]), restricted to the bosonic operators, except for the Yukawa-like interactions, up to operators with four derivatives⁴. Furthermore, only CP-even operators will be taken into account, under the assumption that h is a CP-even scalar.

The most up-to-date analysis to the Higgs results have established that the couplings of h to the gauge bosons and the absolute value of the couplings to fermions are compatible with the SM ones. On the contrary, the sign of the couplings between h and fermions is still to be measured, even if a slight preference for a positive value is indicated in some two parameter fits (see for example [16, 17, 26]) which take into account one-loop induced EW corrections. It is then justified to write the effective Lagrangian as a term \mathcal{L}_0 , which is in fact the SM Lagrangian except for the mentioned sign (would the latter be confirmed positive, \mathcal{L}_0 should be exactly identified with the SM Lagrangian $\mathcal{L}_0 = \mathcal{L}_{SM}$), and to consider as corrections the possible departures from it due to the unknown high-energy strong dynamics:

$$\mathcal{L}_{\text{chiral}} = \mathcal{L}_0 + \Delta\mathcal{L}. \quad (2.1)$$

This description is data-driven and, while being a consistent chiral expansion up to four derivatives, the particular division in Eq. (2.1) does not match that in number of derivatives, usually adopted by chiral Lagrangian practitioners. For instance, the usual custodial breaking term $\text{Tr}(\mathbf{T}\mathbf{V}_\mu)\text{Tr}(\mathbf{T}\mathbf{V}^\mu)$ is a two derivative operator and is often listed among the leading order set in the chiral expansion; however, it is not present in the SM at tree level and thus here it belongs to $\Delta\mathcal{L}$ by definition. Moreover, data strongly constrain its coefficient so that it can be always considered [58] a subleading operator.

The first term in $\mathcal{L}_{\text{chiral}}$ reads then

$$\begin{aligned} \mathcal{L}_0 = & \frac{1}{2}(\partial_\mu h)(\partial^\mu h) - \frac{1}{4}W_{\mu\nu}^a W^{a\mu\nu} - \frac{1}{4}B_{\mu\nu}B^{\mu\nu} - \frac{1}{4}G_{\mu\nu}^a G^{a\mu\nu} - V(h) \\ & - \frac{(v+h)^2}{4}\text{Tr}[\mathbf{V}_\mu\mathbf{V}^\mu] + i\bar{Q}\not{D}Q + i\bar{L}\not{D}L \\ & - \frac{v+s_Y h}{\sqrt{2}}(\bar{Q}_L\mathbf{U}\mathbf{Y}_Q Q_R + \text{h.c.}) - \frac{v+s_Y h}{\sqrt{2}}(\bar{L}_L\mathbf{U}\mathbf{Y}_L L_R + \text{h.c.}), \end{aligned} \quad (2.2)$$

where $\mathbf{V}_\mu \equiv (\mathbf{D}_\mu \mathbf{U}) \mathbf{U}^\dagger$ ($\mathbf{T} \equiv \mathbf{U}\sigma_3\mathbf{U}^\dagger$) is the vector (scalar) chiral field transforming in the adjoint of $SU(2)_L$. The covariant derivative reads

$$\mathbf{D}_\mu \mathbf{U}(x) \equiv \partial_\mu \mathbf{U}(x) + igW_\mu(x)\mathbf{U}(x) - \frac{ig'}{2}B_\mu(x)\mathbf{U}(x)\sigma_3, \quad (2.3)$$

with $W_\mu \equiv W_\mu^a(x)\sigma_a/2$ and B_μ denoting the $SU(2)_L$ and $U(1)_Y$ gauge bosons, respectively. In Eq. (2.2), the first line describes the h and gauge boson kinetic terms, and the effective

⁴As usual, derivative is understood in the sense of covariant derivative. That is, a gauge field and a momentum have both chiral dimension one and their inclusion in non-renormalizable operators is weighted down by the same high-scale Λ_s .

scalar potential $V(h)$, accounting for the breaking of the electroweak symmetry. The second line describes the W and Z masses and their interactions with h , as well as the kinetic terms for GBs and fermions. Finally, the third line corresponds to the Yukawa-like interactions written in the fermionic mass eigenstate basis, where $s_Y \equiv \pm$ encodes the experimental uncertainty on the sign in the h -fermion couplings. A compact notation for the right-handed fields has been adopted, gathering them into doublets⁵ Q_R and L_R . \mathbf{Y}_Q and \mathbf{Y}_L are two 6×6 block-diagonal matrices containing the usual Yukawa couplings:

$$\mathbf{Y}_Q \equiv \mathbf{diag}(Y_U, Y_D), \quad \mathbf{Y}_L \equiv \mathbf{diag}(Y_\nu, Y_L). \quad (2.4)$$

$\Delta\mathcal{L}$ in Eq. (2.1) includes all bosonic (that is, pure gauge and gauge- h operators plus pure Higgs ones) and Yukawa-like operators that describe deviations from the SM picture due to the strong interacting physics present at scales higher than the EW one, in an expansion up to four derivatives [63]:

$$\begin{aligned} \Delta\mathcal{L} = & \xi [c_B\mathcal{P}_B(h) + c_W\mathcal{P}_W(h) + c_G\mathcal{P}_G(h) + c_C\mathcal{P}_C(h) + c_T\mathcal{P}_T(h) + c_H\mathcal{P}_H(h) + c_{\square H}\mathcal{P}_{\square H}(h)] \\ & + \xi \sum_{i=1}^{10} c_i\mathcal{P}_i(h) + \xi^2 \sum_{i=11}^{25} c_i\mathcal{P}_i(h) + \xi^4 c_{26}\mathcal{P}_{26}(h) + \sum_i \xi^{n_i} c_{HH}^i \mathcal{P}_{HH}^i(h) \end{aligned} \quad (2.5)$$

where c_i are model-dependent constant coefficients, and the last term account for all possible pure Higgs operators weighted by ξ^{n_i} with $n_i \geq 2$. The set of pure-gauge and gauge- h operators are defined by [63]⁶:

Weighted by ξ :

$$\begin{aligned} \mathcal{P}_C(h) &= -\frac{v^2}{4} \text{Tr}(\mathbf{V}^\mu \mathbf{V}_\mu) \mathcal{F}_C(h) & \mathcal{P}_4(h) &= ig' B_{\mu\nu} \text{Tr}(\mathbf{T} \mathbf{V}^\mu) \partial^\nu \mathcal{F}_4(h) \\ \mathcal{P}_T(h) &= \frac{v^2}{4} \text{Tr}(\mathbf{T} \mathbf{V}_\mu) \text{Tr}(\mathbf{T} \mathbf{V}^\mu) \mathcal{F}_T(h) & \mathcal{P}_5(h) &= ig \text{Tr}(W_{\mu\nu} \mathbf{V}^\mu) \partial^\nu \mathcal{F}_5(h) \\ \mathcal{P}_B(h) &= -\frac{g'^2}{4} B_{\mu\nu} B^{\mu\nu} \mathcal{F}_B(h) & \mathcal{P}_6(h) &= (\text{Tr}(\mathbf{V}_\mu \mathbf{V}^\mu))^2 \mathcal{F}_6(h) \\ \mathcal{P}_W(h) &= -\frac{g^2}{4} W_{\mu\nu}^a W^{a\mu\nu} \mathcal{F}_W(h) & \mathcal{P}_7(h) &= \text{Tr}(\mathbf{V}_\mu \mathbf{V}^\mu) \partial_\nu \partial^\nu \mathcal{F}_7(h) \\ \mathcal{P}_G(h) &= -\frac{g_s^2}{4} G_{\mu\nu}^a G^{a\mu\nu} \mathcal{F}_G(h) & \mathcal{P}_8(h) &= \text{Tr}(\mathbf{V}_\mu \mathbf{V}_\nu) \partial^\mu \mathcal{F}_8(h) \partial^\nu \mathcal{F}_8'(h) \\ \mathcal{P}_1(h) &= gg' B_{\mu\nu} \text{Tr}(\mathbf{T} W^{\mu\nu}) \mathcal{F}_1(h) & \mathcal{P}_9(h) &= \text{Tr}((\mathcal{D}_\mu \mathbf{V}^\mu)^2) \mathcal{F}_9(h) \\ \mathcal{P}_2(h) &= ig' B_{\mu\nu} \text{Tr}(\mathbf{T} [\mathbf{V}^\mu, \mathbf{V}^\nu]) \mathcal{F}_2(h) & \mathcal{P}_{10}(h) &= \text{Tr}(\mathbf{V}_\nu \mathcal{D}_\mu \mathbf{V}^\mu) \partial^\nu \mathcal{F}_{10}(h) \\ \mathcal{P}_3(h) &= ig \text{Tr}(W_{\mu\nu} [\mathbf{V}^\mu, \mathbf{V}^\nu]) \mathcal{F}_3(h) \end{aligned} \quad (2.6)$$

⁵The Cabibbo-Kobayashi-Maskawa mixing is understood to be encoded in the definition of Q_L .

⁶The set of pure gauge and gauge- h operators exactly matches that in Ref. [63]; nevertheless, the labelling of some operators here and their ξ -weights are corrected with respect to those in Ref. [63], see later.

Weighted by ξ^2 :

$$\begin{aligned}
\mathcal{P}_{11}(h) &= (\text{Tr}(\mathbf{V}_\mu \mathbf{V}_\nu))^2 \mathcal{F}_{11}(h) & \mathcal{P}_{19}(h) &= \text{Tr}(\mathbf{T} \mathcal{D}_\mu \mathbf{V}^\mu) \text{Tr}(\mathbf{T} \mathbf{V}_\nu) \partial^\nu \mathcal{F}_{19}(h) \\
\mathcal{P}_{12}(h) &= g^2 (\text{Tr}(\mathbf{T} W_{\mu\nu}))^2 \mathcal{F}_{12}(h) & \mathcal{P}_{20}(h) &= \text{Tr}(\mathbf{V}_\mu \mathbf{V}^\mu) \partial_\nu \mathcal{F}_{20}(h) \partial^\nu \mathcal{F}'_{20}(h) \\
\mathcal{P}_{13}(h) &= ig \text{Tr}(\mathbf{T} W_{\mu\nu}) \text{Tr}(\mathbf{T} [\mathbf{V}^\mu, \mathbf{V}^\nu]) \mathcal{F}_{13}(h) & \mathcal{P}_{21}(h) &= (\text{Tr}(\mathbf{T} \mathbf{V}_\mu))^2 \partial_\nu \mathcal{F}_{21}(h) \partial^\nu \mathcal{F}'_{21}(h) \\
\mathcal{P}_{14}(h) &= g \varepsilon^{\mu\nu\rho\lambda} \text{Tr}(\mathbf{T} \mathbf{V}_\mu) \text{Tr}(\mathbf{V}_\nu W_{\rho\lambda}) \mathcal{F}_{14}(h) & \mathcal{P}_{22}(h) &= \text{Tr}(\mathbf{T} \mathbf{V}_\mu) \text{Tr}(\mathbf{T} \mathbf{V}_\nu) \partial^\mu \mathcal{F}_{22}(h) \partial^\nu \mathcal{F}'_{22}(h) \\
\mathcal{P}_{15}(h) &= \text{Tr}(\mathbf{T} \mathcal{D}_\mu \mathbf{V}^\mu) \text{Tr}(\mathbf{T} \mathcal{D}_\nu \mathbf{V}^\nu) \mathcal{F}_{15}(h) & \mathcal{P}_{23}(h) &= \text{Tr}(\mathbf{V}_\mu \mathbf{V}^\mu) (\text{Tr}(\mathbf{T} \mathbf{V}_\nu))^2 \mathcal{F}_{23}(h) \\
\mathcal{P}_{16}(h) &= \text{Tr}([\mathbf{T}, \mathbf{V}_\nu] \mathcal{D}_\mu \mathbf{V}^\mu) \text{Tr}(\mathbf{T} \mathbf{V}^\nu) \mathcal{F}_{16}(h) & \mathcal{P}_{24}(h) &= \text{Tr}(\mathbf{V}_\mu \mathbf{V}_\nu) \text{Tr}(\mathbf{T} \mathbf{V}^\mu) \text{Tr}(\mathbf{T} \mathbf{V}^\nu) \mathcal{F}_{24}(h) \\
\mathcal{P}_{17}(h) &= ig \text{Tr}(\mathbf{T} W_{\mu\nu}) \text{Tr}(\mathbf{T} \mathbf{V}^\mu) \partial^\nu \mathcal{F}_{17}(h) & \mathcal{P}_{25}(h) &= (\text{Tr}(\mathbf{T} \mathbf{V}_\mu))^2 \partial_\nu \partial^\nu \mathcal{F}_{25}(h) \\
\mathcal{P}_{18}(h) &= \text{Tr}(\mathbf{T} [\mathbf{V}_\mu, \mathbf{V}_\nu]) \text{Tr}(\mathbf{T} \mathbf{V}^\mu) \partial^\nu \mathcal{F}_{18}(h) & &
\end{aligned} \tag{2.7}$$

Weighted by ξ^4 :

$$\mathcal{P}_{26}(h) = (\text{Tr}(\mathbf{T} \mathbf{V}_\mu) \text{Tr}(\mathbf{T} \mathbf{V}_\nu))^2 \mathcal{F}_{26}(h). \tag{2.8}$$

In Eq. (2.7), \mathcal{D}_μ denotes the covariant derivative on a field transforming in the adjoint representation of $SU(2)_L$, i.e.

$$\mathcal{D}_\mu \mathbf{V}_\nu \equiv \partial_\mu \mathbf{V}_\nu + ig [W_\mu, \mathbf{V}_\nu]. \tag{2.9}$$

Finally, the pure Higgs operators are:

Weighted by ξ : this set includes two operators, one with two derivatives and one with four,

$$\mathcal{P}_H(h) = \frac{1}{2} (\partial_\mu h) (\partial^\mu h) \mathcal{F}_H(h), \quad \mathcal{P}_{\square H} = \frac{1}{v^2} (\partial_\mu \partial^\mu h)^2 \mathcal{F}_{\square H}(h). \tag{2.10}$$

In spite of not containing gauge interactions, they will be considered here as they affect the renormalization of SM parameters, and the propagator of the h field, respectively.

Weighted by $\xi^{\geq 2}$: this class consists of all possible pure Higgs operators with four derivatives weighted by $\xi^{\geq 2}$, $\mathcal{P}_{HH}^i(h)$. We refrain from listing them here, as pure- h operators are beyond the scope of this work and therefore they will not be taken into account in the phenomenological sections below. An example of ξ^2 -weighted operator would be [65, 85]

$$\mathcal{P}_{DH}(h) = \frac{1}{v^4} ((\partial_\mu h) (\partial^\mu h))^2 \mathcal{F}_{DH}(h). \tag{2.11}$$

In another realm, note that $\mathcal{P}_C(h)$, $\mathcal{P}_T(h)$ and $\mathcal{P}_H(h)$ are two-derivative operators and would be considered among the leading terms in any formal analysis of the non-linear expansion (as explained after Eq. (2.1)), a fact of no consequence below.

The ξ weights within $\Delta\mathcal{L}$ do **not** reflect an expansion in ξ , but a reparametrisation that facilitates the tracking of the lowest dimension at which a ‘‘sibling’’ of a given operator appears in the linear expansion. To guarantee the procedure, such an analysis requires to

compare with a specific linear basis; complete linear bases are only available up to $d = 6$ and here we use the completion of the original HISZ basis [6, 76], see Sect. 3.1.

A sibling of a chiral operator $\mathcal{P}_i(h)$ is defined as the operator of the linear expansion whose pure gauge interactions coincide with those described by $\mathcal{P}_i(h)$. The canonical dimension d of the sibling, that is the power of ξ , is thus an indicator of at which order in the linear expansion it is necessary and sufficient to go to account for those gauge interactions: operators weighted by ξ^n require us to consider siblings of canonical dimension $d = 4 + 2n$. It may happen that an operator in Eqs. (2.6)-(2.10) corresponds to a combination of linear operators with different canonical dimensions: the power of ξ refers then to the lowest dimension of such operators that leads to the same phenomenological gauge couplings. The lowest dimensional siblings of the operators in Eqs. (2.6) and (2.10) have $d = 6$; those in Eqs. (2.7) have $d = 8$; that of Eq. (2.8) has $d = 12$. ξ is not a physical quantity *per se* in the framework of the effective Lagrangian. If preferred by the reader, the ξ weights can be reabsorbed in a redefinition of the coefficients c_i and be altogether forgotten; nevertheless, they allow a fast connection with the analyses performed in the linear expansion, as illustrated later on.

In the Lagrangian above, Eq (2.5), we have chosen a definition of the operator coefficients which does not make explicit the weights expected from Naive Dimensional Analysis (NDA) [66, 67, 86]. While the NDA rules are known not to apply to the gauge and scalar kinetic and mass terms, for the higher-order corrections they would imply suppressions by factors of the goldstone boson scale f versus the high energy scale Λ_s . In particular, the coefficients of all operators in Eq. (2.6) except $P_C(h)$, as well as all operators in Eqs. (2.7), (2.8) and (2.10), would be suppressed by the factor $f^2/\Lambda_s^2 = 1/(16\pi^2)$. The coefficients can be easily redefined by the reader if wished.

The $\mathcal{F}(h)$ functions encode the chiral interactions of the light h , through the generic dependence on $(\langle h \rangle + h)$, and are model dependent. Each function can be defined by $\mathcal{F}(h) \equiv g_0(h, v) + \xi g_1(h, v) + \xi^2 g_2(h, v) + \dots$, where $g_i(h, v)$ are model-dependent functions of h and of v , once $\langle h \rangle$ is expressed in terms of ξ and v . Here we will assume that the $\mathcal{F}(h)$ functions are completely general polynomials of $\langle h \rangle$ and h (not including derivatives of h). Notice that when using the equations of motion (EOM) and integration by parts to relate operators, $\mathcal{F}(h)$ would be assumed to be redefined when convenient, much as one customarily redefines the constant operator coefficients.

The insertions of the h field, explicit or through generic functions, deserve a separate comment: given their goldstonic origin, they are expected to be suppressed by the goldstone boson scale as h/f , as it has been already specified above. This is encoded in the present formalism by the combination of the $F_i(h)$ functions as defined in the text and the pertinent ξ -weights which have been explicitly extracted from them, as they constitute a useful tool to establish the relation with the linear expansions. Consider an initial generic dependence on the h field of the form $(h + \langle h \rangle)/f = \sqrt{\xi}(h + \langle h \rangle)/v$: for instance in the linear regime, in which $\langle h \rangle \sim v$, the $F_i(h)$ functions are defined in the text as leading to powers of $(1 + h/v)$, because the functional ξ -dependence has been made explicit in the Lagrangian.

Connection to fermionic operators

Several operators in the list in Eqs. (2.6)-(2.8) are independent only in the presence of massive fermions: these are $\mathcal{P}_9(h)$, $\mathcal{P}_{10}(h)$, $\mathcal{P}_{15}(h)$, $\mathcal{P}_{16}(h)$, $\mathcal{P}_{19}(h)$, one out of $\mathcal{P}_6(h)$, $\mathcal{P}_7(h)$ and $\mathcal{P}_{20}(h)$, and one out of $\mathcal{P}_{21}(h)$, $\mathcal{P}_{23}(h)$ and $\mathcal{P}_{25}(h)$. Indeed, $\mathcal{P}_9(h)$, $\mathcal{P}_{10}(h)$, $\mathcal{P}_{15}(h)$, $\mathcal{P}_{16}(h)$, and $\mathcal{P}_{19}(h)$ contain the contraction $\mathcal{D}_\mu \mathbf{V}^\mu$ that is connected with the Yukawa couplings [63], through the manipulation of the gauge field EOM and the Dirac equations (see App. A for details). When fermion masses are neglected, these five operators can be written in terms of the other operators in the basis (see Eq. (A.16)). Furthermore, using the light h EOM (see Eq. (A.3)), operator $\mathcal{P}_7(h)$ ($\mathcal{P}_{25}(h)$) can be reduced to a combination of $\mathcal{P}_6(h)$ and $\mathcal{P}_{20}(h)$ ($\mathcal{P}_{21}(h)$ and $\mathcal{P}_{23}(h)$), plus a term that can be absorbed in the redefinition of the h -gauge boson couplings, plus a term containing the Yukawa interactions (see App. A for details). In summary, all those operators must be included to have a complete and independent bosonic basis; nevertheless, in the numerical analysis in Sect. 4.2 their effect will be disregarded as the impact of fermion masses on data analysis will be negligible.

Other operators in the basis in Eqs.(2.6)-(2.10) can be traded by fermionic ones independently of the size of fermion masses, applying the EOM for $\mathcal{D}_\mu W^{\mu\nu}$ and $\partial_\mu B^{\mu\nu}$, see Eqs. (A.1), (A.2) and (A.11) in App. A. The complete list of fermionic operators that are related to the pure gauge and gauge- h basis in Eqs. (2.6)-(2.10) can also be found there⁷. This trading procedure can turn out to be very useful [10, 35, 37, 38, 87] when analysing certain experimental data if deviations from the SM values for the h -fermion couplings were found. A basis including all possible fermionic couplings could be more useful in such a hypothetical situation. The bosonic basis defined above is instead “blind” [88] to some deviations in fermionic couplings. This should not come as a surprise: the choice of basis should be optimized with respect to the experimental data under analysis and the presence of blind directions is a common feature of any basis. In this work we are focused in exploring directly the experimental consequences of anomalous gauge and gauge- h couplings and Eqs.(2.6)-(2.10) are the appropriate analysis tool.

Custodial symmetry

In the list in Eqs.(2.6)-(2.10), the operators $\mathcal{P}_{\square H}(h)$, $\mathcal{P}_T(h)$, $\mathcal{P}_1(h)$, $\mathcal{P}_2(h)$, $\mathcal{P}_4(h)$, $\mathcal{P}_9(h)$, $\mathcal{P}_{10}(h)$ and $\mathcal{P}_{12-26}(h)$ are custodial symmetry breaking, as either they: i) are related to fermion masses; ii) are related to the hypercharge through $g' B_{\mu\nu}$; iii) they contain the scalar chiral operator \mathbf{T} but no $B_{\mu\nu}$. Among these, only $\mathcal{P}_T(h)$ and $\mathcal{P}_1(h)$ are strongly constrained from electroweak precision test, while the phenomenological impact of the remaining operators has never been studied and therefore they could lead to interesting effects.

If instead by “custodial breaking” operators one refers only to those in iii), a complete

⁷For completeness, the EOM of the gauge bosons, h and $\mathbf{U}(h)$, and the Dirac equations as well as the full list of fermionic operators that are related to the bosonic ones in Eqs. (2.6)-(2.10) are presented in App. A. In this paper, we will only rely on bosonic observables and therefore we will not consider any fermionic operators other than those mentioned.

set of bosonic custodial preserving operators is given by the following eighteen operators:

$$\mathcal{P}_H(h), \quad \mathcal{P}_{\square H}(h), \quad \mathcal{P}_C(h), \quad \mathcal{P}_B(h), \quad \mathcal{P}_W(h), \quad \mathcal{P}_G(h), \quad \mathcal{P}_{1-11}(h), \quad \mathcal{P}_{20}(h). \quad (2.12)$$

Furthermore, if fermion masses are neglected, this ensemble is further reduced to a set of fourteen independent operators, given by

$$\mathcal{P}_H(h), \quad \mathcal{P}_C(h), \quad \mathcal{P}_B(h), \quad \mathcal{P}_W(h), \quad \mathcal{P}_G(h), \quad \mathcal{P}_{1-5}(h), \quad \mathcal{P}_8(h), \quad \mathcal{P}_{11}(h), \quad (2.13)$$

plus any two among the following three operators:

$$\mathcal{P}_6(h), \quad \mathcal{P}_7(h), \quad \mathcal{P}_{20}(h). \quad (2.14)$$

Under the same assumptions (no beyond SM sources of custodial breaking and massless fermions), a subset of only twelve operators has been previously proposed in Ref. [62], as this reference in addition restricted to operators that lead to cubic and quartic vertices of GBs and gauge bosons *and* including one or two Higgs bosons.

The Lagrangian in Eq.(2.1) is very general and can be used to describe an extended class of Higgs models, from the SM scenario with a linear Higgs sector (for $\langle h \rangle = v$, $\xi = 0$ and $s_Y = 1$), to the technicolor-like ansatz (for $f \sim v$ and omitting all terms in h) and intermediate situations with a light scalar h from composite/holographic Higgs models [41–49, 56] (in general for $f \neq v$) up to dilaton-like scalar frameworks [85, 89–94] (for $f \sim v$), where the dilaton participates in the electroweak symmetry breaking.

3 Comparison with the linear regime

The chiral and linear approaches are essentially different from each other, as explained in the introduction. The reshuffling with respect to the linear case of the order at which the leading operators appear plus the generic dependence on h imply that correlations among observables present in one scenario may not hold in the other and, moreover, interactions that are strongly suppressed in one case may be leading corrections in the other. As the symmetry respected by the non-linear Lagrangian is smaller, more freedom is generically expected for the latter. In this section, for the sake of comparison we will first present the effective Lagrangian in the linear regime, restricting to the HISZ basis [76, 77], and discuss then the coincidences and differences expected in observable predictions. The relation to another basis [87] can be found in App. B.

3.1 The effective Lagrangian in the linear regime

Following the description pattern in Eq. (2.1), the effective Lagrangian in the linear regime can be written accordingly as

$$\mathcal{L}_{\text{linear}} = \mathcal{L}_{SM} + \Delta\mathcal{L}_{\text{linear}}, \quad (3.1)$$

where the relation with the non-linear Lagrangian in Eq. (2.2) is given by $\mathcal{L}_{SM} = \mathcal{L}_0|_{s_Y=1}$, and $\Delta\mathcal{L}_{\text{linear}}$ contains operators with canonical dimension $d > 4$, weighted down by suitable

powers of the ultraviolet cut-off scale Λ . Restricting to CP -even and baryon and lepton number preserving operators, the leading $d = 6$ corrections

$$\Delta\mathcal{L}_{\text{linear}}^{d=6} = \sum_i \frac{f_i}{\Lambda^2} \mathcal{O}_i, \quad (3.2)$$

may be parametrized via a complete basis of operators [5, 6]. Only a small subset of those modify the Higgs couplings to gauge bosons. Consider the HISZ basis [76, 77]:

$$\begin{aligned} \mathcal{O}_{GG} &= \Phi^\dagger \Phi G_{\mu\nu}^a G^{a\mu\nu}, & \mathcal{O}_{WW} &= \Phi^\dagger \hat{W}_{\mu\nu} \hat{W}^{\mu\nu} \Phi, \\ \mathcal{O}_{BB} &= \Phi^\dagger \hat{B}_{\mu\nu} \hat{B}^{\mu\nu} \Phi, & \mathcal{O}_{BW} &= \Phi^\dagger \hat{B}_{\mu\nu} \hat{W}^{\mu\nu} \Phi, \\ \mathcal{O}_W &= (D_\mu \Phi)^\dagger \hat{W}^{\mu\nu} (D_\nu \Phi), & \mathcal{O}_B &= (D_\mu \Phi)^\dagger \hat{B}^{\mu\nu} (D_\nu \Phi), \\ \mathcal{O}_{\Phi,1} &= (D_\mu \Phi)^\dagger \Phi \Phi^\dagger (D^\mu \Phi), & \mathcal{O}_{\Phi,2} &= \frac{1}{2} \partial^\mu (\Phi^\dagger \Phi) \partial_\mu (\Phi^\dagger \Phi), \\ \mathcal{O}_{\Phi,4} &= (D_\mu \Phi)^\dagger (D^\mu \Phi) (\Phi^\dagger \Phi), \end{aligned} \quad (3.3)$$

where $D_\mu \Phi = (\partial_\mu + \frac{i}{2}g'B_\mu + \frac{i}{2}g\sigma_i W_\mu^i) \Phi$ and $\hat{B}_{\mu\nu} \equiv \frac{i}{2}g'B_{\mu\nu}$ and $\hat{W}_{\mu\nu} \equiv \frac{i}{2}g\sigma_i W_{\mu\nu}^i$. An additional operator is commonly added in phenomenological analysis,

$$\mathcal{O}_{\Phi,3} = \frac{1}{3} (\Phi^\dagger \Phi)^3, \quad (3.4)$$

which is a pure Higgs operator. An equivalent basis of ten operators in the linear expansion is often used nowadays instead of the previous set of ten linear operators: the so-called SILH [87] Lagrangian, in which four of the operators above are traded by combinations of them and/or by a fermionic one via EOM (the exact relation with the SILH basis can be found in App. B).

The pure Higgs interactions described by the ξ -weighted operator $\mathcal{P}_{\square H}$ of the chiral expansion, Eq. (2.10), are contained in the linear operator,

$$\mathcal{O}_{\square\Phi} = (D_\mu D^\mu \Phi)^\dagger (D_\nu D^\nu \Phi). \quad (3.5)$$

Let us now explore the relation between the linear and non-linear analyses. Beyond the different h -dependence of the operators, that is (in the unitary gauge):

$$\Phi = \frac{1}{\sqrt{2}} \begin{pmatrix} 0 \\ v + h(x) \end{pmatrix} \quad \text{vs.} \quad \mathcal{F}(h), \quad (3.6)$$

it is interesting to explore the relation among the linear operators in Eqs. (3.3) and those in the chiral expansion. A striking distinct feature when comparing both basis is the different number of independent couplings they span. This is best illustrated for instance truncating the non-linear expansion at order ξ -which may be specially relevant for small ξ - and comparing the result with the $d = 6$ linear basis that contributes to gauge-Higgs couplings: while the latter basis exhibits ten independent couplings, the former depends on

sixteen. A more precise illustration follows when taking momentarily $\mathcal{F}_i(h) = (1 + h/v)^n$, with $n = 2$ in general, in all $\mathcal{P}_i(h)$ under discussion, which would lead to:

$$\begin{aligned}
\mathcal{O}_{BB} &= \frac{v^2}{2} \mathcal{P}_B(h), & \mathcal{O}_{WW} &= \frac{v^2}{2} \mathcal{P}_W(h), \\
\mathcal{O}_{GG} &= -\frac{2v^2}{g_s^2} \mathcal{P}_G(h), & \mathcal{O}_{BW} &= \frac{v^2}{8} \mathcal{P}_1(h), \\
\mathcal{O}_B &= \frac{v^2}{16} \mathcal{P}_2(h) + \frac{v^2}{8} \mathcal{P}_4(h), & \mathcal{O}_W &= \frac{v^2}{8} \mathcal{P}_3(h) - \frac{v^2}{4} \mathcal{P}_5(h), \\
\mathcal{O}_{\Phi,1} &= \frac{v^2}{2} \mathcal{P}_H(h) - \frac{v^2}{4} \mathcal{F}(h) \mathcal{P}_T(h), & \mathcal{O}_{\Phi,2} &= v^2 \mathcal{P}_H(h), \\
\mathcal{O}_{\Phi,4} &= \frac{v^2}{2} \mathcal{P}_H(h) + \frac{v^2}{2} \mathcal{F}(h) \mathcal{P}_C(h), \\
\mathcal{O}_{\square\Phi} &= \frac{v^2}{2} \mathcal{P}_{\square H}(h) + \frac{v^2}{8} \mathcal{P}_6(h) + \frac{v^2}{4} \mathcal{P}_7(h) - v^2 \mathcal{P}_8(h) - \frac{v^2}{4} \mathcal{P}_9(h) - \frac{v^2}{2} \mathcal{P}_{10}(h).
\end{aligned} \tag{3.7}$$

These relations show that five chiral operators, $\mathcal{P}_B(h)$, $\mathcal{P}_W(h)$, $\mathcal{P}_G(h)$, $\mathcal{P}_1(h)$ and $\mathcal{P}_H(h)$ are then in a one-to-one correspondence with the linear operators \mathcal{O}_{BB} , \mathcal{O}_{WW} , \mathcal{O}_{GG} , \mathcal{O}_{BW} and $\mathcal{O}_{\Phi,2}$, respectively. Also the operator $\mathcal{P}_T(h)$ ($\mathcal{P}_C(h)$) corresponds to a combination of the linear operators $\mathcal{O}_{\Phi,1}$ and $\mathcal{O}_{\Phi,2}$ ($\mathcal{O}_{\Phi,4}$ and $\mathcal{O}_{\Phi,2}$). In contrast, it follows from Eq. (3.7) above that:

- Only a specific combination of the non-linear operators $\mathcal{P}_2(h)$ and $\mathcal{P}_4(h)$ corresponds to the linear operator \mathcal{O}_B .
- Similarly, a specific combination of the non-linear operators $\mathcal{P}_3(h)$ and $\mathcal{P}_5(h)$ corresponds to the linear operator \mathcal{O}_W .
- Only a specific combination of the non-linear operators $\mathcal{P}_{\square H}(h)$, $\mathcal{P}_6(h)$, $\mathcal{P}_7(h)$, $\mathcal{P}_8(h)$, $\mathcal{P}_9(h)$ and $\mathcal{P}_{10}(h)$ corresponds to the linear operator $\mathcal{O}_{\square\Phi}$.

It is necessary to go to the next order in the linear basis, $d = 8$, to identify the operators which break these correlations (see Eq. (C.2)). It can be checked that, for example for the first two correlations, the linear $d = 8$ operators

$$((D_\mu \Phi)^\dagger \Phi) \hat{B}^{\mu\nu} (\Phi^\dagger D_\nu \Phi) \quad \text{and} \quad ((D_\mu \Phi)^\dagger \Phi) \hat{W}^{\mu\nu} (\Phi^\dagger D_\nu \Phi) \tag{3.8}$$

correspond separately to $\mathcal{P}_4(h)$ and $\mathcal{P}_5(h)$, respectively.

A comment is pertinent when considering the ξ truncation. In the $\xi \rightarrow 0$ limit, in which $\mathcal{F}(h) \rightarrow (1 + h/v)^2$, if the underlying theory is expected to account for EWSB, the ensemble of the non-linear Lagrangian should converge to a linear-like pattern. Nevertheless, the size of ξ is not known in a model-independent way; starting an analysis by formulating the problem (only) in the linear expansion is somehow assuming an answer from the start: that ξ is necessarily small in any possible BSM construction. Furthermore, the non-linear Lagrangian accounts for more exotic singlet scalars, and that convergence is not granted in general.

The maximal set of CP-even independent operators involving gauge and/or the Higgs boson in any $d = 6$ linear basis is made out of 16 operators: the ten [76,77] in Eqs. (3.3) and (3.4), plus the operator [6] $\mathcal{O}_{\square\Phi}$ defined in Eq. (3.5), and another five which only modify the gauge boson couplings and do not involve the Higgs field⁸ [76,77]:

$$\begin{aligned}\mathcal{O}_{WWW} &= i\epsilon_{ijk}\hat{W}_\mu^{i\nu}\hat{W}_\nu^{j\rho}\hat{W}_\rho^{k\mu}, & \mathcal{O}_{GGG} &= if_{abc}G_\mu^{a\nu}G_\nu^{b\rho}G_\rho^{c\mu}, \\ \mathcal{O}_{DW} &= \left(\mathcal{D}^\mu\hat{W}_{\mu\nu}\right)^i\left(\mathcal{D}_\rho\hat{W}^{\rho\nu}\right)^i, & \mathcal{O}_{DB} &= \left(\partial^\mu\hat{B}_{\mu\nu}\right)\left(\partial_\rho\hat{B}^{\rho\nu}\right), \\ \mathcal{O}_{DG} &= \left(\mathcal{D}^\mu G_{\mu\nu}\right)^a\left(\mathcal{D}_\rho G^{\rho\nu}\right)^a.\end{aligned}\quad (3.9)$$

The Lorentz structures contained in these five operators are *not* present in the non-linear Lagrangian expanded up to four derivatives: they would appear only at higher order in that expansion, i.e. six derivatives. They are not the siblings of any of the chiral operators discussed in this work, Eqs. (2.6)-(2.10).

The rest of this paper will focus on how the present and future LHC gauge and gauge- h data, as well as other data, may generically shed light on the (non-)linearity of the underlying physics. In particular exploiting the decorrelations implied by the discussion above as well as via new anomalous discriminating signals.

Disregarding fine tunings, that is, assuming in general all dimensionless operator coefficients of $\mathcal{O}(1)$, the pattern of dominant signals expected from each expansion varies because the nature of some leading corrections is different, or because the expected relation between some couplings varies. In the next subsections we analyze first how some correlations among couplings expected in the linear regime are broken in the non-linear one. Next, it is pointed out that some couplings expected if the EWSB is linearly realized are instead expected to appear only as higher order corrections in the non-linear case. Conversely and finally, attention is paid to new anomalous couplings expected as leading corrections in the non-linear regime which appear only at $d \geq 8$ of the linear expansion.

3.2 Decorrelation of signals with respect to the linear analysis

The parameter ξ is a free parameter in the effective approach. Nevertheless, in concrete composite Higgs models electroweak corrections imply $\xi \lesssim 0.2 - 0.4$ [95] (more constraining bounds $\xi \lesssim 0.1 - 0.2$ have been advocated in older analyses [29,96,97]), and it is therefore interesting for the sake of comparison to consider the truncation of $\Delta\mathcal{L}$ which keeps only the terms weighted by ξ and disregard first those weighted by higher ξ powers. We will thus analyze first only those operators in Eqs. (2.6) and (2.10). We will refer to this truncation as $\Delta\mathcal{L}^\xi$ and define $\mathcal{L}_{chiral}^\xi \equiv \mathcal{L}_0 + \Delta\mathcal{L}^\xi$.

All operators in $\Delta\mathcal{L}^\xi$ have by definition lowest dimensional linear siblings of $d = 6$. We will thus compare first \mathcal{L}_{chiral}^ξ with the $d = 6$ linear expansion [5,6,87]. For low enough values of ξ , that is when the new physics scale $\Lambda_s \gg v$, \mathcal{L}_{chiral}^ξ is expected to collapse into the $d = 6$ linear Lagrangian if it should account correctly for EW symmetry breaking via

⁸The Operators \mathcal{O}_{DW} , \mathcal{O}_{DB} and \mathcal{O}_{DG} are usually traded by \mathcal{O}_{WWW} and \mathcal{O}_{GGG} plus fermionic operators. As in this paper we focus on bosonic observables, such translation is not pertinent. Taken by themselves, the ensembles discussed constitute a non-redundant and complete set of gauge and/or Higgs operators. In \mathcal{O}_{DG} , \mathcal{D}^μ denotes the covariant derivative acting on a field transforming in the adjoint of $SU(3)_C$.

an $SU(2)_L$ doublet scalar, but the non-linear Lagrangian encodes more general scenarios (for instance that for a SM singlet) as well.

The comparison of the effects in the non-linear versus the linear expansion is illuminating when done in the context of the maximal set of independent (and thus non-redundant) operators on the gauge-boson/Higgs sector for each expansion: comparing complete bases of those characteristics. The number of independent bosonic operators that induce leading deviations in gauge- h couplings turns out to be then different for both expansions: ten $d = 6$ operators in the linear expansion, see Eq. (3.3) and Eq. (3.5), for sixteen ξ -weighted operators⁹ in the chiral one, see Eq. (2.6) and (2.10). For illustration, further details are given here on one example pointed out in Sect. 3.1: $\mathcal{P}_2(h)$ and $\mathcal{P}_4(h)$ versus the $d = 6$ operator \mathcal{O}_B . From Eq. (3.7) it followed that only the combinations $\mathcal{P}_2(h) + 2\mathcal{P}_4(h)$ have a $d = 6$ linear equivalent (with $\mathcal{F}_i(h)$ substituted by $(1 + h/v)^2$). In the unitary gauge $\mathcal{P}_2(h)$ and $\mathcal{P}_4(h)$ read:

$$\mathcal{P}_2(h) = 2ieg^2 A_{\mu\nu} W^{-\mu} W^{+\nu} \mathcal{F}_2(h) - 2 \frac{ie^2 g}{\cos \theta_W} Z_{\mu\nu} W^{-\mu} W^{+\nu} \mathcal{F}_2(h), \quad (3.10)$$

$$\mathcal{P}_4(h) = -\frac{eg}{\cos \theta_W} A_{\mu\nu} Z^\mu \partial^\nu \mathcal{F}_4(h) + \frac{e^2}{\cos^2 \theta_W} Z_{\mu\nu} Z^\mu \partial^\nu \mathcal{F}_4(h), \quad (3.11)$$

with their coefficients c_2 and c_4 taking arbitrary (model-dependent) values. In contrast, their $d = 6$ sibling \mathcal{O}_B results in the combination:

$$\begin{aligned} \mathcal{O}_B = & \frac{ieg^2}{8} A_{\mu\nu} W^{-\mu} W^{+\nu} (v + h)^2 - \frac{ie^2 g}{8 \cos \theta_W} Z_{\mu\nu} W^{-\mu} W^{+\nu} (v + h)^2 \\ & - \frac{eg}{4 \cos \theta_W} A_{\mu\nu} Z^\mu \partial^\nu h (v + h) + \frac{e^2}{4 \cos^2 \theta_W} Z_{\mu\nu} Z^\mu \partial^\nu h (v + h). \end{aligned} \quad (3.12)$$

In consequence, the following interactions encoded in \mathcal{O}_B -and for the precise Lorentz structures shown above- get decorrelated in a general non-linear analysis:

- $\gamma - W - W$ from $\gamma - Z - h$, and $Z - W - W$ from $Z - Z - h$; these are examples of interactions involving different number of external h legs.
- $\gamma - W - W - h$ from $\gamma - Z - h$, and $Z - W - W - h$ from $Z - Z - h$, which are interactions involving the same number of external h legs.

While such decorrelations are expected among the leading SM deviations in a generic non-linear approach, they require us to consider $d = 8$ operators in scenarios with linearly realized EW symmetry breaking. This statement is a physical effect, which means that it holds irrespective of the linear basis used, for instance it also holds in the bases in Refs. [97, 98]. The study of the correlations/decorrelations described represents an interesting method to investigate the intimate nature of the light Higgs h .

The argument developed above focused on just one operator, for illustration. A parallel analysis on correlations/decorrelations also applies in another case, i.e. the interactions

⁹Note that the first operator in Eq. (2.10) impacts on the gauge- h couplings via the renormalization of the h field.

described by $\mathcal{P}_3(h)$ and $\mathcal{P}_5(h)$ versus those in the $d = 6$ linear operator \mathcal{O}_W . Obviously, in order to firmly establish the pattern of deviations expected, all possible operators at a given order of an expansion should be considered together, and this will be done in the phenomenological Sect. 4 below.

3.3 Signals specific to the linear expansion

The $d = 6$ operators in Eq. (3.9) have no equivalent among the dominant corrections of the non-linear expansion, Eqs. (2.6)-(2.10), all ξ weights considered. This fact results in an interesting method to test the nature of the Higgs. Considering for example the operator \mathcal{O}_{WWW} in Eq. (3.9), the couplings

$$\begin{array}{l}
 \begin{array}{c}
 W_\mu^+ \\
 \text{---} \\
 A_\rho \\
 \text{---} \\
 W_\nu^-
 \end{array}
 \end{array}
 \quad
 \begin{aligned}
 f_{WWW} & \frac{3ieg^2}{4} \left[g_{\rho\mu} ((p_+ \cdot p_-) p_{A\nu} - (p_A \cdot p_-) p_{+\nu}) \right. \\
 & + g_{\mu\nu} ((p_A \cdot p_-) p_{+\rho} - (p_A \cdot p_+) p_{-\rho}) \\
 & \left. + g_{\rho\nu} ((p_A \cdot p_+) p_{-\mu} - (p_+ \cdot p_-) p_{A\mu}) + p_{A\mu} p_{+\nu} p_{-\rho} - p_{A\nu} p_{+\rho} p_{-\mu} \right],
 \end{aligned}
 \tag{3.13}$$

$$\begin{array}{l}
 \begin{array}{c}
 W_\mu^+ \\
 \text{---} \\
 Z_\rho \\
 \text{---} \\
 W_\nu^-
 \end{array}
 \end{array}
 \quad
 \begin{aligned}
 f_{WWW} & \frac{3ig^3 \cos \theta_W}{4} \left[g_{\rho\mu} ((p_+ \cdot p_-) p_{Z\nu} - (p_Z \cdot p_-) p_{+\nu}) \right. \\
 & + g_{\mu\nu} ((p_Z \cdot p_-) p_{+\rho} - (p_Z \cdot p_+) p_{-\rho}) \\
 & \left. + g_{\rho\nu} ((p_Z \cdot p_+) p_{-\mu} - (p_+ \cdot p_-) p_{Z\mu}) + p_{Z\mu} p_{+\nu} p_{-\rho} - p_{Z\nu} p_{+\rho} p_{-\mu} \right],
 \end{aligned}$$

should be observable with a strength similar to that of other couplings described by $d = 6$ operators, if the EW breaking is linearly realized by the underlying physics. On the contrary, for a subjacent non-linear dynamics their strength is expected to be suppressed (i.e. be of higher order) [64]¹⁰. A similar discussion holds for the other operators in Eq. (3.9).

3.4 New signals specific to the non-linear expansion

For large ξ , all chiral operators weighted by ξ^n with $n \geq 2$, Eqs. (2.7)-(2.10), are equally relevant to the ξ -weighted ones in Eq. (2.6), and therefore their siblings require operators of dimension $d \geq 8$. Of special interest is $\mathcal{P}_{14}(h)$ which belongs to the former class, as some of the couplings encoded in it are absent from the SM Lagrangian. This fact provides a viable strategy to test the nature of the physical Higgs.

In App. D, the Feynman rules for all couplings appearing in the non-linear Lagrangian for gauge and gauge- h operators can be found. A special column indicates directly the non-standard structures and it is easy to identify among those entries the couplings weighted only by ξ^n with $n \geq 2$. Here, we report explicitly only the example of the anomalous $Z - W - W$ and $\gamma - Z - W - W$ vertices, assuming for simplicity that the $\mathcal{F}_{14}(h)$ function admits a polynomial expansion in h/v . The operator $\mathcal{P}_{14}(h)$ contains the couplings

$$\varepsilon^{\mu\nu\rho\lambda} \partial_\mu W_\nu^+ W_\rho^- Z_\lambda \mathcal{F}_{14}(h), \quad \varepsilon^{\mu\nu\rho\lambda} Z_\mu A_\nu W_\rho^- W_\lambda^+ \mathcal{F}_{14}(h), \tag{3.14}$$

¹⁰This coupling is usually referred to in the literature as λ_V [4].

which correspond to an anomalous $Z - W - W$ triple vertex and to an anomalous $\gamma - Z - W - W$ quartic vertex, respectively. The corresponding Feynman diagrams and rules read

$$\begin{aligned}
 & - \xi^2 \frac{g^3}{\cos \theta_W} \varepsilon^{\mu\nu\rho\lambda} [p_{+\lambda} - p_{-\lambda}], \\
 & - 2 \xi^2 \frac{eg^3}{\cos \theta_W} \varepsilon^{\mu\nu\rho\lambda}.
 \end{aligned} \tag{3.15}$$

These couplings are present neither in the SM nor in the $d = 6$ linear Lagrangian and are anomalous couplings due to their Lorentz nature. A signal of these type of interactions at colliders with a strength comparable with that expected for the couplings in the $d = 6$ linear Lagrangian would be a clear hint of a strong dynamics in the EWSB sector. More details are given in the phenomenological sections below.

4 Phenomenology

Prior to developing the strategies suggested above to investigate the nature of the Higgs particle, the renormalization procedure is illustrated next.

4.1 Renormalization Procedure

Five electroweak parameters of the SM-like Lagrangian \mathcal{L}_0 are relevant in our analysis, when neglecting fermion masses: g_s, g, g', v and the h self-coupling λ . The first four can be optimally constrained by four observables that are extremely well determined nowadays, while as a fifth one the Higgs mass m_h can be used; in summary:

$$\begin{aligned}
 \alpha_s & \text{ world average [99]}, \\
 G_F & \text{ extracted from the muon decay rate [99]}, \\
 \alpha_{\text{em}} & \text{ extracted from Thomson scattering [99]}, \\
 m_Z & \text{ extracted from the } Z \text{ lineshape at LEP I [99]}, \\
 m_h & \text{ now measured at LHC [11, 12]}.
 \end{aligned} \tag{4.1}$$

This ensemble of observables defines the so-called Z-scheme: they will be kept as input parameters, and all predictions will be expressed as functions of them. Accordingly, whenever a dependence on the parameters g, g', v (and e) or the weak mixing angle θ_W may appear in the expressions below, it should be interpreted as corresponding to the combinations of experimental inputs as follows:

$$\begin{aligned}
 e^2 &= 4\pi\alpha_{\text{em}}, & \sin^2 \theta_W &= \frac{1}{2} \left(1 - \sqrt{1 - \frac{4\pi\alpha_{\text{em}}}{\sqrt{2}G_F m_Z^2}} \right), \\
 v^2 &= \frac{1}{\sqrt{2}G_F}, & \left(g = \frac{e}{\sin \theta_W}, \quad g' = \frac{e}{\cos \theta_W} \right) & \Big|_{\theta_W, e \text{ as above}}.
 \end{aligned} \tag{4.2}$$

The abbreviations s_θ ($s_{2\theta}$) and c_θ ($c_{2\theta}$) will stand below for $\sin\theta_W$ ($\sin 2\theta_W$) and $\cos\theta_W$ ($\cos 2\theta_W$), respectively. Furthermore, for concreteness, we assume a specific parametrization for the $\mathcal{F}_i(h)$ functions:

$$\mathcal{F}_i(h) \equiv 1 + 2\tilde{a}_i \frac{h}{v} + \tilde{b}_i \frac{h^2}{v^2} + \dots \quad (4.3)$$

where the dots stand for higher powers of h/v that will not be considered in what follows; to further simplify the notation a_i and b_i will indicate below the products $a_i \equiv c_i \tilde{a}_i$ and $b_i \equiv c_i \tilde{b}_i$, respectively, where c_i are the global operator coefficients.

Working in the unitary gauge to analyze the impact that the couplings in $\Delta\mathcal{L}$ in Eq. (2.5) have on \mathcal{L}_0 , it is straightforward to show that $\mathcal{P}_B(h)$, $\mathcal{P}_W(h)$, $\mathcal{P}_G(h)$, $\mathcal{P}_H(h)$, $\mathcal{P}_1(h)$ and $\mathcal{P}_{12}(h)$ introduce corrections to the SM kinetic terms, and in consequence field redefinitions are necessary to obtain canonical kinetic terms. Among these operators, $\mathcal{P}_B(h)$, $\mathcal{P}_W(h)$ and $\mathcal{P}_G(h)$ can be considered innocuous operators with respect to \mathcal{L}_0 , as the impact on the latter of c_B , c_W and c_G can be totally eliminated from the Lagrangian by ineffectual field and coupling constant redefinitions; they do have a physical impact though on certain BSM couplings in $\Delta\mathcal{L}$ involving external scalar fields.

With canonical kinetic terms, it is then easy to identify the contribution of $\Delta\mathcal{L}$ to the input parameters¹¹:

$$\begin{aligned} \frac{\delta\alpha_{\text{em}}}{\alpha_{\text{em}}} &\simeq 4e^2 c_1 \xi + 4e^2 c_{12} \xi^2, & \frac{\delta G_F}{G_F} &\simeq 0, \\ \frac{\delta m_Z}{m_Z} &\simeq -c_T \xi - 2e^2 c_1 \xi + 2e^2 \cot^2 \theta_W c_{12} \xi^2, & \frac{\delta m_h}{m_h} &\simeq 0, \end{aligned} \quad (4.4)$$

keeping only terms linear in the coefficients c_i . Expressing all other SM parameters in $\mathcal{L}_{\text{chiral}}$ in terms of the four input parameters leads to the predictions to be described next.

W mass

The prediction for the W mass departs from the SM expectation by

$$\begin{aligned} \frac{\Delta m_W^2}{m_W^2} &= \frac{4e^2}{c_{2\theta}} c_1 \xi + \frac{2c_\theta^2}{c_{2\theta}} c_T \xi - \frac{4e^2}{s_\theta^2} c_{12} \xi^2 \\ &\equiv \frac{e^2}{2c_{2\theta}} f_{BW} \frac{v^2}{\Lambda^2} - \frac{c_\theta^2}{2c_{2\theta}} f_{\Phi,1} \frac{v^2}{\Lambda^2}, \end{aligned} \quad (4.5)$$

where the second line shows for comparison the corresponding expression in the linear expansion at order $d = 6$.

S and T parameters

$\mathcal{P}_1(h)$ and $\mathcal{P}_T(h)$ generate tree-level contributions to the oblique parameters S and T [100], which read

$$\alpha_{\text{em}} \Delta S = -8e^2 c_1 \xi \quad \text{and} \quad \alpha_{\text{em}} \Delta T = 2c_T \xi. \quad (4.6)$$

¹¹The BSM corrections that enter into the definition of the input parameters will be generically denoted by the sign “ δ ”, while the predicted measurable departures from SM expectations will be indicated below by “ Δ ”.

Triple gauge–boson couplings

The effective operators described in the non-linear Lagrangian, Eqs. (2.6)-(2.8), give rise to triple gauge–boson couplings $\gamma W^+ W^-$ and $Z W^+ W^-$. Following Ref. [4], the CP-even sector of the Lagrangian that describes trilinear gauge boson vertices (TGV) can be parametrized as:

$$\begin{aligned} \mathcal{L}_{WWV} = & - ig_{WWV} \left\{ g_1^V \left(W_{\mu\nu}^+ W^{-\mu} V^\nu - W_\mu^+ V_\nu W^{-\mu\nu} \right) + \kappa_V W_\mu^+ W_\nu^- V^{\mu\nu} \right. \\ & \left. - ig_5^V \epsilon^{\mu\nu\rho\sigma} \left(W_\mu^+ \partial_\rho W_\nu^- - W_\nu^- \partial_\rho W_\mu^+ \right) V_\sigma + g_6^V \left(\partial_\mu W^{+\mu} W^{-\nu} - \partial_\mu W^{-\mu} W^{+\nu} \right) V_\nu \right\}, \end{aligned} \quad (4.7)$$

where $V \equiv \{\gamma, Z\}$ and $g_{WW\gamma} \equiv e = g \sin \theta_W$, $g_{WWZ} = g \cos \theta_W$ (see Eq. (4.2) for their relation to observables). In this equation $W_{\mu\nu}^\pm$ and $V_{\mu\nu}$ stand exclusively for the kinetic part of the gauge field strengths. In contrast with the usual parameterization proposed in Ref. [4], the coefficient λ_V (associated with a linear $d = 6$ operator) is omitted here as this coupling does not receive contributions from the non-linear effective chiral Lagrangian expanded up to four derivatives. Conversely, we have introduced the coefficients g_6^V associated to operators that contain the contraction $\mathcal{D}_\mu \mathbf{V}^\mu$; its $\partial_\mu \mathbf{V}^\mu$ part vanishes only for on-shell gauge bosons; in all generality $\mathcal{D}_\mu \mathbf{V}^\mu$ insertions could only be disregarded¹² in the present context when fermion masses are neglected, as explained in Sect. 2 and App. A.

Electromagnetic gauge invariance requires $g_1^\gamma = 1$ and $g_5^\gamma = 0$, and in consequence the TGV CP-even sector described in Eq. (4.7) depends in all generality on six dimensionless couplings g_1^Z , g_5^Z , $g_6^{\gamma,Z}$ and $\kappa_{\gamma,Z}$. Their SM values are $g_1^Z = \kappa_\gamma = \kappa_Z = 1$ and $g_5^Z = g_6^Z = g_6^\gamma = 0$. Table 1 shows the departures from those SM values due to the effective couplings in Eq. (2.5); it illustrates the ξ and ξ^2 -weighted chiral operator contributions. For the sake of comparison, the corresponding expressions in terms of the coefficients of $d = 6$ operators in the linear expansion are shown as well. A special case is that of the linear operator $\mathcal{O}_{\square\Phi}$, whose physical interpretation is not straightforward [102–104] and will be analyzed in detail in Ref. [105]; the corresponding coefficient $f_{\square\Phi}$ does not appear in Table 1 as contributing to the measurable couplings, while nevertheless the symbol (*) recalls the theoretical link between some chiral operators and their sibling $\mathcal{O}_{\square\Phi}$. The analysis of Table 1 leads as well to relations between measurable quantities, which are collected later on in Eq. (4.14) and subsequent ones.

h couplings to SM gauge-boson pairs

The effective operators described in Eqs. (2.6)-(2.8) also give rise to interactions involving the Higgs and two gauge bosons, to which we will refer as HVV couplings. The latter

¹²See for example Ref. [101] for a general discussion on possible “off-shell” vertices associated to $d = 4$ and $d = 6$ operators.

	Coeff.	Chiral		Linear
	$\times e^2/s_\theta^2$	$\times \xi$	$\times \xi^2$	$\times v^2/\Lambda^2$
$\Delta\kappa_\gamma$	1	$-2c_1 + 2c_2 + c_3$	$-4c_{12} + 2c_{13}$	$\frac{1}{8}(f_W + f_B - 2f_{BW})$
Δg_6^γ	1	$-c_9$	–	(*)
Δg_1^Z	$\frac{1}{c_\theta^2}$	$\frac{s_\theta^2}{4e^2 c_{2\theta}} c_T + \frac{2s_\theta^2}{c_{2\theta}} c_1 + c_3$	–	$\frac{1}{8}f_W + \frac{s_\theta^2}{4c_{2\theta}}f_{BW} - \frac{s_\theta^2}{16e^2 c_{2\theta}}f_{\Phi,1}$
$\Delta\kappa_Z$	1	$\frac{s_\theta^2}{e^2 c_{2\theta}} c_T + \frac{4s_\theta^2}{c_{2\theta}} c_1 - \frac{2s_\theta^2}{c_\theta^2} c_2 + c_3$	$-4c_{12} + 2c_{13}$	$\frac{1}{8}f_W - \frac{s_\theta^2}{8c_\theta^2}f_B + \frac{s_\theta^2}{2c_{2\theta}}f_{BW} - \frac{s_\theta^2}{4e^2 c_{2\theta}}f_{\Phi,1}$
Δg_5^Z	$\frac{1}{c_\theta^2}$	–	c_{14}	–
Δg_6^Z	$\frac{1}{c_\theta^2}$	$s_\theta^2 c_9$	$-c_{16}$	(*)

Table 1: *Effective couplings parametrizing the VW^+W^- vertices defined in Eq. (4.7). The coefficients in the second column are common to both the chiral and linear expansions. In the third and fourth columns the specific contributions from the operators in the chiral Lagrangian are shown. For comparison, the last column exhibits the corresponding contributions from the linear $d = 6$ operators. The star (*) in the last column indicates the link between the chiral operator $\mathcal{P}_9(h)$ and its linear sibling $\mathcal{O}_{\square\Phi}$, without implying a physical impact of the latter on the VW^+W^- observables, as explained in the text and in Ref. [105].*

can be phenomenologically parametrized as

$$\begin{aligned}
\mathcal{L}_{HVV} \equiv & g_{Hgg} G_{\mu\nu}^a G^{a\mu\nu} h + g_{H\gamma\gamma} A_{\mu\nu} A^{\mu\nu} h + g_{HZ\gamma}^{(1)} A_{\mu\nu} Z^\mu \partial^\nu h + g_{HZ\gamma}^{(2)} A_{\mu\nu} Z^{\mu\nu} h \\
& + g_{HZZ}^{(1)} Z_{\mu\nu} Z^\mu \partial^\nu h + g_{HZZ}^{(2)} Z_{\mu\nu} Z^{\mu\nu} h + g_{HZZ}^{(3)} Z_\mu Z^\mu h + g_{HZZ}^{(4)} Z_\mu Z^\mu \square h \\
& + g_{HZZ}^{(5)} \partial_\mu Z^\mu Z_\nu \partial^\nu h + g_{HZZ}^{(6)} \partial_\mu Z^\mu \partial_\nu Z^\nu h \\
& + g_{HWW}^{(1)} (W_{\mu\nu}^+ W^{-\mu} \partial^\nu h + \text{h.c.}) + g_{HWW}^{(2)} W_{\mu\nu}^+ W^{-\mu\nu} h + g_{HWW}^{(3)} W_\mu^+ W^{-\mu} h \\
& + g_{HWW}^{(4)} W_\mu^+ W^{-\mu} \square h + g_{HWW}^{(5)} (\partial_\mu W^{+\mu} W_\nu^- \partial^\nu h + \text{h.c.}) + g_{HWW}^{(6)} \partial_\mu W^{+\mu} \partial_\nu W^{-\nu} h,
\end{aligned} \tag{4.8}$$

where $V_{\mu\nu} = \partial_\mu V_\nu - \partial_\nu V_\mu$ with $V = \{A, Z, W, G\}$. Separating the contributions into SM ones plus corrections,

$$g_i^{(j)} \simeq g_i^{(j)SM} + \Delta g_i^{(j)}, \tag{4.9}$$

it turns out that

$$g_{HZZ}^{(3)SM} = \frac{m_Z^2}{v}, \quad g_{HWW}^{(3)SM} = \frac{2m_Z^2 c_\theta^2}{v}, \tag{4.10}$$

while the tree-level SM value for all other couplings in Eq. (4.8) vanishes (the SM loop-induced value for g_{Hgg} , $g_{H\gamma\gamma}$ and $g_{HZ\gamma}^{(2)}$ will be taken into account in our numerical analysis, though); in these expressions, v is as defined in Eq. (4.2). Table 2 shows the expressions for the corrections Δg_{Hgg} , $\Delta g_{H\gamma\gamma}$, $\Delta g_{HZ\gamma}^{(1,2)}$, $\Delta g_{HWW}^{(1,2,3,4,5,6)}$, and $\Delta g_{HZZ}^{(1,2,3,4,5,6)}$ induced at tree-level by the effective non-linear couplings under discussion. In writing Eq. (4.8) we have introduced the coefficients $\Delta g_{HZZ}^{(4,5,6)}$ and $\Delta g_{HWW}^{(4,5,6)}$: $\Delta g_{HVV}^{(4)}$ become redundant for on-shell h ; $\Delta g_{HVV}^{(5,6)}$ vanish for on-shell W_μ and Z_μ or massless fermions. Notice also that the leading chiral corrections include operators weighted by ξ powers up to ξ^2 . For the sake of

comparison, the corresponding expressions in terms of the coefficients of the linear $d = 6$ operators in Eq. (3.7) are also shown¹³.

	Coeff. $\times e^2/4v$	Chiral		Linear $\times v^2/\Lambda^2$
		$\times \xi$	$\times \xi^2$	
Δg_{Hgg}	$\frac{g^2}{e^2}$	$-2a_G$	—	$-4f_{GG}$
$\Delta g_{H\gamma\gamma}$	1	$-2(a_B + a_W) + 8a_1$	$8a_{12}$	$-(f_{BB} + f_{WW}) + f_{BW}$
$\Delta g_{HZ\gamma}^{(1)}$	$\frac{1}{s_{2\theta}}$	$-8(a_5 + 2a_4)$	$-16a_{17}$	$2(f_W - f_B)$
$\Delta g_{HZ\gamma}^{(2)}$	$\frac{c_\theta}{s_\theta}$	$4\frac{s_\theta^2}{c_\theta^2}a_B - 4a_W + 8\frac{c_{2\theta}}{c_\theta^2}a_1$	$16a_{12}$	$2\frac{s_\theta^2}{c_\theta^2}f_{BB} - 2f_{WW} + \frac{c_{2\theta}}{c_\theta^2}f_{BW}$
$\Delta g_{HZZ}^{(1)}$	$\frac{1}{c_\theta^2}$	$-4\frac{c_\theta^2}{s_\theta^2}a_5 + 8a_4$	$-8\frac{c_\theta^2}{s_\theta^2}a_{17}$	$\frac{c_\theta^2}{s_\theta^2}f_W + f_B$
$\Delta g_{HZZ}^{(2)}$	$-\frac{c_\theta^2}{s_\theta^2}$	$2\frac{s_\theta^4}{c_\theta^4}a_B + 2a_W + 8\frac{s_\theta^2}{c_\theta^2}a_1$	$-8a_{12}$	$\frac{s_\theta^4}{c_\theta^4}f_{BB} + f_{WW} + \frac{s_\theta^2}{c_\theta^2}f_{BW}$
$\Delta g_{HZZ}^{(3)}$	$\frac{m_Z^2}{e^2}$	$-2c_H + 2(2a_C - c_C) - 8(a_T - c_T)$	—	$f_{\Phi,1} + 2f_{\Phi,4} - 2f_{\Phi,2}$
$\Delta g_{HZZ}^{(4)}$	$-\frac{1}{s_{2\theta}^2}$	$16a_7$	$32a_{25}$	(*)
$\Delta g_{HZZ}^{(5)}$	$-\frac{1}{s_{2\theta}^2}$	$16a_{10}$	$32a_{19}$	(*)
$\Delta g_{HZZ}^{(6)}$	$-\frac{1}{s_{2\theta}^2}$	$16a_9$	$32a_{15}$	(*)
$\Delta g_{HWW}^{(1)}$	$\frac{1}{s_\theta^2}$	$-4a_5$	—	f_W
$\Delta g_{HWW}^{(2)}$	$\frac{1}{s_\theta^2}$	$-4a_W$	—	$-2f_{WW}$
$\Delta g_{HWW}^{(3)}$	$\frac{m_Z^2 c_\theta^2}{e^2}$	$-4c_H + 4(2a_C - c_C) + \frac{32e^2}{c_{2\theta}}c_1 + \frac{16c_\theta^2}{c_{2\theta}}c_T$	$-\frac{32e^2}{s_\theta^2}c_{12}$	$-\frac{2(3c_\theta^2 - s_\theta^2)}{c_{2\theta}}f_{\Phi,1} + 4f_{\Phi,4} - 4f_{\Phi,2} + \frac{4e^2}{c_{2\theta}}f_{BW}$
$\Delta g_{HWW}^{(4)}$	$-\frac{1}{s_\theta^2}$	$8a_7$	—	(*)
$\Delta g_{HWW}^{(5)}$	$-\frac{1}{s_\theta^2}$	$4a_{10}$	—	(*)
$\Delta g_{HWW}^{(6)}$	$-\frac{1}{s_\theta^2}$	$8a_9$	—	(*)

Table 2: The trilinear Higgs-gauge bosons couplings defined in Eq. (4.8). The coefficients in the second column are common to both the chiral and linear expansions. The contributions from the operators weighted by ξ and ξ^2 are listed in the third and fourth columns, respectively. For comparison, the last column exhibits the corresponding expressions for the linear expansion at order $d = 6$. The star (*) in the last column indicates the link between the chiral operators $\mathcal{P}_7(h)$, $\mathcal{P}_9(h)$ and $\mathcal{P}_{10}(h)$, and their linear sibling $\mathcal{O}_{\square\Phi}$, without implying a physical impact of the latter on the observables considered, as explained in the text and in Ref. [105].

Notice that the bosonic operators $\mathcal{P}_H(h)$ and $\mathcal{P}_C(h)$ induce universal shifts to the SM-like couplings of the Higgs to weak gauge bosons. Similarly $\mathcal{P}_H(h)$, induces universal shifts to the Yukawa couplings to fermions, see Eq. (FR.32) in Appendix D. It is straightforward

¹³Alternatively the coefficient of $\Delta g_{HWW}^{(3)}$ can be defined in terms of the measured value of M_W as M_W^2/e^2 . In this case the entries in columns 3–5 read $-4c_H + 4(2a_C - c_C)$, $-32\frac{e^2}{s_\theta^2}$, and $-2f_{\Phi,1} + 4f_{\Phi,4} - 4f_{\Phi,2}$ respectively.

to identify the link between the coefficients of these operators and the parameters a and c defined in Refs. [17, 26, 62] assuming custodial invariance, which reads¹⁴

$$a = 1 - \frac{\xi c_H}{2} + \frac{\xi(2a_C - c_C)}{2}, \quad c = s_Y \left(1 - \frac{\xi c_H}{2}\right). \quad (4.11)$$

Quartic gauge–boson couplings

The quartic gauge boson couplings also receive contributions from the operators in Eqs. (2.6)-(2.8). The corresponding effective Lagrangian reads

$$\begin{aligned} \mathcal{L}_{4X} \equiv g^2 \left\{ & g_{ZZ}^{(1)}(Z_\mu Z^\mu)^2 + g_{WW}^{(1)} W_\mu^+ W^{+\mu} W_\nu^- W^{-\nu} - g_{WW}^{(2)}(W_\mu^+ W^{-\mu})^2 \right. \\ & + g_{VV'}^{(3)} W^{+\mu} W^{-\nu} (V_\mu V'_\nu + V'_\mu V_\nu) - g_{VV'}^{(4)} W_\nu^+ W^{-\nu} V^\mu V'_\mu \\ & \left. + i g_{VV'}^{(5)} \varepsilon^{\mu\nu\rho\sigma} W_\mu^+ W_\nu^- V_\rho V'_\sigma \right\}, \end{aligned} \quad (4.12)$$

where $VV' = \{\gamma\gamma, \gamma Z, ZZ\}$. Notice that all these couplings are C and P even, except for $g_{VV'}^{(5)}$ that is CP even but both C and P odd. Some of these couplings are nonvanishing at tree-level in the SM:

$$\begin{aligned} g_{WW}^{(1)SM} &= \frac{1}{2}, & g_{WW}^{(2)SM} &= \frac{1}{2}, & g_{ZZ}^{(3)SM} &= \frac{c_\theta^2}{2}, & g_{\gamma\gamma}^{(3)SM} &= \frac{s_\theta^2}{2}, \\ g_{Z\gamma}^{(3)SM} &= \frac{s_{2\theta}}{2}, & g_{ZZ}^{(4)SM} &= c_\theta^2, & g_{\gamma\gamma}^{(4)SM} &= s_\theta^2, & g_{Z\gamma}^{(4)SM} &= s_{2\theta}, \end{aligned} \quad (4.13)$$

where the notation defined in Eq. (4.9) has been used and the expression for the weak mixing angle can be found in Eq. (4.2). Table 3 shows the contributions to the effective quartic couplings from the chiral operators in Eqs. (2.6)-(2.8) and from the linear operator in Eq. (3.3).

(De)correlation formulae

Some operators of the non-linear Lagrangian in Sect. 2 participate in more than one of the couplings in Tables 1 and 2. This fact leads to interesting series of relations that relate different couplings. First, simple relations on the TGV sector results:

$$\Delta\kappa_Z + \frac{s_\theta^2}{c_\theta^2} \Delta\kappa_\gamma - \Delta g_1^Z = \frac{16e^2}{s_\theta^2} (2c_{12} - c_{13}) \xi^2, \quad (4.14)$$

$$\Delta g_6^\gamma + \frac{c_\theta^2}{s_\theta^2} \Delta g_6^Z = -\frac{e^2}{s_\theta^4} c_{16} \xi^2, \quad (4.15)$$

¹⁴Supplementary terms are present when taking into account the custodial breaking couplings considered in this paper.

	Coeff. $\times e^2/4s_\theta^2$	Chiral		Linear
		$\times \xi$	$\times \xi^2$	$\times v^2/\Lambda^2$
$\Delta g_{WW}^{(1)}$	1	$\frac{s_{2\theta}^2}{e^2 c_{2\theta}} c_T + \frac{8s_\theta^2}{c_{2\theta}} c_1 + 4c_3$	$2c_{11} - 16c_{12} + 8c_{13}$	$\frac{f_W}{2} + \frac{s_\theta^2}{c_{2\theta}} f_{BW} - \frac{s_{2\theta}^2}{4c_{2\theta} e^2} f_{\Phi 1}$
$\Delta g_{WW}^{(2)}$	1	$\frac{s_{2\theta}^2}{e^2 c_{2\theta}} c_T + \frac{8s_\theta^2}{c_{2\theta}} c_1 + 4c_3 - 4c_6$	$-2c_{11} - 16c_{12} + 8c_{13}$	$\frac{f_W}{2} + \frac{s_\theta^2}{c_{2\theta}} f_{BW} - \frac{s_{2\theta}^2}{4c_{2\theta} e^2} f_{\Phi 1} + (*)$
$\Delta g_{ZZ}^{(1)}$	$\frac{1}{c_\theta^4}$	c_6	$c_{11} + 2c_{23} + 2c_{24} + 4c_{26}\xi^2$	$(*)$
$\Delta g_{ZZ}^{(3)}$	$\frac{1}{c_\theta^2}$	$\frac{s_{2\theta}^2 c_\theta^2}{e^2 c_{2\theta}} c_T + \frac{2s_{2\theta}^2}{c_{2\theta}} c_1 + 4c_\theta^2 c_3 - 2s_\theta^4 c_9$	$2c_{11} + 4s_\theta^2 c_{16} + 2c_{24}$	$\frac{f_W c_\theta^2}{2} + \frac{s_{2\theta}^2}{4c_{2\theta}} f_{BW} - \frac{s_{2\theta}^2 c_\theta^2}{4e^2 c_{2\theta}} f_{\Phi 1} + (*)$
$\Delta g_{ZZ}^{(4)}$	$\frac{1}{c_\theta^2}$	$\frac{2s_{2\theta}^2 c_\theta^2}{e^2 c_{2\theta}} c_T + \frac{4s_{2\theta}^2}{c_{2\theta}} c_1 + 8c_\theta^2 c_3 - 4c_6$	$-4c_{23}$	$f_W c_\theta^2 + 2\frac{s_{2\theta}^2}{4c_{2\theta}} f_{BW} - \frac{s_{2\theta}^2 c_\theta^2}{2e^2 c_{2\theta}} f_{\Phi 1} + (*)$
$\Delta g_{\gamma\gamma}^{(3)}$	s_θ^2	$-2c_9$	$-$	$(*)$
$\Delta g_{\gamma Z}^{(3)}$	$\frac{s_\theta}{c_\theta}$	$\frac{s_{2\theta}^2}{e^2 c_{2\theta}} c_T + \frac{8s_\theta^2}{c_{2\theta}} c_1 + 4c_3 + 4s_\theta^2 c_9$	$-4c_{16}$	$\frac{f_W}{2} + \frac{s_\theta^2}{c_{2\theta}} f_{BW} - \frac{s_{2\theta}^2}{4c_{2\theta} e^2} f_{\Phi 1} + (*)$
$\Delta g_{\gamma Z}^{(4)}$	$\frac{s_\theta}{c_\theta}$	$\frac{2s_{2\theta}^2}{e^2 c_{2\theta}} c_T + \frac{16s_\theta^2}{c_{2\theta}} c_1 + 8c_3$	$-$	$f_W + 2\frac{s_\theta^2}{c_{2\theta}} f_{BW} - \frac{s_{2\theta}^2}{2c_{2\theta} e^2} f_{\Phi 1}$
$\Delta g_{\gamma Z}^{(5)}$	$\frac{s_\theta}{c_\theta}$	$-$	$8c_{14}$	$-$

Table 3: *Effective couplings parametrizing the vertices of four gauge bosons defined in Eq. (4.12). The contributions from the operators weighted by ξ and $\xi^{\geq 2}$ are listed in the third and fourth columns, respectively. For comparison, the last column exhibits the corresponding expressions for the linear expansion at order $d = 6$. The star (*) in the last column indicates the link between the chiral operators $\mathcal{P}_6(h)$ and $\mathcal{P}_9(h)$, and their linear sibling $\mathcal{O}_{\square\Phi}$, without implying a physical impact of the latter on the observables considered, as explained in the text and in Ref. [105].*

while other examples of relations involving HVV couplings are:

$$g_{HWW}^{(1)} - c_\theta^2 g_{HZZ}^{(1)} - c_\theta s_\theta g_{HZ\gamma}^{(1)} = \frac{2e^2}{vs_\theta^2} a_{17} \xi^2, \quad (4.16)$$

$$2c_\theta^2 g_{HZZ}^{(2)} + 2s_\theta c_\theta g_{HZ\gamma}^{(2)} + 2s_\theta^2 g_{H\gamma\gamma} - g_{HWW}^{(2)} = \frac{4e^2}{vs_\theta^2} a_{12} \xi^2, \quad (4.17)$$

$$\Delta g_{HZZ}^{(4)} - \frac{1}{2c_\theta^2} \Delta g_{HWW}^{(4)} = -\frac{8e^2}{vs_{2\theta}^2} a_{25} \xi^2, \quad (4.18)$$

$$\Delta g_{HZZ}^{(5)} - \frac{1}{c_\theta^2} \Delta g_{HWW}^{(5)} = -\frac{8e^2}{vs_{2\theta}^2} a_{19} \xi^2, \quad (4.19)$$

$$\Delta g_{HZZ}^{(6)} - \frac{1}{2c_\theta^2} \Delta g_{HWW}^{(6)} = -\frac{8e^2}{vs_{2\theta}^2} a_{15} \xi^2. \quad (4.20)$$

The non-vanishing terms on the right-hand side of Eqs. (4.14)-(4.17) stem from ξ^2 -weighted terms in the non-linear Lagrangian. It is interesting to note that they would vanish in the

following cases: i) the $d = 6$ linear limit¹⁵; ii) in the ξ -truncated non-linear Lagrangian; iii) in the custodial preserving limit. The first two relations with a vanishing right-hand side were already found in Ref. [33]. Any hypothetical deviation from zero in the data combinations indicated by the left-hand side of those equations would thus be consistent with either $d = 8$ corrections of the linear expansion or a non-linear realisation of the underlying dynamics.

Furthermore, we found an interesting correlation which only holds in the linear regime at order $d = 6$, mixes TGV and HVV couplings, and stems from comparing Tables 1 and 2:

$$\Delta\kappa_Z - \Delta g_1^Z = \frac{vs_\theta}{2c_\theta} \left[(c_\theta^2 - s_\theta^2) \left(g_{HZ\gamma}^{(1)} + 2g_{HZ\gamma}^{(2)} \right) + 2s_\theta c_\theta \left(2g_{H\gamma\gamma} - g_{HZZ}^{(1)} - 2g_{HZZ}^{(2)} \right) \right]. \quad (4.21)$$

This relation does not hold in the non-linear regime, not even when only ξ -weighted operators are considered. Its verification from experimental data would be an excellent test of BSM physics in which the EWSB is linearly realized and dominated by $d = 6$ corrections.

The above general (de)correlations are a few examples among many [68].

When in addition the strong experimental constraints on the S and T parameters are applied, disregarding thus c_T and c_1 (equivalently, $f_{\phi 1}$ and f_{BW} for the linear case), supplementary constraints follow, *e.g.*:

$$\begin{aligned} \frac{2}{m_Z^2} g_{HZZ}^{(3)} - \frac{1}{m_W^2 + \delta m_W^2} g_{HWW}^{(3)} &= \frac{16e^2}{v s_\theta^2} a_{12} \xi^2, \\ 2g_{H\gamma\gamma} + \frac{c_\theta}{s_\theta} g_{HZ\gamma}^{(2)} - g_{HWW}^{(2)} &= -\frac{4e^2}{v s_\theta^2} a_{12} \xi^2, \\ 2g_{HZZ}^{(2)} + \frac{s_\theta}{c_\theta} g_{HZ\gamma}^{(2)} - g_{HWW}^{(2)} &= -\frac{4e^2}{v s_\theta^2} a_{12} \xi^2, \\ \frac{-2s_\theta^2}{c_\theta^2 - s_\theta^2} g_{H\gamma\gamma} + \frac{2c_\theta^2}{c_\theta^2 - s_\theta^2} g_{HZZ}^{(2)} - g_{HWW}^{(2)} &= -\frac{4e^2}{v s_\theta^2} a_{12} \xi^2. \end{aligned} \quad (4.22)$$

where again the non-zero entries on the right-hand sides vanish in either the $d = 6$ linear or the ξ -truncated non-linear limits.

Counting of degrees of freedom for the HVV Lagrangian

Given the present interest in the gauge- h sector, we analyze here the number of degrees of freedom involved in the HVV Lagrangian, Eq. (4.8), for on-shell and off-shell gauge and Higgs bosons, with massive and massless fermions.

This can be schematically resumed as follows: for the massive fermion case,

$$\begin{array}{llll} \text{phen. couplings:} & 16 & \xrightarrow{\text{i)}} & 12 \ (\Delta g_{HVV}^{5,6} = 0) & \xrightarrow{\text{ii)}} & 10 \ (\Delta g_{HVV}^4 \text{ redundant}) \\ \text{op. coefficients:} & 17 & \xrightarrow{\text{i)}} & 13 \ (\mathcal{P}_{11}, \mathcal{P}_{12}, \mathcal{P}_{16}, \mathcal{P}_{17} \text{ irrelevant}) & \xrightarrow{\text{ii)}} & 11 \ (\mathcal{P}_7, \mathcal{P}_{25} \text{ redundant}) \end{array}$$

¹⁵Eq. (4.14) with vanishing right-hand side was already known [76, 106] to hold in the linear regime at order $d = 6$.

where the first line refers to the phenomenological couplings appearing in Eq. (4.8), while the second one to the operator coefficients of the non-linear basis in Eq. (2.5). Moreover, i) denotes the limit of on-shell gauge bosons, i.e. $\partial^\mu Z_\mu = 0$ and $\partial^\mu W_\mu^\pm = 0$, while ii) refers to the limit of, in addition, on-shell h . In brackets we indicate the couplings and the operator coefficients that are irrelevant for redundant under the conditions i) or ii).

If fermion masses are set to zero, the conditions $\partial^\mu Z_\mu = 0$ and $\partial^\mu W_\mu^\pm = 0$ hold also for off-shell gauge bosons, and therefore the counting starts with 12 phenomenological couplings and 13 operator coefficients.

This analysis for the number of operator coefficients refers to the full non-linear Lagrangian in Eq. (2.5), which includes the custodial breaking operators.

Up to this point, as well as in Apps. A, C and D for the EOM, $d = 6$ siblings and Feynman rules, respectively, all non-linear pure gauge and gauge- h operators of the chiral Lagrangian Eq. (2.1) have been taken into account. The next subsection describes the results of the numerical analysis, and there instead the value of fermion masses on external legs will be neglected. This means that operators $\mathcal{P}_9(h)$, $\mathcal{P}_{10}(h)$, $\mathcal{P}_{15}(h)$, $\mathcal{P}_{16}(h)$, and $\mathcal{P}_{19-21}(h)$ become redundant then, and will not be analyzed.

4.2 Present bounds on operators weighted by ξ

At present, the most precise determination of S , T , U from a global fit to electroweak precision data (EWPD) yields the following values and correlation matrix [99]

$$\Delta S = 0.00 \pm 0.10 \quad \Delta T = 0.02 \pm 0.11 \quad \Delta U = 0.03 \pm 0.09 \quad (4.23)$$

$$\rho = \begin{pmatrix} 1 & 0.89 & -0.55 \\ 0.89 & 1 & -0.8 \\ -0.55 & -0.8 & 1 \end{pmatrix}. \quad (4.24)$$

Operators $\mathcal{P}_1(h)$ and $\mathcal{P}_T(h)$ contribute at tree-level to these observables, see Eq. (4.6) and consequently they are severely constrained. The corresponding 95% CL allowed ranges for their coefficients read

$$-4.7 \times 10^{-3} \leq \xi c_1 \leq 4 \times 10^{-3} \quad \text{and} \quad -2 \times 10^{-3} \leq \xi c_T \leq 1.7 \times 10^{-3}. \quad (4.25)$$

These constraints render the contribution of $\mathcal{P}_1(h)$ and $\mathcal{P}_T(h)$ to the gauge-boson self-couplings and to the present Higgs data too small to give any observable effect. Consequently we will not include them in the following discussion.

As for the ξ -weighted TGV contributions from $\mathcal{P}_2(h)$ and $\mathcal{P}_3(h)$, their impact on the coefficients $\Delta\kappa_\gamma$, Δg_1^Z and $\Delta\kappa_Z$ was described in Table 1. At present, the most precise determination of TGV in this scenario results from the two-dimensional analysis in Ref. [107] which was performed in terms of $\Delta\kappa_\gamma$ and Δg_1^Z with $\Delta\kappa_Z$ determined by the relation Eq. (4.14) with the right-handed side set to zero:

$$\kappa_\gamma = 0.984_{-0.049}^{+0.049} \quad \text{and} \quad g_1^Z = 1.004_{-0.025}^{+0.024}, \quad (4.26)$$

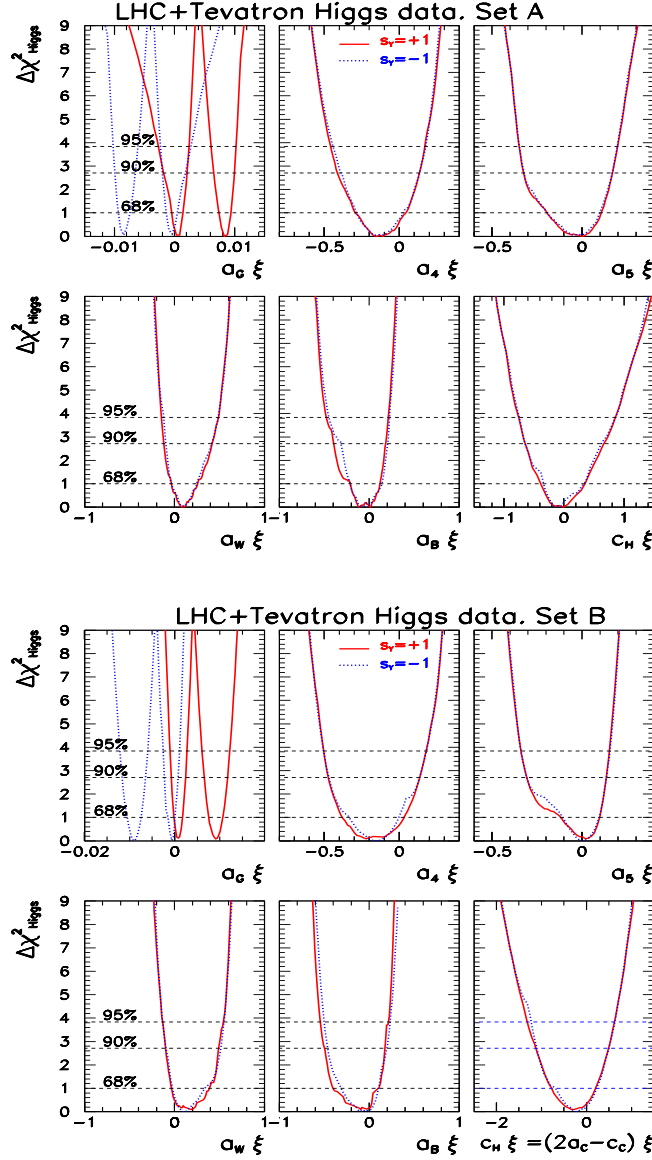


Figure 1: $\Delta\chi_{\text{Higgs}}^2$ dependence on the coefficients of the seven bosonic operators in Eq. (4.27) from the analysis of all Higgs collider (ATLAS, CMS and Tevatron) data. In each panel, we marginalized over the five undisplayed variables. The six upper (lower) panels corresponds to analysis with set **A** (**B**). In each panel the red solid (blue dotted) line stands for the analysis with the discrete parameter $s_Y = +(-)$.

with a correlation factor $\rho = 0.11$. In Table 4 we list the corresponding 90% CL allowed ranges on the coefficients c_2 and c_3 from the analysis of the TGV data.

Now, let us focus on the constraints on ξ -weighted operators stemming from the presently available Higgs data on HVV couplings. There are seven bosonic operators in

this category ¹⁶

$$\mathcal{P}_G(h), \mathcal{P}_4(h), \mathcal{P}_5(h), \mathcal{P}_B(h), \mathcal{P}_W(h), \mathcal{P}_H(h), \mathcal{P}_C(h). \quad (4.27)$$

To perform a seven-parameter fit to the present Higgs data is technically beyond the scope of this paper and we will consider sets of “only” six of them simultaneously. We are presenting below two such analysis. Leaving out a different coupling in each set. In the first one, **A**, we will neglect $\mathcal{P}_C(h)$ and in the second one, **B**, we will link its contribution to that of $\mathcal{P}_H(h)$, so the 6 parameters in each set read:

$$\text{Set A :} \quad a_G, a_4, a_5, a_B, a_W, c_H, 2a_C - c_C = 0, \quad (4.28)$$

$$\text{Set B :} \quad a_G, a_4, a_5, a_B, a_W, c_H = 2a_C - c_C. \quad (4.29)$$

For both sets we will explore the sensitivity of the results to the sign of the h -fermion couplings by performing analysis with both values of the discrete parameter $s_Y = \pm$.

As mentioned above, $\mathcal{P}_H(h)$ and $\mathcal{P}_C(h)$ induce a universal shift to the SM-like HVV couplings involving electroweak gauge bosons, see Eq. (FR.15) and (FR.17), while $\mathcal{P}_H(h)$ also induces a universal shift to the Yukawa Higgs-fermion couplings, see Eq. (FR.32). In consequence, the two sets above correspond to the case in which the shift of the Yukawa Higgs-fermion couplings is totally unrelated to the modification of the HVV couplings involving electroweak bosons (**set B**), and to the case in which the shift of SM-like HVV couplings involving electroweak bosons and to the Yukawa Higgs-fermion couplings are the same (**set A**). In both sets we keep all other five operators which induce modifications of the HVV couplings with different Lorentz structures than those of the SM as well as tree-level contributions to the loop-induced vertices $h\gamma\gamma$, $h\gamma Z$ and hgg .

Notice also that a combination of $\mathcal{P}_H(h)$ and $\mathcal{P}_C(h)$ can be traded via the EOM (see third line in Eq. (A.11)) by that of fermion-Higgs couplings $\mathcal{P}_{f,\alpha\beta}(h)$ plus that of other operators already present in the six-dimensional gauge- h set analyzed. So our choice allows us to stay close to the spirit of this work (past and future data confronting directly the gauge and gauge- h sector), while performing a powerful six-dimensional exploration of possible correlations.

Technically, in order to obtain the present constraints on the coefficients of the bosonic operators listed in Eqs. (4.28) and (4.29) we perform a chi-square test using the available data on the signal strengths (μ). We took into account data from Tevatron D0 and CDF Collaborations and from LHC, CMS, and ATLAS Collaborations at 7 TeV and 8 TeV for final states $\gamma\gamma$, W^+W^- , ZZ , $Z\gamma$, $b\bar{b}$, and $\tau\bar{\tau}$ [108–121]. For CMS and ATLAS data, the included results on W^+W^- , ZZ and $Z\gamma$ correspond to leptonic final states, while for $\gamma\gamma$ all the different categories are included which in total accounts for 56 data points. We refer the reader to Refs. [9, 78] for details of the Higgs data analysis.

The results of the analysis are presented in Fig. 1 which displays the chi-square ($\Delta\chi_{\text{Higgs}}^2$) dependence from the analysis of the Higgs data on the six bosonic couplings for the two sets **A** and **B** of operators and for the two values of the discrete parameter $s_Y = \pm$. In

¹⁶ In present Higgs data analysis, the Higgs state is on-shell and in this case $\Delta g_{HVV}^{(4)}$ can be recasted as a m_H^2 correction to $\Delta g_{HVV}^{(3)}$. Thus the contribution from c_7 , i.e. the coefficient of $\mathcal{P}_7(h)$ to the Higgs observables, can be reabsorbed in a redefinition of $2a_C - c_C$.

each panel $\Delta\chi_{\text{Higgs}}^2$ is shown after marginalizing over the other five parameters. As seen in this figure, there are no substantial difference between both sets in the determination of the five common parameters with only slight differences in a_G (more below). The quality of the fit is equally good for both sets ($|\chi_{\text{min,A}}^2 - \chi_{\text{min,B}}^2| < 0.5$). The SM lays at $\chi_{SM}^2 = 68.1$ within the 4% CL region in the six dimensional parameter space of either set.

In Fig. 1, for each set, the two curves of $\Delta\chi_{\text{Higgs}}^2$ for $s_Y = \pm$ are defined with respect to the same χ_{min}^2 corresponding to the minimum value of the two signs. However, as seen in the figure, the difference is inappreciable. In other words, we find that in both six-parameter analysis the quality of the description of the data is equally good for both signs of the h -fermion couplings. Quantitatively for either set $|\chi_{\text{min,+}}^2 - \chi_{\text{min,-}}^2|$ is compatible with zero within numerical accuracy. If all the anomalous couplings are set to zero the quality of the fit is dramatically different for both signs with $\chi_-^2 - \chi_+^2 = 26$. This arises from the different sign of the interference between the W - and top-loop contributions to $h\gamma\gamma$ which is negative for the SM value $s_Y = +$ and positive for $s_Y = -$ which increases $BR_-(h \rightarrow \gamma\gamma)/BR_{SM}(h \rightarrow \gamma\gamma) \sim 2.5$, a value strongly disfavoured by data. However, once the effect of the 6 bosonic operators is included – in particular that of $\mathcal{P}_B(h)$ and $\mathcal{P}_W(h)$ which give a tree-level contribution to the $h\gamma\gamma$ vertex – we find that both signs of the h -fermion couplings are equally probable.

In the figure we also see that in all cases $\Delta\chi_{\text{Higgs}}^2$ as a function of a_G exhibits two degenerate minima. They are due to the interference between SM and anomalous contributions possessing exactly the same momentum dependence. Around the secondary minimum the anomalous contribution is approximately twice the one due to the top-loop but with an opposite sign. The gluon fusion Higgs production cross section is too depleted for a_G values between the minima, giving rise to the intermediate barrier. Obviously the allowed values of a_G around both minima are different for $s_Y = +$ and $s_Y = -$ as a consequence of the different relative sign of the a_G and the top-loop contributions to the hgg vertex. In the convention chosen for the chiral Lagrangian, the relative sign of both contributions is negative (positive) for $s_Y = +$, ($s_Y = -$) so that the non-zero minimum occurs for a_G around 0.01 (-0.01). The precise value of the a_G coupling at the minima is slightly different for the analysis with set **A** and **B** due to the effect of the coefficient c_H near the minima, which shifts the contribution of the top-loop by a slightly different quantity in both analysis.

Fig. 1 also shows that in all cases the curves for a_4 and a_5 are almost “mirror symmetric”. This is due to the strong anticorrelation between those two coefficients, because they are the dominant contributions to the Higgs branching ratio into two photons, which is proportional to $a_4 + a_5$. In Table 4 we list the corresponding 90% CL allowed ranges for the six coefficients, for the different variants of the analysis. With the expected uncertainties attainable in the Higgs signal strengths in CMS and ATLAS at 14 TeV with an integrated luminosity of 300 fb^{-1} [122, 123], we estimate that the sensitivity to those couplings can improve by a factor $\mathcal{O}(3 - 5)$ with a similar analysis.

We finish by stressing that in the context of ξ -weighted operators in the chiral expansion the results from TGV analysis and those from the HVV analysis apply to two independent sets of operators as discussed in Sec. 3.2. This is unlike the case of the linear expansion for which $2c_2 = a_4$ and $2c_3 = -a_5$, which establishes an interesting complementarity in the experimental searches for new signals in TGV and HVV couplings in the linear regime [78].

90% CL allowed range		
	Set A	Set B
$a_G \xi (\cdot 10^{-3})$	$s_Y = +1: [-1.8, 2.1] \cup [6.5, 10]$ $s_Y = -1: [-9.9, -6.5] \cup [-2.1, 1.8]$	$s_Y = +1: [-0.78, 2.4] \cup [6.5, 12]$ $s_Y = -1: [-12, -6.5] \cup [-2.3, 0.75]$
$a_4 \xi$	[-0.47, 0.14]	
$a_5 \xi$	[-0.33, 0.17]	
$a_W \xi$	[-0.12, 0.51]	
$a_B \xi$	[-0.50, 0.21]	
$c_H \xi$	[-0.66, 0.66]	[-1.1, 0.49]
$c_2 \xi$	[-0.12, 0.076]	
$c_3 \xi$	[-0.064, 0.079]	

Table 4: 90% CL allowed ranges of the coefficients of the operators contributing to Higgs data (a_G , a_4 , a_5 , a_W , a_B , and c_H) and to TGV (c_2 and c_3). For the coefficients a_4 , a_5 , a_W , and a_B , for which the range is almost the same for analysis with both sets and both values of s_Y we show the inclusive range of the four analysis. For c_H the allowed range is the same for both signs of s_Y .

Conversely, in the event of some anomalous observation in either of these two sectors, the presence of this (de)correlation would allow for direct testing of the nature of the Higgs boson. This is illustrated in Fig. 2, where the results of the combined analysis of the TGV and HVV data are projected into combinations of the coefficients of the operators $\mathcal{P}_2(h)$, $\mathcal{P}_3(h)$, $\mathcal{P}_4(h)$ and $\mathcal{P}_5(h)$:

$$\begin{aligned}
\Sigma_B &\equiv 4(2c_2 + a_4), & \Sigma_W &\equiv 2(2c_3 - a_5), \\
\Delta_B &\equiv 4(2c_2 - a_4), & \Delta_W &\equiv 2(2c_3 + a_5),
\end{aligned}
\tag{4.30}$$

defined such that at order $d = 6$ of the linear regime $\Sigma_B = c_B$, $\Sigma_W = c_W$, while $\Delta_B = \Delta_W = 0$. With these variables, the $(0, 0)$ coordinate corresponds to the SM in Fig. 2 left panel, while in Fig. 2 right panel it corresponds to the linear regime (at order $d = 6$). Would future data point to a departure from $(0, 0)$ in the variables of the first figure it would indicate BSM physics irrespective of the linear or non-linear character of the underlying dynamics; while such a departure in the second figure would be consistent with a non-linear realization of EWSB. For concreteness the figures are shown for the $s_Y = +$ analysis with set **A**, but very similar results hold for the other variants of the analysis.

4.3 ξ^2 -weighted couplings: LHC potential to study g_5^Z

One interesting property of the ξ^2 -chiral Lagrangian is the presence of operator $\mathcal{P}_{14}(h)$ that generates a non-vanishing g_5^Z TGV, which is a C and P odd, but CP even operator;

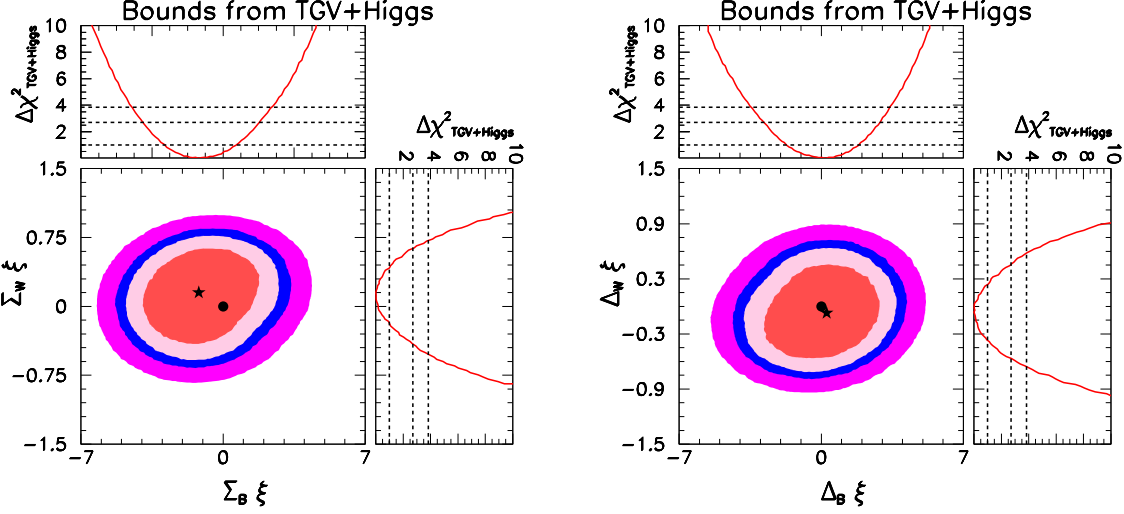


Figure 2: **Left:** A BSM sensor irrespective of the type of expansion: constraints from TGV and Higgs data on the combinations $\Sigma_B = 4(2c_2 + a_4)$ and $\Sigma_W = 2(2c_3 - a_5)$, which converge to f_B and f_W in the linear $d = 6$ limit. The dot at $(0, 0)$ signals the SM expectation. **Right:** A non-linear versus linear discriminator: constraints on the combinations $\Delta_B = 4(2c_2 - a_4)$ and $\Delta_W = 2(2c_3 + a_5)$, which would take zero values in the linear (order $d = 6$) limit (as well as in the SM), indicated by the dot at $(0, 0)$. For both figures the lower left panels shows the 2-dimensional allowed regions at 68%, 90%, 95%, and 99% CL after marginalization with respect to the other six parameters ($a_G, a_W, a_B, c_H, \Delta_B,$ and Δ_W) and ($a_G, a_W, a_B, c_H, \Sigma_B,$ and Σ_W) respectively. The star corresponds to the best fit point of the analysis. The upper left and lower right panels give the corresponding 1-dimensional projections over each of the two combinations.

see Eq. (4.7). Presently, the best direct limits on this anomalous coupling come from the study of W^+W^- pairs and single W production at LEP II energies [124–126]. Moreover, the strongest bounds on g_5^Z originate from its impact on radiative corrections to Z physics [127–129]; see Table 5 for the available direct and indirect limits on g_5^Z .

We can use the relation in Table 1 to translate the existing bounds on g_5^Z into limits on $\mathcal{P}_{14}(h)$. The corresponding limits can be seen in the last column of Table 5. We note here that these limits were obtained assuming only a non-vanishing g_5^Z while the rest of anomalous TGV were set to their corresponding SM value.

At present, the LHC collaborations have presented some data analyses of anomalous TGV [130–134] but in none of them have they included the effects of g_5^Z . A preliminary study on the potential of LHC 7 to constrain this coupling was presented in Ref. [135] where it was shown that the LHC 7 with a very modest luminosity had the potential of probing g_5^Z at the level of the present indirect bounds. In Ref. [135] it was also discussed the use of some kinematic distributions to characterize the presence of a non-vanishing g_5^Z . So far the LHC has already collected almost 25 times more data than the luminosity considered in this preliminary study which we update here. Furthermore, in this update we take advantage of a more realistic background evaluation, by using the results of the

experimental LHC analysis on other anomalous TGV couplings [130].

At the LHC, the anomalous coupling g_5^Z contributes to WW and WZ pair production, with the strongest limits originating from the last reaction [135]. Hence, the present study is focused on the WZ production channel, where we consider only the leptonic decays of the gauge bosons for a better background suppression, *i.e.*, we analyze the reaction

$$pp \rightarrow \ell'^{\pm} \ell^+ \ell^- E_T^{miss}, \quad (4.31)$$

where $\ell^{(\prime)} = e$ or μ . The main background for the g_5^Z analysis is the irreducible SM production of WZ pairs. There are further reducible backgrounds like W or Z production with jets, ZZ production followed by the leptonic decay of the Z 's with one charged lepton escaping detection and $t\bar{t}$ pair production.

We simulated the signal and the SM irreducible background using an implementation of the anomalous operator g_5^Z in FeynRules [136] interfaced with MadGraph 5 [137] for event generation. We account for the different detection efficiencies by rescaling our simulation to the one done by ATLAS [130] for the study of $\Delta\kappa_Z$, g_1^Z and λ_Z . However, we also cross checked the results using a setup where the signal simulation is based on the same FeynRules [136] and MadGraph5 [137] implementation, interfaced then with PYTHIA [138] for parton shower and hadronization and with PGS 4 [139] for detector simulation. Finally, the reducible backgrounds for the 7 TeV analysis were obtained from the simulations presented in the ATLAS search [130], and they were properly rescaled for the 8 TeV and 14 TeV runs.

In order to make our simulations more realistic, we closely follow the TGV analysis performed by ATLAS [130]. Thus, the kinematic study of the WZ production starts with the usual detection and isolation cuts on the final state leptons. Muons are considered if their transverse momentum with respect to the collision axis z , $p_T \equiv \sqrt{p_x^2 + p_y^2}$, and

	Measurement ($\pm 68\%$ CL region)	95% CL region	
Experiment	g_5^Z	g_5^Z	$c_{14}\xi^2$
OPAL [124]	$-0.04_{-0.12}^{+0.13}$	$[-0.28, 0.21]$	$[-0.16, 0.12]$
L3 [125]	$0.00_{-0.13}^{+0.13}$	$[-0.21, 0.20]$	$[-0.12, 0.11]$
ALEPH [126]	$-0.064_{-0.13}^{+0.13}$	$[-0.317, 0.19]$	$[-0.18, 0.11]$
90% CL region from indirect bounds [127–129]		$g_5^Z: [-0.08, 0.04]$	$c_{14}\xi^2: [-0.04, 0.02]$

Table 5: *Existing direct measurements of g_5^Z coming from LEP analyses [124–126] as well as the strongest constraints from the existing indirect bounds on g_5^Z in the literature [127–129]. In the last column we show the translated bounds on $c_{14}\xi^2$. These bounds were obtained assuming only g_5^Z different from zero while the rest of anomalous TGV were set to the SM values.*

pseudorapidity $\eta \equiv \frac{1}{2} \ln \frac{|\vec{p}|+p_z}{|\vec{p}|-p_z}$, satisfy

$$p_T^\ell > 15 \text{ GeV} , |\eta^\mu| < 2.5 . \quad (4.32)$$

Electrons must comply with the same transverse momentum requirement than that applied to muons; however, the electron pseudo-rapidity cut is

$$|\eta^e| < 1.37 \text{ or } 1.52 < |\eta^e| < 2.47 . \quad (4.33)$$

To guarantee the isolation of muons (electrons), we required that the scalar sum of the p_T of the particles within $\Delta R \equiv \sqrt{\Delta\eta^2 + \Delta\phi^2} = 0.3$ of the muon (electron), excluding the muon (electron) track, is smaller than 15% (13%) of the charged lepton p_T . In the case where the final state contains both muons and electrons, a further isolation requirement has been imposed:

$$\Delta R_{e\mu} > 0.1 . \quad (4.34)$$

It was also required that at least two leptons with the same flavour and opposite charge are present in the event and that their invariant mass is compatible with the Z mass, *i.e.*

$$M_{\ell^+\ell^-} \in [M_Z - 10, M_Z + 10] \text{ GeV} . \quad (4.35)$$

A further constraint imposed is that a third lepton is present which passes the above detection requirements and whose transverse momentum satisfies

$$p_T^\ell > 20 \text{ GeV} . \quad (4.36)$$

Moreover, with the purpose of suppressing most of the Z +jets and other diboson production background, we required

$$E_T^{\text{miss}} > 25 \text{ GeV and } M_T^W > 20 \text{ GeV} , \quad (4.37)$$

where E_T^{miss} is the missing transverse energy and the transverse mass is defined as

$$M_T^W = \sqrt{2p_T^\ell E_T^{\text{miss}} (1 - \cos(\Delta\phi))} , \quad (4.38)$$

with p_T^ℓ being the transverse momentum of the third lepton, and where $\Delta\phi$ is the azimuthal angle between the missing transverse momentum and the third lepton. Finally, it was required that at least one electron or one muon has a transverse momentum complying with

$$p_T^{e(\mu)} > 25 \text{ (20) GeV} . \quad (4.39)$$

Our Monte Carlo simulations have been tuned to the ATLAS ones [130], so as to incorporate more realistic detection efficiencies. Initially, a global k -factor was introduced to account for the higher order corrections to the process in Eq. (4.31) by comparing our leading order prediction to the NLO one used in the ATLAS search [130], leading to

$k \sim 1.7$. Next, we compared our results after cuts with the ones quoted by ATLAS in Table 1 of Ref. [130]. We tuned our simulation by applying a correction factor per flavour channel (eee , $ee\mu$, $e\mu\mu$ and $\mu\mu\mu$) that is equivalent to introducing a detection efficiency of $\epsilon^e = 0.8$ for electrons and $\epsilon^\mu = 0.95$ for muons. These efficiencies have been employed in our simulations for signal and backgrounds.

After applying all the above cuts and efficiencies, the cross section for the process (4.31) in the presence of a non-vanishing g_5^Z can be written as ¹⁷

$$\sigma = \sigma_{\text{bck}} + \sigma_{SM} + \sigma_{\text{int}} g_5^Z + \sigma_{\text{ano}} (g_5^Z)^2, \quad (4.40)$$

where σ_{SM} denotes the SM contribution to $W^\pm Z$ production, σ_{int} stands for the interference between this SM process and the anomalous g_5^Z contribution and σ_{ano} is the pure anomalous contribution. Furthermore, σ_{bck} corresponds to all background sources except for the SM EW $W^\pm Z$ production. We present in Table 6 the values of σ_{SM} , σ_{int} and σ_{ano} for center-of-mass energies of 7, 8 and 14 TeV, as well as the cross section for the reducible backgrounds.

COM Energy	σ_{bck} (fb)	σ_{SM} (fb)	σ_{int} (fb)	σ_{ano} (fb)
7 TeV	14.3	47.7	6.5	304
8 TeV	16.8	55.3	6.6	363
14 TeV	29.0	97.0	9.1	707

Table 6: Values of the cross section predictions for the process $pp \rightarrow \ell'^{\pm} \ell^+ \ell^- E_T^{\text{miss}}$ after applying all the cuts described in the text. σ_{SM} is the SM contribution coming from EW $W^\pm Z$ production, σ_{int} is the interference between this SM process and the anomalous g_5^Z contribution, σ_{ano} is the pure anomalous contribution and σ_{bck} corresponds to all background sources except for the SM EW $W^\pm Z$ production.

In order to quantify the expected limits on g_5^Z , advantage has been taken in this analysis of the fact that anomalous TGVs enhance the cross sections at high energies. Ref. [135] shows that the variables M_{WZ}^{rec} (the reconstructed $W-Z$ invariant mass), $p_T^{\ell, \text{max}}$ and p_T^Z are able to trace well this energy dependence, leading to similar sensitivities to the anomalous TGV. Here, we chose p_T^Z to study g_5^Z because this variable is strongly correlated with the subprocess center-of-mass energy (\hat{s}), and, furthermore, it can be directly reconstructed with good precision from the measured lepton momenta. The left (right) panel of Figure 3 depicts the number of expected events with respect to the Z transverse momentum for the 7 (14) TeV run and an integrated luminosity of 4.64 (300) fb^{-1} . As illustrated by this figure, the existence of an anomalous g_5^Z contribution enhances the tail of the p_T^Z spectrum, signaling the existence of new physics.

¹⁷ We assumed in this study that all anomalous TGV vanish except for g_5^Z .

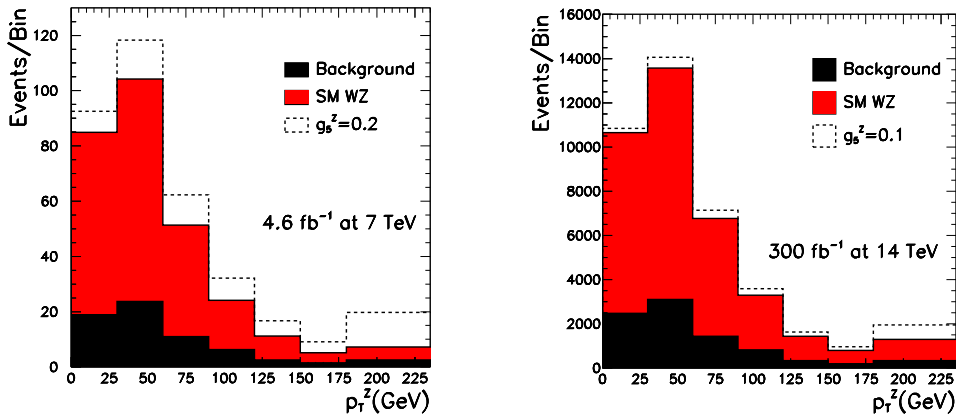


Figure 3: The left (right) panel displays the number of expected events as a function of the Z transverse momentum for a center-of-mass energy of 7 (14) TeV, assuming an integrated luminosity of 4.64 (300) fb^{-1} . The black histogram corresponds to the sum of all background sources except for the SM electroweak $pp \rightarrow W^\pm Z$ process, while the red histogram corresponds to the sum of all SM backgrounds, and the dashed distribution corresponds to the addition of the anomalous signal for $g_5^Z = 0.2$ ($g_5^Z = 0.1$). The last bin contains all the events with $p_T^Z > 180$ GeV.

Two procedures have been used to estimate the LHC potential to probe anomalous g_5^Z couplings. In the first approach, we performed a simple event counting analysis assuming that the number of observed events correspond to the SM prediction ($g_5^Z = 0$) and we look for the values of g_5^Z which are inside the 68% and 95% CL allowed regions. As suggested by Ref. [135], the following additional cut was applied in this analysis to enhance the sensitivity to g_5^Z :

$$p_T^Z > 90 \text{ GeV}. \quad (4.41)$$

On a second analysis, a simple χ^2 was built based on the contents of the different bins of the p_T^Z distribution, in order to obtain more stringent bounds. The binning used is shown in Fig. 3. Once again, it was assumed that the observed p_T^Z spectrum corresponds to the SM expectations and we sought for the values of g_5^Z that are inside the 68% and 95% allowed regions. The results of both analyses are presented in Table 7.

We present in the first row of Table 7 the expected LHC limits for the combination of the 7 TeV and 8 TeV existing data sets, where we considered an integrated luminosity of 4.64 fb^{-1} for the 7 TeV run and 19.6 fb^{-1} for the 8 TeV one. Therefore, the attainable precision on g_5^Z at the LHC 7 and 8 TeV runs is already higher than the present direct bounds stemming from LEP and it is also approaching the present indirect limits. Finally, the last row of Table 7 displays the expected precision on g_5^Z when the 14 TeV run with an integrated luminosity of 300 fb^{-1} is included in the combination. Here, once more, it was assumed that the observed number of events is the SM expected one. The LHC precision on g_5^Z will approach the per cent level, clearly improving the present both direct and indirect bounds.

Data sets used	68% CL range		95% CL range	
	Counting $p_T^Z > 90$ GeV	p_T^Z binned analysis	Counting $p_T^Z > 90$ GeV	p_T^Z binned analysis
7+8 TeV (4.64+19.6 fb ⁻¹)	(-0.066, 0.058)	(-0.057, 0.050)	(-0.091, 0.083)	(-0.080, 0.072)
7+8+14 TeV (4.64+19.6+300 fb ⁻¹)	(-0.030, 0.022)	(-0.024, 0.019)	(-0.040, 0.032)	(-0.033, 0.028)

Table 7: *Expected sensitivity on g_5^Z at the LHC for the two different procedures described in the text.*

4.4 Anomalous quartic couplings

As shown in Sect. 3.4, in the chiral expansion several operators weighted by ξ or higher powers contribute to quartic gauge boson vertices without inducing any modification to TGVs. Therefore, their coefficients are much less constrained at present, and one can expect still larger deviations on future studies of quartic vertices at LHC for large values of ξ . This is unlike in the linear expansion, in which the modifications of quartic gauge couplings that do not induce changes to TGVs appear only when the $d = 8$ operators are considered [83]. For instance, the linear operators similar to $\mathcal{P}_6(h)$ and $\mathcal{P}_{11}(h)$ are $\mathcal{L}_{S,0}$ and $\mathcal{L}_{S,1}$ in Ref. [83].

Of the five operators giving rise to purely quartic gauge boson vertices ($\mathcal{P}_6(h)$, $\mathcal{P}_{11}(h)$, $\mathcal{P}_{23}(h)$, $\mathcal{P}_{24}(h)$, $\mathcal{P}_{26}(h)$), none modifies quartic vertices including photons while all generate the anomalous quartic vertex $ZZZZ$ that is not present in the SM. Moreover, all these operators but $\mathcal{P}_{26}(h)$ modify the ZZW^+W^- vertex, while only $\mathcal{P}_6(h)$ and $\mathcal{P}_{11}(h)$ also induce anomalous contributions to $W^+W^-W^+W^-$.

Presently, the most stringent bounds on the coefficients of these operators are indirect, from their one-loop contribution to the EWPD derived in Ref. [79] where it was shown that the five operators correct $\alpha\Delta T$ while render $\alpha\Delta S = \alpha\Delta U = 0$. In Table 8 we give the updated indirect bounds using the determination of the oblique parameters in Eq. (4.24).

At the LHC these anomalous quartic couplings can be directly tested in the production of three vector bosons (VVV) or in vector boson fusion (VBF) production of two gauge bosons [81]. At lower center-of-mass energies the best limits originate from the VVV processes, while the VBF channel dominates for the 14 TeV run [80–83, 140].

At the LHC with 14 TeV center-of-mass energy, the couplings c_6 and c_{11} can be constrained by combining their impact on the VBF channels

$$pp \rightarrow jjW^+W^- \quad \text{and} \quad pp \rightarrow jj(W^+W^+ + W^-W^-), \quad (4.42)$$

where j stands for a tagging jet and the final state W 's decay into electron or muon plus neutrino. It was shown in Ref. [83] that the attainable 99% CL limits on these couplings are

$$-12 \times 10^{-3} < c_6 \xi < 10 \times 10^{-3} \quad , \quad -7.7 \times 10^{-3} < c_{11} \xi^2 < 14 \times 10^{-3} \quad (4.43)$$

for an integrated luminosity of 100 fb⁻¹. Notice that the addition of the channel $pp \rightarrow jjZZ$ does not improve significantly the above limits [80].

coupling	90% CL allowed region
$c_6 \xi$	$[-0.23, 0.26]$
$c_{11} \xi^2$	$[-0.094, 0.10]$
$c_{23} \xi^2$	$[-0.092, 0.10]$
$c_{24} \xi^2$	$[-0.012, 0.013]$
$c_{26} \xi^4$	$[-0.0061, 0.0068]$

Table 8: *90% CL limits on the anomalous quartic couplings from their one-loop contribution to the EWPD. The bounds were obtained assuming only one operator different from zero at a time and for a cutoff scale $\Lambda_s = 2 \text{ TeV}$.*

5 Conclusions

In this paper we have made a comparative study of the departures from the Standard Model predictions in theories based on linear and non-linear realizations of $SU(2)_L \times U(1)_Y$ gauge symmetry breaking. To address this question in a model-independent way, we have considered effective Lagrangians containing either a light fundamental Higgs in the linear realization or a light dynamical Higgs in the non-linear one. We have exploited the fact that these two expansions are intrinsically different from the point of view of the presence or absence, respectively, of a global $SU(2)_L$ symmetry in the effective Lagrangian, with the light Higgs scalar behaving as a singlet in the chiral case. Less symmetry means more possible invariant operators at a given order, and the result is that the non-linear realization for a light dynamical Higgs particle is expected to exhibit a larger number of independent couplings than linear ones. This has been explored here concentrating on the CP-even operators involving pure gauge and gauge- h couplings. First, in Sec. 2 we have presented the maximal set of independent (and thus non-redundant) operators of that type contained in the effective chiral Lagrangian for a light dynamical Higgs, up to operators with four derivatives. In Sec. 3.1 the analogous complete basis of independent operators up to dimension six in the linear expansion is presented. Comparing both sets of operators, we have established the relations and differences between the chiral and the linear bases.

In particular, in Secs. 3.2 and 3.4 we have identified two sources of discriminating signatures. For small values of the ξ parameter the counting of operators is not the same in both sets, being larger by six for the chiral expansion. This implies that, even keeping only operators weighted by ξ , the expected deviations from the SM predictions in the Higgs couplings to gauge bosons and that of the triple gauge boson self-couplings are independent in the chiral expansion, unlike in the linear expansion at dimension six; one interesting set of (de)correlated couplings is explored in details as indicators of a non-linear character. Conversely, when considering operators weighted by ξ^n with $n \geq 2$ in the chiral expansion, we find anomalous signals which appear only at dimension eight of the linear Lagrangian; they may thus be detected with larger (leading) strength for a non-linear realization of

EWSB than for a linear one, for sizeable values of ξ .

In order to quantify the observability of the above effects we have implemented the renormalization procedure as described in Sec. 4.1 and derived the corresponding Feynman rules for the non-linear expansion (which we present in the detail in Appendix D, for the complete set of independent operators under discussion). Neglecting external fermion masses only in the numerical analysis, the results of our simulations for some of the discriminating signatures at LHC are presented in Secs. 4.2–4.4. To our knowledge, this is the first six-parameter analysis in the context of the non-linear expansion, focusing on the ξ -weighted pure gauge and gauge- h effective couplings. In particular we have derived the present bounds on the coefficients of the latter from the analysis of electroweak precision physics, triple gauge boson coupling studies and Higgs data. The results are summarized in Fig. 1 and Table 4 and the corresponding level of decorrelation between the triple gauge couplings and Higgs effects is illustrated in Fig. 2: the presently allowed values for the parameters $c_i\xi$ and $a_i\xi$ turn out to be of order 1, with only few exceptions bounded to the per cent level. With the expected uncertainties attainable in CMS and ATLAS at 14 TeV, that sensitivity can be improved by a factor $\mathcal{O}(3 - 5)$. Furthermore, our study of the present sensitivity to the C and P odd operator in the analysis of WWZ vertex, with the accumulated luminosity of LHC7+8 and with LHC14 in the future, show that per cent precision on the coupling of the operator $\mathcal{P}_{14}(h)$ is foreseeable. Similar precision should be attainable for the coefficients of the operators leading to generic quartic gauge couplings $\mathcal{P}_6(h)$ and $\mathcal{P}_{11}(h)$.

Acknowledgements

We acknowledge illuminating conversations with Rodrigo Alonso, Gino Isidori, Aneesh Manohar, Michael Trott, and Juan Yepes. We also acknowledge partial support of the European Union network FP7 ITN INVISIBLES (Marie Curie Actions, PITN-GA-2011-289442), of CiCYT through the project FPA2009-09017, of CAM through the project HEPHACOS P-ESP-00346, of the European Union FP7 ITN UNILHC (Marie Curie Actions, PITN-GA-2009-237920), of MICINN through the grant BES-2010-037869, of the Spanish MINECOs Centro de Excelencia Severo Ochoa Programme under grant SEV-2012-0249, and of the Italian Ministero dell'Università e della Ricerca Scientifica through the COFIN program (PRIN 2008) and the contract MRTN-CT-2006-035505. The work of I.B. is supported by an ESR contract of the European Union network FP7 ITN INVISIBLES mentioned above. The work of L.M. is supported by the Juan de la Cierva programme (JCI-2011-09244). The work of O.J.P.E. is supported in part by Conselho Nacional de Desenvolvimento Científico e Tecnológico (CNPq) and by Fundação de Amparo à Pesquisa do Estado de São Paulo (FAPESP), M.C.G-G and T.C are supported by USA-NSF grant PHY-09-6739, M.C.G-G is also supported by CUR Generalitat de Catalunya grant 2009SGR502 and together with J.G-F by MICINN FPA2010-20807 and consolider-ingenio 2010 program CSD-2008-0037. J.G-F is further supported by ME FPU grant AP2009-2546. I.B., J.G-F., M.C.G-G., B.G., L.M, and S.R. acknowledge CERN TH department and J.G-F. also acknowledges ITP Heidelberg for hospitality during part of this work.

A EOM and fermion operators

The EOM can be extracted from the \mathcal{L}_0 part of the chiral Lagrangian, Eq. (2.2); as we will work at first order in $\Delta\mathcal{L}$ they read¹⁸:

$$(\mathcal{D}^\mu W_{\mu\nu})^a = \frac{g}{2}\bar{Q}_L\sigma^a\gamma_\nu Q_L + \frac{g}{2}\bar{L}_L\sigma^a\gamma_\nu L_L + \frac{igv^2}{4}\text{Tr}[\mathbf{V}_\nu\sigma^a] \left(1 + \frac{h}{v}\right)^2 \quad (\text{A.1})$$

$$\partial^\mu B_{\mu\nu} = -\frac{ig'v^2}{4}\text{Tr}[\mathbf{T}\mathbf{V}_\mu] \left(1 + \frac{h}{v}\right)^2 + g' \sum_{i=L,R} \left(\bar{Q}_i\mathbf{h}_i\gamma_\nu Q_i + \frac{1}{6}\bar{L}_L\gamma_\nu L_L\right) \quad (\text{A.2})$$

$$\square h = -\frac{\delta V(h)}{\delta h} - \frac{v+h}{2}\text{Tr}[\mathbf{V}_\mu\mathbf{V}^\mu] - \frac{s_Y}{\sqrt{2}}(\bar{Q}_L\mathbf{U}\mathbf{Y}_Q Q_R + \bar{L}_L\mathbf{U}\mathbf{Y}_L L_R + \text{h.c.}) \quad (\text{A.3})$$

$$\left[\mathbf{D}_\mu\left(\frac{(v+h)^2}{2\sqrt{2}}\mathbf{U}^\dagger\mathbf{D}^\mu\mathbf{U}\right)\right]_{ij} = \begin{cases} -(v+s_Y h) \left[(\bar{Q}_R\mathbf{Y}_Q^\dagger)_j(\mathbf{U}^\dagger Q_L)_i + (\bar{L}_R\mathbf{Y}_L^\dagger)_j(\mathbf{U}^\dagger L_L)_i \right] & \text{for } i \neq j \\ 0 & \text{for } i = j \end{cases} \quad (\text{A.4})$$

$$i\not{D}Q_L = \frac{v+s_Y h}{\sqrt{2}}\mathbf{U}\mathbf{Y}_Q Q_R \quad i\not{D}Q_R = \frac{v+s_Y h}{\sqrt{2}}\mathbf{Y}_Q^\dagger\mathbf{U}^\dagger Q_L \quad (\text{A.5})$$

$$i\not{D}L_L = \frac{v+s_Y h}{\sqrt{2}}\mathbf{U}\mathbf{Y}_L L_R \quad i\not{D}L_R = \frac{v+s_Y h}{\sqrt{2}}\mathbf{Y}_L^\dagger\mathbf{U}^\dagger L_L, \quad (\text{A.6})$$

where $\mathbf{h}_{L,R}$ are the 2×2 matrices of hypercharge for the left- and right-handed quarks.

By using these EOM, it is possible to identify relations between some bosonic operators listed in Eqs.(2.6)-(2.8) and specific fermion operators. This allows us to trade those bosonic operators by the corresponding fermionic ones: this procedure can turn out to be very useful when analysing specific experimental data. For instance, if deviations from the SM values of the h -fermion couplings were found, then the following three operators,

$$\begin{aligned} \mathcal{P}_{U,\alpha\beta}(h) &= -\frac{v}{\sqrt{2}}\bar{Q}_{L\alpha}\mathbf{U}(\mathcal{F}_U(h)P_\uparrow Q_R)_\beta + \text{h.c.}, \\ \mathcal{P}_{D,\alpha\beta}(h) &= -\frac{v}{\sqrt{2}}\bar{Q}_{L\alpha}\mathbf{U}(\mathcal{F}_D(h)P_\downarrow Q_R)_\beta + \text{h.c.}, \\ \mathcal{P}_{E,\alpha\beta}(h) &= -\frac{v}{\sqrt{2}}\bar{L}_{L\alpha}\mathbf{U}(\mathcal{F}_E(h)P_\downarrow L_R)_\beta + \text{h.c.}, \end{aligned} \quad (\text{A.7})$$

would be a good choice for an operator basis. In the previous equations the two projectors

$$P_\uparrow = \begin{pmatrix} 1 & \\ & 0 \end{pmatrix} \quad P_\downarrow = \begin{pmatrix} 0 & \\ & 1 \end{pmatrix}, \quad (\text{A.8})$$

have been introduced.

On the contrary, without including the operators in Eqs. (A.7), the bosonic basis defined in Eqs. (2.6)- (2.10) is blind to these directions. The fermionic operators that arise applying the EOM to bosonic operators in the basis above is presented in the following list:

¹⁸With alternative choices for the separation \mathcal{L}_0 versus $\Delta\mathcal{L}$ the EOM are correspondingly modified [63, 64, 73]: this is of no relevance to the focus of this paper, which explores the tree-level impact of effective operators.

Weighted by ξ :

$$\begin{aligned}
\mathcal{P}_{U,\alpha\beta}(h) &= -\frac{v}{\sqrt{2}}\bar{Q}_{L\alpha}\mathbf{U}(\mathcal{F}_U(h)P_{\uparrow}Q_R)_{\beta} + \text{h.c.} \\
\mathcal{P}_{D,\alpha\beta}(h) &= -\frac{v}{\sqrt{2}}\bar{Q}_{L\alpha}\mathbf{U}(\mathcal{F}_D(h)P_{\downarrow}Q_R)_{\beta} + \text{h.c.} \\
\mathcal{P}_{E,\alpha\beta}(h) &= -\frac{v}{\sqrt{2}}\bar{L}_{L\alpha}\mathbf{U}(\mathcal{F}_E(h)P_{\downarrow}L_R)_{\beta} + \text{h.c.} \\
\mathcal{P}_{1Q,\alpha\beta}(h) &= \frac{\alpha}{2}\bar{Q}_{L\alpha}\gamma^{\mu}\{\mathbf{T}, \mathbf{V}_{\mu}\}(\mathcal{F}_{1Q}(h)Q_L)_{\beta} \\
\mathcal{P}_{1L,\alpha\beta}(h) &= \frac{\alpha}{2}\bar{L}_{L\alpha}\gamma^{\mu}\{\mathbf{T}, \mathbf{V}_{\mu}\}(\mathcal{F}_{1L}(h)L_L)_{\beta} \\
\mathcal{P}_{1U,\alpha\beta}(h) &= \frac{\alpha}{2}\bar{Q}_{R\alpha}\gamma^{\mu}\{\sigma^3, \tilde{\mathbf{V}}_{\mu}\}(\mathcal{F}_{1U}(h)P_{\uparrow}Q_R)_{\beta} \\
\mathcal{P}_{1D,\alpha\beta}(h) &= \frac{\alpha}{2}\bar{Q}_{R\alpha}\gamma^{\mu}\{\sigma^3, \tilde{\mathbf{V}}_{\mu}\}(\mathcal{F}_{1D}(h)P_{\downarrow}Q_R)_{\beta} \\
\mathcal{P}_{1N,\alpha\beta}(h) &= \frac{\alpha}{2}\bar{L}_{R\alpha}\gamma^{\mu}\{\sigma^3, \tilde{\mathbf{V}}_{\mu}\}(\mathcal{F}_{1N}(h)P_{\uparrow}L_R)_{\beta} \\
\mathcal{P}_{1E,\alpha\beta}(h) &= \frac{\alpha}{2}\bar{L}_{R\alpha}\gamma^{\mu}\{\sigma^3, \tilde{\mathbf{V}}_{\mu}\}(\mathcal{F}_{1E}(h)P_{\downarrow}L_R)_{\beta} \\
\mathcal{P}_{2Q,\alpha\beta}(h) &= i\bar{Q}_{L\alpha}\gamma^{\mu}\mathbf{V}_{\mu}(\mathcal{F}_{2Q}(h)Q_L)_{\beta} \\
\mathcal{P}_{2L,\alpha\beta}(h) &= i\bar{L}_{L\alpha}\gamma^{\mu}\mathbf{V}_{\mu}(\mathcal{F}_{2L}(h)L_L)_{\beta} \\
\mathcal{P}_{3Q,\alpha\beta}(h) &= i\bar{Q}_{L\alpha}\gamma^{\mu}\mathbf{T}\mathbf{V}_{\mu}\mathbf{T}(\mathcal{F}_{3Q}(h)Q_L)_{\beta} \\
\mathcal{P}_{3L,\alpha\beta}(h) &= i\bar{L}_{L\alpha}\gamma^{\mu}\mathbf{T}\mathbf{V}_{\mu}\mathbf{T}(\mathcal{F}_{3L}(h)L_L)_{\beta}
\end{aligned} \tag{A.9}$$

Weighted by $\xi\sqrt{\xi}$:

$$\begin{aligned}
\mathcal{P}_{6U,\alpha\beta}(h) &= \bar{Q}_{L\alpha} \mathbf{V}_\mu \mathbf{U} (\partial^\mu \mathcal{F}_{6U}(h) P_\uparrow Q_R)_\beta \\
\mathcal{P}_{6D,\alpha\beta}(h) &= \bar{Q}_{L\alpha} \mathbf{V}_\mu \mathbf{U} (\partial^\mu \mathcal{F}_{6D}(h) P_\downarrow Q_R)_\beta \\
\mathcal{P}_{6N,\alpha\beta}(h) &= \bar{L}_{L\alpha} \mathbf{V}_\mu \mathbf{U} (\partial^\mu \mathcal{F}_{6N}(h) P_\uparrow L_R)_\beta \\
\mathcal{P}_{6E,\alpha\beta}(h) &= \bar{L}_{L\alpha} \mathbf{V}_\mu \mathbf{U} (\partial^\mu \mathcal{F}_{6E}(h) P_\downarrow L_R)_\beta \\
\mathcal{P}_{7U,\alpha\beta}(h) &= \text{Tr}[\mathbf{T}\mathbf{V}^\mu] \bar{Q}_{L\alpha} \mathbf{T}\mathbf{U} (\partial^\mu \mathcal{F}_{7U}(h) P_\uparrow Q_R)_\beta \\
\mathcal{P}_{7D,\alpha\beta}(h) &= \text{Tr}[\mathbf{T}\mathbf{V}^\mu] \bar{Q}_{L\alpha} \mathbf{T}\mathbf{U} (\partial^\mu \mathcal{F}_{7D}(h) P_\downarrow Q_R)_\beta \\
\mathcal{P}_{7N,\alpha\beta}(h) &= \text{Tr}[\mathbf{T}\mathbf{V}^\mu] \bar{L}_{L\alpha} \mathbf{T}\mathbf{U} (\partial^\mu \mathcal{F}_{7N}(h) P_\uparrow L_R)_\beta \\
\mathcal{P}_{7E,\alpha\beta}(h) &= \text{Tr}[\mathbf{T}\mathbf{V}^\mu] \bar{L}_{L\alpha} \mathbf{T}\mathbf{U} (\partial^\mu \mathcal{F}_{7E}(h) P_\downarrow L_R)_\beta \\
\mathcal{P}_{8U,\alpha\beta}(h) &= \text{Tr}[\mathbf{T}\mathbf{V}^\mu] \bar{Q}_{L\alpha} [\mathbf{T}, \mathbf{V}_\mu] \mathbf{U} (\mathcal{F}_{8U}(h) P_\uparrow Q_R)_\beta \\
\mathcal{P}_{8D,\alpha\beta}(h) &= \text{Tr}[\mathbf{T}\mathbf{V}^\mu] \bar{Q}_{L\alpha} [\mathbf{T}, \mathbf{V}_\mu] \mathbf{U} (\mathcal{F}_{8D}(h) P_\downarrow Q_R)_\beta \\
\mathcal{P}_{8N,\alpha\beta}(h) &= \text{Tr}[\mathbf{T}\mathbf{V}^\mu] \bar{L}_{L\alpha} [\mathbf{T}, \mathbf{V}_\mu] \mathbf{U} (\mathcal{F}_{8N}(h) P_\uparrow L_R)_\beta \\
\mathcal{P}_{8E,\alpha\beta}(h) &= \text{Tr}[\mathbf{T}\mathbf{V}^\mu] \bar{L}_{L\alpha} [\mathbf{T}, \mathbf{V}_\mu] \mathbf{U} (\mathcal{F}_{8E}(h) P_\downarrow L_R)_\beta .
\end{aligned} \tag{A.10}$$

Rearranging Eqs. (A.1)-(A.4), one can derive the following relations between bosonic and fermionic operators:

$$\begin{aligned}
2\mathcal{P}_B(h) + \frac{1}{2}\mathcal{P}_1(h) + \frac{1}{2}\mathcal{P}_2(h) + \mathcal{P}_4(h) - g'^2\mathcal{P}_T(h) \left(1 + \frac{h}{v}\right)^2 &= \sum_\alpha \left\{ \frac{1}{3}g'^2\mathcal{P}_{1Q,\alpha\alpha}(h) + \frac{4}{3}g'^2\mathcal{P}_{1U,\alpha\alpha}(h) \right. \\
&\quad \left. - \frac{2}{3}g'^2\mathcal{P}_{1D,\alpha\alpha}(h) - g'^2\mathcal{P}_{1L,\alpha\alpha}(h) - 2g'^2\mathcal{P}_{1E,\alpha\alpha}(h) \right\}, \\
-\mathcal{P}_W(h) - g^2\mathcal{P}_C(h) \left(1 + \frac{h}{v}\right)^2 - \frac{1}{4}\mathcal{P}_1(h) - \frac{1}{2}\mathcal{P}_3(h) + \mathcal{P}_5(h) &= \frac{g^2}{2} \sum_\alpha \left\{ \mathcal{P}_{2Q,\alpha\alpha}(h) + \mathcal{P}_{2L,\alpha\alpha}(h) \right\}, \\
\mathcal{P}_H(h) + 2\mathcal{P}_C(h) \left(1 + \frac{h}{v}\right)^2 + (v+h)\mathcal{F}(h) \frac{\delta V}{\delta h} &= s_Y \frac{v+h}{\sqrt{2}} \sum_{f=U,D,E} \sum_{\alpha\beta} \left\{ Y_{f,\alpha\beta} \mathcal{P}_{f,\alpha\beta}(h) + \text{h.c.} \right\}, \\
g^2\mathcal{P}_T(h) \left(1 + \frac{h}{v}\right)^2 - \frac{1}{2}\mathcal{P}_1(h) - \mathcal{P}_3(h) + \frac{1}{2}\mathcal{P}_{12}(h) + \mathcal{P}_{13}(h) + \mathcal{P}_{17}(h) &= \\
&= \frac{g^2}{2} \sum_\alpha \left\{ (\mathcal{P}_{3Q,\alpha\alpha}(h) + \mathcal{P}_{2Q,\alpha\alpha}(h)) + (\mathcal{P}_{3L,\alpha\alpha}(h) + \mathcal{P}_{2L,\alpha\alpha}(h)) \right\}.
\end{aligned} \tag{A.11}$$

The $\mathcal{F}_i(h)$ functions in all operators in these relations are the same, except for \mathcal{P}_H in the third line of Eq. (A.11), which is related to it by

$$\mathcal{F}_H(h) = \mathcal{F}_C(h) + \left(1 + \frac{h}{v}\right) \frac{\delta \mathcal{F}_C(h)}{\delta h}. \tag{A.12}$$

Applying the EOM in Eq. (A.3) to the operators $\mathcal{P}_{20}(h)$ and $\mathcal{P}_{21}(h)$ allows us to express them

in terms of other operators in the basis, h -gauge boson couplings and Yukawa-like interactions:

$$\begin{aligned}
\mathcal{P}_{20}(h) &= 2\mathcal{F}(h)\mathcal{P}_6(h) + 2\mathcal{F}(h)\mathcal{P}_7(h) - \frac{16}{v^3}\sqrt{\mathcal{F}(h)}\mathcal{P}_C(h)\frac{\delta V}{\delta h} \\
&\quad - \frac{8\sqrt{2}s_y}{v^3}\sqrt{\mathcal{F}(h)}\mathcal{P}_C(h) (\bar{Q}_L\mathbf{U}\mathbf{Y}_Q Q_R + \bar{L}_L\mathbf{U}\mathbf{Y}_L L_R + \text{h.c.}) , \\
\mathcal{P}_{21}(h) &= 2\mathcal{F}(h)\mathcal{P}_{23}(h) + 2\mathcal{F}(h)\mathcal{P}_{25}(h) + \frac{16}{v^3}\sqrt{\mathcal{F}(h)}\mathcal{P}_T(h)\frac{\delta V}{\delta h} \\
&\quad + \frac{8\sqrt{2}s_y}{v^3}\sqrt{\mathcal{F}(h)}\mathcal{P}_T(h) (\bar{Q}_L\mathbf{U}\mathbf{Y}_Q Q_R + \bar{L}_L\mathbf{U}\mathbf{Y}_L L_R + \text{h.c.}) ,
\end{aligned} \tag{A.13}$$

where all $\mathcal{F}_i(h)$ appearing explicitly in these expressions and included in the definition of the operators $\mathcal{P}_i(h)$ are the same and defined by

$$\mathcal{F}(h) = \left(1 + \frac{h}{v}\right)^2 . \tag{A.14}$$

From Eqs. (A.1), (A.2) and (A.5), it follows that

$$\begin{aligned}
\frac{iv}{\sqrt{2}}\text{Tr}(\sigma^j \mathcal{D}_\mu \mathbf{V}^\mu) \left(1 + \frac{h}{v}\right)^2 &= \frac{v + s_Y h}{v} (i\bar{Q}_L \sigma^j \mathbf{U}\mathbf{Y}_Q Q_R + i\bar{L}_L \sigma^j \mathbf{U}\mathbf{Y}_L L_R + \text{h.c.}) \\
&\quad - \frac{iv}{\sqrt{2}}\text{Tr}(\sigma^j \mathbf{V}_\mu) \partial^\mu \left(1 + \frac{h}{v}\right)^2 , \\
\frac{iv}{\sqrt{2}}\text{Tr}(\mathbf{T} \mathcal{D}_\mu \mathbf{V}^\mu) \left(1 + \frac{h}{v}\right)^2 &= \frac{v + s_Y h}{v} (i\bar{Q}_L \mathbf{T}\mathbf{U}\mathbf{Y}_Q Q_R + i\bar{L}_L \mathbf{T}\mathbf{U}\mathbf{Y}_L L_R + \text{h.c.}) \\
&\quad - \frac{iv}{\sqrt{2}}\text{Tr}(\mathbf{T}\mathbf{V}_\mu) \partial^\mu \left(1 + \frac{h}{v}\right)^2 ,
\end{aligned} \tag{A.15}$$

which allows us to rewrite the pure bosonic operators $\mathcal{P}_{11-13}(h)$, $\mathcal{P}_{10}(h)$ and $\mathcal{P}_{19}(h)$ as combination of other pure bosonic ones in Eqs. (2.6)-(2.8) plus fermionic operators in Eqs. (A.9) and (A.10):

$$\begin{aligned}
\mathcal{P}_9(h) - \mathcal{P}_8(h) &= \frac{1}{v^2} \sum_{f_1, f_2=U, D, E} \sum_{\alpha\beta\gamma\delta} Y_{f_1, \alpha\beta} Y_{f_2, \gamma\delta} \mathcal{P}_{4f_1 f_2, \alpha\beta\gamma\delta}(h) \\
&\quad - \frac{2\sqrt{2}}{v} \sum_{f=U, D, N, E} \sum_{\alpha\beta} (Y_{f, \alpha\beta} \mathcal{P}_{6f, \alpha\beta}(h) - \text{h.c.}) , \\
\mathcal{P}_{15}(h) - \mathcal{P}_{22}(h) &= \frac{2}{v^2} \sum_{f_1, f_2=U, D, E} \sum_{\alpha\beta\gamma\delta} Y_{f_1, \alpha\beta\gamma\delta} Y_{f_2, \gamma\delta} \mathcal{P}_{5f_1 f_2, \alpha\beta\gamma\delta}(h) \\
&\quad - \frac{2\sqrt{2}}{v \cos \theta_W} \sum_{f=U, D, N, E} \sum_{\alpha\beta} (Y_{f, \alpha\beta} \mathcal{P}_{7f, \alpha\beta}(h) - \text{h.c.}) , \\
\mathcal{P}_{16}(h) + \mathcal{P}_{18}(h) &= \sum_{f=U, D, N, E} \sum_{\alpha\beta} \frac{\sqrt{2}}{v} (Y_{f, \alpha\beta} \mathcal{P}_{8f, \alpha\beta}(h) - \text{h.c.}) , \\
\mathcal{P}_{10}(h) + \mathcal{P}_8(h) &= \sum_{f=U, D, N, E} \sum_{\alpha\beta} \frac{\sqrt{2}}{v} (Y_{f, \alpha\beta} \mathcal{P}_{6f, \alpha\beta}(h) - \text{h.c.}) , \\
\mathcal{P}_{19}(h) + \mathcal{P}_{22}(h) &= \sum_{f=U, D, N, E} \sum_{\alpha\beta} \frac{\sqrt{2}}{v} (Y_{f, \alpha\beta} \mathcal{P}_{7f, \alpha\beta}(h) - \text{h.c.}) .
\end{aligned} \tag{A.16}$$

A straightforward consequence is that once the $\mathcal{F}_i(h)$ functions in the operators on the left-hand side of Eq. (A.16) are specified, then the $\mathcal{F}_i(h)$ functions in the operators on the right-hand side are no longer general, but take the form of specific expressions.

B Equivalence of the $d = 6$ basis with the SILH Lagrangian

The SILH Lagrangian [87] is defined by the following 10 $d = 6$ linear operators:

$$\begin{aligned}
\mathcal{O}_g^{\text{SILH}} &= \Phi^\dagger \Phi G_{\mu\nu}^a G^{a\mu\nu}, & \mathcal{O}_\gamma^{\text{SILH}} &= \Phi^\dagger \hat{B}_{\mu\nu} \hat{B}^{\mu\nu} \Phi, \\
\mathcal{O}_B^{\text{SILH}} &= \left(\Phi^\dagger \overleftrightarrow{D}_\mu \Phi \right) \partial_\nu \hat{B}^{\mu\nu}, & \mathcal{O}_W^{\text{SILH}} &= \frac{ig}{2} \left(\Phi^\dagger \sigma^i \overleftrightarrow{D}_\mu \Phi \right) D_\nu W_i^{\mu\nu}, \\
\mathcal{O}_{HB}^{\text{SILH}} &= (D_\mu \Phi)^\dagger (D_\nu \Phi) \hat{B}^{\mu\nu}, & \mathcal{O}_{HW}^{\text{SILH}} &= (D_\mu \Phi)^\dagger \hat{W}^{\mu\nu} (D_\nu \Phi), \\
\mathcal{O}_T^{\text{SILH}} &= \frac{1}{2} \left(\Phi^\dagger \overleftrightarrow{D}_\mu \Phi \right) \left(\Phi^\dagger \overleftrightarrow{D}^{\mu} \Phi \right), & \mathcal{O}_H^{\text{SILH}} &= \frac{1}{2} \partial^\mu \left(\Phi^\dagger \Phi \right) \partial_\mu \left(\Phi^\dagger \Phi \right), \\
\mathcal{O}_6^{\text{SILH}} &= \frac{1}{3} \left(\Phi^\dagger \Phi \right)^3, & \mathcal{O}_y^{\text{SILH}} &= \left(\Phi^\dagger \Phi \right) f_L \Phi \mathbf{Y} f_R + \text{h.c.},
\end{aligned} \tag{B.1}$$

where $\Phi^\dagger \overleftrightarrow{D}_\mu \Phi \equiv \Phi^\dagger D_\mu \Phi - D_\mu \Phi^\dagger \Phi$ and $\Phi^\dagger \sigma^i \overleftrightarrow{D}_\mu \Phi \equiv \Phi^\dagger \sigma^i D_\mu \Phi - D_\mu \Phi^\dagger \sigma^i \Phi$. They can be related directly to the operators in Eqs. (3.3) and (3.4):

$$\begin{aligned}
\mathcal{O}_g^{\text{SILH}} &\equiv \mathcal{O}_{GG}, & \mathcal{O}_\gamma^{\text{SILH}} &\equiv \mathcal{O}_{BB}, \\
\mathcal{O}_B^{\text{SILH}} &\equiv 2\mathcal{O}_B + \mathcal{O}_{BW} + \mathcal{O}_{BB}, & \mathcal{O}_W^{\text{SILH}} &\equiv 2\mathcal{O}_W + \mathcal{O}_{BW} + \mathcal{O}_{WW}, \\
\mathcal{O}_{HW}^{\text{SILH}} &\equiv \mathcal{O}_W, & \mathcal{O}_{HB}^{\text{SILH}} &\equiv \mathcal{O}_B, \\
\mathcal{O}_T^{\text{SILH}} &\equiv \mathcal{O}_{\Phi,2} - 2\mathcal{O}_{\Phi,1}, & \mathcal{O}_H^{\text{SILH}} &\equiv \mathcal{O}_{\Phi,2}, \\
\mathcal{O}_6^{\text{SILH}} &\equiv \mathcal{O}_{\Phi,3}, & \mathcal{O}_y^{\text{SILH}} &\equiv 2\mathcal{O}_{\Phi,2} + 2\mathcal{O}_{\Phi,4} - \left(\Phi^\dagger \Phi \right) \Phi^\dagger \frac{\delta V(h)}{\delta \Phi^\dagger}.
\end{aligned} \tag{B.2}$$

This shows the equivalence of the two linear expansions.

It can also be interesting to show explicitly the connection between the SILH operators and those of the chiral basis in Eqs. (2.6)-(2.8), which is as follows:

$$\begin{aligned}
\mathcal{O}_g^{\text{SILH}} &= \frac{v^2}{2g_s^2} \mathcal{P}_G(h), & \mathcal{O}_\gamma^{\text{SILH}} &= \frac{v^2}{2} \mathcal{P}_B(h), \\
\mathcal{O}_B^{\text{SILH}} &= \frac{v^2}{8} (\mathcal{P}_2(h) + 2\mathcal{P}_4(h)) + \frac{v^2}{8} \mathcal{P}_1(h) + \frac{v^2}{2} \mathcal{P}_B(h), & \mathcal{O}_{HB}^{\text{SILH}} &= \frac{v^2}{16} (\mathcal{P}_2(h) + 2\mathcal{P}_4(h)), \\
\mathcal{O}_W^{\text{SILH}} &= \frac{v^2}{4} (\mathcal{P}_3(h) - 2\mathcal{P}_5(h)) + \frac{v^2}{8} \mathcal{P}_1(h) + \frac{v^2}{2} \mathcal{P}_W(h), & \mathcal{O}_{HW}^{\text{SILH}} &= \frac{v^2}{8} (\mathcal{P}_3(h) - 2\mathcal{P}_5(h)), \\
\mathcal{O}_T^{\text{SILH}} &= \frac{v^2}{2} \mathcal{F}(h) \mathcal{P}_T(h), & \mathcal{O}_H^{\text{SILH}} &= v^2 \mathcal{P}_H(h), \\
\mathcal{O}_y^{\text{SILH}} &= 3v^2 \mathcal{P}_H(h) + v^2 \mathcal{F}(h) \mathcal{P}_C(h) - \frac{(v+h)^3}{2} \frac{\delta V(h)}{\delta h},
\end{aligned} \tag{B.3}$$

where the $\mathcal{F}_i(h)$ appearing in these relations and inside the individual $\mathcal{P}_i(h)$ operators are all defined by

$$\mathcal{F}(h) = \left(1 + \frac{h}{v} \right)^2. \tag{B.4}$$

C Relations between chiral and linear operators

In this Appendix, the connections between the operators of the chiral and linear bases is discussed. As the number and nature of the leading order operators in the chiral and linear expansion are not the same, there are pairs of chiral operators that correspond to the same lowest dimensional linear one: in order to get then a one-to-one correspondence between these chiral operators and (combinations of) linear ones, operators of higher dimension should be taken into consideration. For those weighted by a single power of ξ , the list of the siblings can be read from Eq. (3.7). Below, we also indicate which chiral operators, weighted by higher powers of ξ , should be combined in order to generate the gauge interactions contained in specific linear ones.

For operators weighted by ξ :

$$\begin{aligned}
\mathcal{P}_B(h) &\rightarrow \mathcal{O}_{BB} & \mathcal{P}_W(h) &\rightarrow \mathcal{O}_{WW} & \mathcal{P}_G(h) &\rightarrow \mathcal{O}_{GG} \\
\mathcal{P}_C(h) &\rightarrow \mathcal{O}_{\Phi,4} & \mathcal{P}_T(h) &\rightarrow \mathcal{O}_{\Phi,1} & \mathcal{P}_H(h) &\rightarrow \mathcal{O}_{\Phi,2} \\
\mathcal{P}_1(h) &\rightarrow \mathcal{O}_{BW} & \mathcal{P}_2(h), \mathcal{P}_4(h) &\rightarrow \mathcal{O}_B & \mathcal{P}_3(h), \mathcal{P}_5(h) &\rightarrow \mathcal{O}_W \\
&& \mathcal{P}_6(h), \mathcal{P}_7(h), \mathcal{P}_8(h), \mathcal{P}_9(h), \mathcal{P}_{10}(h), \mathcal{P}_{\square H}(h) &\rightarrow \mathcal{O}_{\square\Phi}
\end{aligned} \tag{C.1}$$

For operators weighted by ξ^2 :

$$\begin{aligned}
&\mathcal{P}_{DH}(h), \mathcal{P}_{20}(h) \rightarrow \left[D_\mu \Phi^\dagger D^\mu \Phi \right]^2 \\
\mathcal{P}_{11}(h), \mathcal{P}_{18}(h), \mathcal{P}_{21}(h), \mathcal{P}_{22}(h), \mathcal{P}_{23}(h), \mathcal{P}_{24}(h) &\rightarrow \left[D^\mu \Phi^\dagger D^\nu \Phi \right]^2 \\
&\mathcal{P}_{12}(h) \rightarrow \left(\Phi^\dagger W^{\mu\nu} \Phi \right)^2 \\
\mathcal{P}_{13}(h), \mathcal{P}_{17}(h) &\rightarrow \left(\Phi^\dagger W^{\mu\nu} \Phi \right) D_\mu \Phi^\dagger D_\nu \Phi \\
\mathcal{P}_{14}(h) &\rightarrow \varepsilon^{\mu\nu\rho\lambda} \left(\Phi^\dagger \overleftrightarrow{D}_\rho \Phi \right) \left(\Phi^\dagger \sigma_i \overleftrightarrow{D}_\lambda \Phi \right) W_{\mu\nu}^i \\
\mathcal{P}_{15}(h), \mathcal{P}_{19}(h) &\rightarrow \left[\Phi^\dagger D_\mu D^\mu \Phi - D_\mu D^\mu \Phi^\dagger \Phi \right]^2 \\
\mathcal{P}_{16}(h), \mathcal{P}_{25}(h) &\rightarrow \left(D^\nu \Phi^\dagger D_\mu D^\mu \Phi - D_\mu D^\mu \Phi^\dagger D^\nu \Phi \right) \left(\Phi^\dagger \overleftrightarrow{D}_\nu \Phi \right)
\end{aligned} \tag{C.2}$$

For operators weighted by ξ^4 :

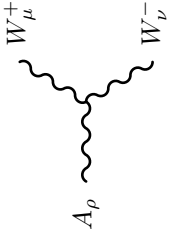
$$\mathcal{P}_{26}(h) \rightarrow \left[\left(\Phi^\dagger \overleftrightarrow{D}_\mu \Phi \right) \left(\Phi^\dagger \overleftrightarrow{D}_\nu \Phi \right) \right]^2. \tag{C.3}$$

D Feynman rules

This Appendix provides a complete list of all the Feynman rules resulting from the operators discussed here in the Lagrangian \mathcal{L}_{chiral} of Eq. (2.1) (except for the pure Higgs ones weighted by powers of ξ higher than one). Only diagrams with up to four legs are shown and the notation $\mathcal{F}_i(h) = 1 + 2\tilde{a}_i h/v + \tilde{b}_i h^2/v^2 + \dots$ has been adopted. Moreover, for brevity, the products $c_i \tilde{a}_i$ and $c_i \tilde{b}_i$ have been redefined as a_i and b_i , respectively. For the operators \mathcal{P}_8 , and \mathcal{P}_{20-22} , that contain two functions $\mathcal{F}_X(h)$ and $\mathcal{F}'_X(h)$ we redefine $c_X \tilde{a}_X \tilde{a}'_X \rightarrow a_X$. In all Feynman diagrams

the momenta are chosen to be flowing inwards in the vertices and are computed in the unitary gauge, with the exception of the propagator of the photon which is written in a generic gauge.

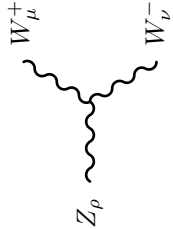
Finally, the standard (that is SM-like) and non-standard Lorentz structures are reported in two distinct columns, on the left and on the right, respectively. Greek indices indicate flavour and are assumed to be summed over when repeated; whenever they do not appear, it should be understood that the vertex is flavour diagonal. All the quantities entering the Feynman diagrams can be expressed in terms of the parameters of the Z -renormalization scheme, as shown in Eq. (4.2).

(FR.7) 

$$ie[g_{\mu\nu}(p_+ - p_-)_\rho - g_{\nu\rho}p_{-\mu} + g_{\mu\rho}p_{+\nu}]$$

$$-ieg^2\xi(p_+^\mu g_{\nu\rho} - p_-^\nu g_{\mu\rho})c_9$$

$$-ie[-g_{\mu\rho}p_{A\nu} + g_{\nu\rho}p_{A\mu}](1 - g^2\xi(2c_1 - 2c_2 - c_3) + 2g^2\xi^2(c_{13} - 2c_{12}))$$

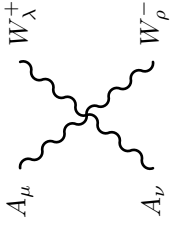
(FR.8) 

$$igc_\theta [g_{\mu\nu}(p_+ - p_-)_\rho - g_{\nu\rho}p_{-\mu} + g_{\mu\rho}p_{+\nu}] \left(1 + \frac{\xi c_T}{c_\theta^2 - s_\theta^2} + \frac{g^2\xi c_3}{c_\theta^2} + \frac{2e^2\xi c_1}{c_\theta^2(c_\theta^2 - s_\theta^2)} \right)$$

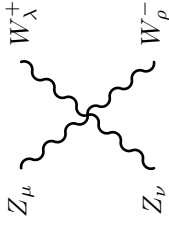
$$-\varepsilon^{\mu\nu\rho\lambda}[p_{+\lambda} - p_{-\lambda}] \frac{g^3\xi^2 c_{14}}{c_\theta}$$

$$-igc_\theta [-g_{\mu\rho}p_{Z\nu} + g_{\nu\rho}p_{Z\mu}] \left(1 + \frac{\xi(c_T + 4e^2c_1)}{c_\theta^2 - s_\theta^2} + \xi g^2 c_3 - \frac{2e^2\xi c_2}{c_\theta^2} + 2g^2\xi^2(c_{13} - 2c_{12}) \right)$$

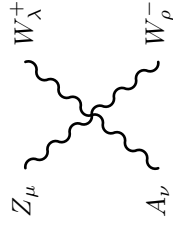
$$+\frac{ig^3\xi}{c_\theta^2}[p_+^\mu g_{\nu\rho} - p_-^\nu g_{\mu\rho}](s_\theta^2 c_9 - \xi c_{16})$$

(FR.9) 

$$-ie^2[2g_{\mu\nu}g_{\lambda\rho} - (g_{\lambda\mu}g_{\rho\nu} + g_{\lambda\nu}g_{\rho\mu})](1 - g^2\xi c_9)]$$

(FR.10) 

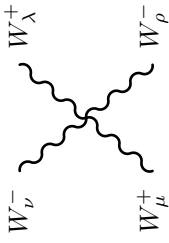
$$-ig^2c_\theta^2 \left(1 + \frac{2\xi c_T}{c_\theta^2 - s_\theta^2} + \frac{4e^2\xi c_1}{c_\theta^2(c_\theta^2 - s_\theta^2)} + \frac{2g^2\xi c_3}{c_\theta^2} \right) \left[2g_{\mu\nu}g_{\lambda\rho} \left(1 - \frac{g^2\xi c_6}{c_\theta^4} - \frac{g^2\xi^2 c_{23}}{c_\theta^4} \right) - (g_{\lambda\mu}g_{\rho\nu} + g_{\lambda\nu}g_{\rho\mu}) \left(1 + \frac{\xi(-e^2s_\theta^2c_9 + g^2\xi c_{11} + 2e^2\xi c_{16})}{c_\theta^4} + \frac{g^2\xi^2 c_{24}}{c_\theta^4} \right) \right]$$

(FR.11) 

$$-iegc_\theta \left(1 + \frac{\xi c_T}{c_\theta^2 - s_\theta^2} + \frac{2\xi e^2 c_1}{c_\theta^2(c_\theta^2 - s_\theta^2)} + \frac{g^2\xi c_3}{c_\theta^2} \right) \cdot$$

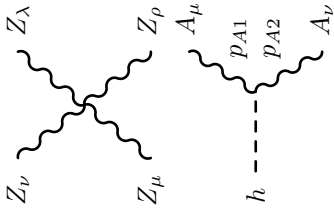
$$-\varepsilon^{\mu\nu\rho\lambda} \frac{2eg^3\xi^2 c_{14}}{c_\theta}$$

$$\cdot \left[2g_{\mu\nu}g_{\lambda\rho} - (g_{\lambda\nu}g_{\rho\mu} + g_{\lambda\mu}g_{\rho\nu}) \left(1 + \frac{\xi(e^2c_9 - g^2\xi c_{16})}{c_\theta^2} \right) \right]$$



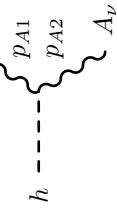
(FR.12)

$$ig^2 \left(1 + \frac{2\xi(c_T c_\theta^2 + 2e^2 c_1)}{c_\theta^2 - s_\theta^2} + 2g^2 \xi c_3 \right) \cdot \left[- (g_{\mu\nu} g_{\lambda\rho} + g_{\lambda\nu} g_{\mu\rho}) (1 + g^2 \xi (-2c_6 - \xi c_{11} - 8\xi c_{12} + 4\xi c_{13})) + 2g_{\lambda\mu} g_{\nu\rho} (1 + g^2 \xi^2 (c_{11} - 8c_{12} + 4c_{13})) \right]$$



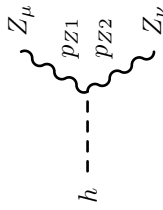
(FR.13)

$$\frac{ig^4 \xi}{c_\theta^4} [g_{\mu\nu} g_{\lambda\rho} + g_{\mu\lambda} g_{\nu\rho} + g_{\mu\rho} g_{\nu\lambda}] (c_6 + \xi(c_{11} + 2c_{23} + 2c_{24}) + 4\xi^3 c_{26})$$



(FR.14)

$$i \frac{8e^2 \xi}{v} [g^{\mu\nu} p_{A1} \cdot p_{A2} - p_{A1}^\nu p_{A2}^\mu] \left(\frac{a_B + a_W}{4} - a_1 - \xi a_{12} \right)$$

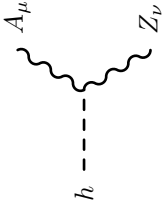


(FR.15)

$$2i \frac{m_Z^2}{v} g^{\mu\nu} \left(1 - \frac{\xi c_H}{2} + \frac{\xi}{2} (2a_C - c_C) - 2\xi (a_T - c_T) \right) \\ - \frac{ie^2 \xi}{v} [p_{Z1}^\nu p_h^\mu + p_{Z2}^\mu p_h^\nu - (p_{Z1} + p_{Z2}) \cdot p_h g^{\mu\nu}] \left(\frac{2a_4}{c_\theta^2} - \frac{a_5 + 2\xi a_{17}}{s_\theta^2} \right) \\ + \frac{2ig^2 \xi}{vc_\theta^2} g_{\mu\nu} p_h^2 (2a_7 + 4\xi a_{25}) + \frac{2ig^2 \xi}{vc_\theta^2} p_{Z1}^\mu p_{Z2}^\nu (a_9 + 2\xi a_{15}) \\ + \frac{ig^2 \xi}{vc_\theta^2} [p_{Z1}^\mu p_h^\nu + p_{Z2}^\nu p_h^\mu] (a_{10} + 2\xi a_{19})$$

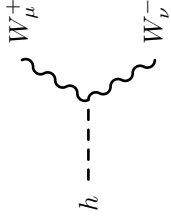
standard structure

non-standard structure



(FR.16)

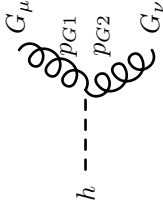
$$\begin{aligned}
 & -\frac{2ig^2c_\theta s_\theta \xi}{v} [g^{\mu\nu}(p_A \cdot p_Z) - p_A^\nu p_Z^\mu] \cdot \\
 & \cdot \left(a_B \frac{s_\theta^2}{c_\theta^2} - a_W + 2a_1 \frac{c_\theta^2 - s_\theta^2}{c_\theta^2} + 4\xi a_{12} \right) \\
 & + \frac{ieg\xi}{vc_\theta} [p_A^\nu p_h^\mu - p_A \cdot p_h g^{\mu\nu}] (2a_4 + a_5 + 2\xi a_{17})
 \end{aligned}$$



(FR.17)

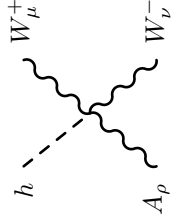
$$\begin{aligned}
 & i \frac{2m_Z^2 c_\theta^2}{v} g_{\mu\nu} \left(1 - \frac{\xi c_H}{2} + \frac{\xi}{2} (2a_C - c_C) + \frac{4e^2 \xi c_1}{(c_\theta^2 - s_\theta^2)} \right) \\
 & + \frac{2c_\theta^2 \xi c_T}{(c_\theta^2 - s_\theta^2)} - 4g^2 \xi^2 c_{12}
 \end{aligned}$$

$$\begin{aligned}
 & \frac{ig^2 \xi}{v} [2g^{\mu\nu}(p_+ \cdot p_-) - 2p_+^\nu p_-^\mu] a_W \\
 & - \frac{ig^2 \xi}{v} [(p_+^\nu p_h^\mu + p_-^\mu p_h^\nu) - (p_+ + p_-) \cdot p_h g^{\mu\nu}] a_5 \\
 & + \frac{2ig^2 \xi}{v} g_{\mu\nu} p_h^2 a_7 + \frac{2ig^2 \xi}{v} p_+^\mu p_-^\nu a_9 + \frac{ig^2 \xi}{v} (p_+^\mu p_h^\nu + p_-^\nu p_h^\mu) c_{10}
 \end{aligned}$$



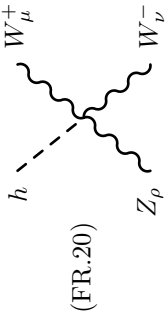
(FR.18)

$$i \frac{2g_s^2 \xi}{v} [g^{\mu\nu} p_{G1} \cdot p_{G2} - p_{G1}^\nu p_{G2}^\mu] a_G$$



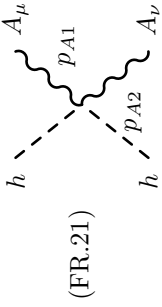
(FR.19)

$$\begin{aligned}
 & -\frac{2ieg^2 \xi}{v} [g_{\mu\nu}(p_+ - p_-)_\rho + g_{\mu\rho} p_{-\nu} + g_{\nu\rho} p_{+\mu}] a_W \\
 & -\frac{2ieg^2 \xi}{v} [-g_{\mu\rho} p_{A\nu} + g_{\nu\rho} p_{A\mu}] (a_W - 2a_1 + 2a_2 + a_3 + 2\xi(a_{13} - 2a_{12})) \\
 & -\frac{ieg^2 \xi}{v} [g_{\mu\rho} p_{h\nu} - g_{\nu\rho} p_{h\mu}] (a_5 - a_{10}) - \frac{2ieg^2 \xi}{v} (p_+^\mu g_{\nu\rho} - p_-^\nu g_{\mu\rho}) a_9
 \end{aligned}$$



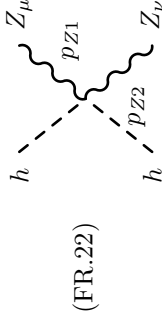
(FR.20)

$$\begin{aligned}
 & -\frac{2ig^3c_\theta\xi}{v}[g_{\mu\nu}(p_+ - p_-)_\rho + g_{\mu\rho}p_{-\nu} + g_{\nu\rho}p_{+\mu}]\left(a_W + \frac{a_3}{c_\theta}\right) \\
 & -\frac{2ig^3c_\theta\xi}{v}[-g_{\mu\rho}p_{Z\nu} + g_{\nu\rho}p_{Z\mu}]\left(a_W + a_3 + 2\frac{s_\theta^2}{c_\theta^2}(a_1 - a_2) + 2\xi(a_{13} - 2a_{12})\right) \\
 & +\frac{ige^2\xi}{vc_\theta}[g_{\mu\rho}p_{h\nu} - g_{\nu\rho}p_{h\mu}]\left(a_5 - a_{10} + \frac{2\xi(a_{17} + a_{18})}{s_\theta^2}\right) \\
 & +\frac{i2g^3\xi}{vc_\theta^2}[p_+^\mu g_{\nu\rho} - p_-^\nu g_{\mu\rho}](s_\theta^2 a_9 - \xi a_{16}) - \frac{2g^3\xi^2}{vc_\theta}\varepsilon^{\mu\nu\rho\lambda}[p_{+\lambda} - p_{-\lambda}]a_{14}
 \end{aligned}$$



(FR.21)

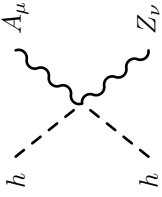
$$i\frac{8e^2\xi}{v^2}[g^{\mu\nu}p_{A1} \cdot p_{A2} - p_{A1}^\nu p_{A2}^\mu]\left(\frac{b_B + b_W}{4} - b_1 - \xi b_{12}\right)$$



(FR.22)

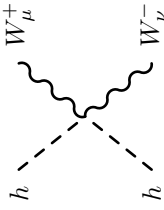
$$\begin{aligned}
 & i\frac{2g^2c_\theta^2\xi}{v^2}[g^{\mu\nu}p_{Z1} \cdot p_{Z2} - p_{Z1}^\nu p_{Z2}^\mu]\left(b_B\frac{s_\theta^4}{c_\theta^4} + b_W + 4\frac{s_\theta^2}{c_\theta^2}b_1 - \xi b_{12}\right) \\
 & -\frac{ie^2\xi}{v^2}[p_{Z1}^\nu(p_{h1} + p_{h2})^\mu + p_{Z2}^\mu(p_{h1} + p_{h2})^\nu - (p_{Z1} + p_{Z2}) \cdot (p_{h1} + p_{h2})g^{\mu\nu}]\left(\frac{2b_4}{c_\theta^2} - \frac{b_5 + 2\xi b_{17}}{s_\theta^2}\right) \\
 & +\frac{2ig^2\xi}{v^2c_\theta^2}g_{\mu\nu}\left[2p_{h1} \cdot p_{h2}(b_7 + 2\xi a_{20} + 4\xi a_{21} + 2\xi b_{25}) + (p_{h1}^2 + p_{h2}^2)(b_7 + 2\xi b_{25})\right] \\
 & +\frac{2ig^2\xi}{v^2c_\theta^2}p_{Z1}^\mu p_{Z2}^\nu(b_9 + 2\xi b_{15}) + \frac{4ig^2\xi}{v^2c_\theta^2}[p_{h1}^\mu p_{h2}^\nu + p_{h1}^\nu p_{h2}^\mu](a_8 + 2\xi a_{22}) \\
 & +\frac{ig^2\xi}{v^2c_\theta^2}[p_{Z1}^\mu(p_{h1} + p_{h2})^\nu + p_{Z2}^\nu(p_{h1} + p_{h2})^\mu](b_{10} + 2\xi b_{19})
 \end{aligned}$$

$$i\frac{2m_Z^2}{v^2}g^{\mu\nu}(1 - \xi c_H + \xi b_C - 2\xi(b_T - c_T))$$



(FR.23)

$$\begin{aligned} & \frac{-2ig^2 c_\theta s_\theta \xi}{v^2} [g^{\mu\nu} (p_A \cdot p_Z) - p_A^\nu p_Z^\mu] \cdot \\ & \cdot \left(b_B \frac{s_\theta^2}{c_\theta^2} - b_W + 2b_1 \frac{c_\theta^2 - s_\theta^2}{c_\theta^2} + 4\xi b_{12} \right) \\ & + \frac{ieg\xi}{v^2 c_\theta} [p_A^\nu (p_{h1} + p_{h2})^\mu - p_A \cdot (p_{h1} + p_{h2}) g^{\mu\nu}] (2b_4 + b_5 + 2\xi b_{17}) \end{aligned}$$



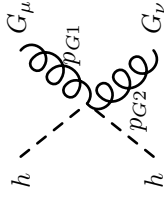
(FR.24)

$$\begin{aligned} & i \frac{2m_Z^2 c_\theta^2}{v^2} g_{\mu\nu} \left(1 - \xi c_H + \xi b_C + \frac{4e^2 \xi c_1}{(c_\theta^2 - s_\theta^2)} \right) \\ & + \frac{2c_\theta^2 \xi c_T}{(c_\theta^2 - s_\theta^2)} - 4g^2 \xi^2 c_{12} \end{aligned}$$

$$\frac{i\xi}{v^2} [2g^{\mu\nu} (p_+ \cdot p_-) - 2p_+^\nu p_-^\mu] g^2 b_W + \frac{2ig^2 \xi}{v^2} p_+^\mu p_-^\nu b_9$$

$$\begin{aligned} & + \frac{ig^2 \xi}{v^2} [p_+^\nu (p_{h1} + p_{h2})^\mu + p_-^\mu (p_{h1} + p_{h2})^\nu - (p_+ + p_-) \cdot (p_{h1} + p_{h2}) g^{\mu\nu}] b_5 \\ & + \frac{2ig^2 \xi}{v^2} g_{\mu\nu} [2p_{h1} \cdot p_{h2} (b_7 + 2\xi a_{20}) + (p_{h1}^2 + p_{h2}^2) b_7] \\ & + \frac{4ig^2 \xi}{v^2} [p_{h1}^\mu p_{h2}^\nu + p_{h1}^\nu p_{h2}^\mu] a_8 \end{aligned}$$

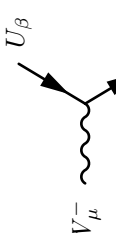
$$+ \frac{ig^2 \xi}{v^2} [p_+^\mu (p_{h1} + p_{h2})^\nu + p_-^\nu (p_{h1} + p_{h2})^\mu] b_{10}$$

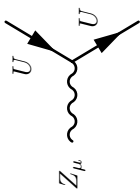


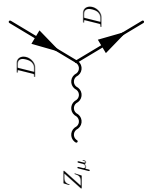
(FR.25)

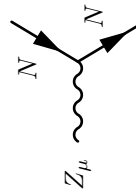
$$i \frac{2g_s^2 \xi}{v^2} [g^{\mu\nu} p_{G1} \cdot p_{G2} - p_{G1}^\nu p_{G2}^\mu] b_G$$

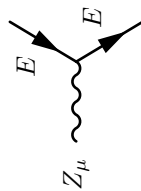
(FR.26)  $q_U = \frac{2}{3}, q_D = -\frac{1}{3}, q_N = 0, q_E = -1$
 $-ieq_f \gamma_\mu;$

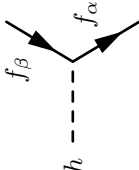
(FR.27)  $\frac{ig}{\sqrt{2}} \frac{\gamma_\mu (1 - \gamma_5)}{2} (V^\dagger)_{\alpha\beta} \left(1 + \frac{\xi(c_T c_\theta^2 + 2e^2 c_1)}{c_\theta^2 - s_\theta^2} - 2g^2 \xi^2 c_{12} \right)$

(FR.28)  $\frac{igc_\theta}{2} \left(\frac{s_\theta^2}{3c_\theta^2} - 1 \right) \frac{\gamma_\mu (1 - \gamma_5)}{2} \left[1 + \frac{8\xi e^2 c_1}{(c_\theta^2 - s_\theta^2)(1 + 2(c_\theta^2 - s_\theta^2))} + \frac{\xi c_T}{c_\theta^2 - s_\theta^2} \frac{1 + 2c_\theta^2}{1 + 2(c_\theta^2 - s_\theta^2)} \right]$
 $\frac{2}{3} \frac{ie}{c_\theta} \frac{s_\theta \gamma_\mu (1 + \gamma_5)}{2} \left[1 - \frac{\xi(c_T + 2g^2 c_1)}{c_\theta^2 - s_\theta^2} \right]$

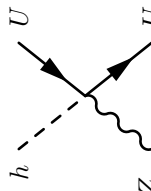
(FR.29)  $\frac{igc_\theta}{2} \left(\frac{s_\theta^2}{3c_\theta^2} + 1 \right) \frac{\gamma_\mu (1 - \gamma_5)}{2} \left[1 + \frac{\xi 4e^2 c_1}{(c_\theta^2 - s_\theta^2)(2 + (c_\theta^2 - s_\theta^2))} + \frac{\xi c_T}{c_\theta^2 - s_\theta^2} \frac{4c_\theta^2 - 1}{2 + (c_\theta^2 - s_\theta^2)} \right]$
 $-\frac{1}{3} \frac{ie}{c_\theta} \frac{s_\theta \gamma_\mu (1 + \gamma_5)}{2} \left[1 - \frac{\xi(c_T + 2g^2 c_1)}{c_\theta^2 - s_\theta^2} \right]$

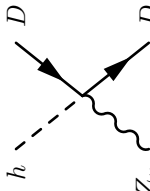
(FR.30)  $-\frac{ig}{2c_\theta} \frac{\gamma_\mu (1 - \gamma_5)}{2} \left[1 + \frac{\xi 4e^2 c_1}{(c_\theta^2 - s_\theta^2)(2 + (c_\theta^2 - s_\theta^2))} + \frac{\xi c_T}{c_\theta^2 - s_\theta^2} \frac{4c_\theta^2 - 1}{2 + (c_\theta^2 - s_\theta^2)} \right]$

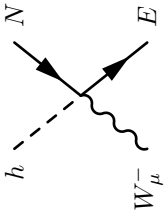
(FR.31)  $\frac{ig(c_\theta^2 - s_\theta^2)}{2c_\theta} \frac{\gamma_\mu (1 - \gamma_5)}{2} \left[1 + \frac{\xi 4e^2 c_1}{(c_\theta^2 - s_\theta^2)(2 + (c_\theta^2 - s_\theta^2))} + \frac{\xi c_T}{c_\theta^2 - s_\theta^2} \frac{4c_\theta^2 - 1}{2 + (c_\theta^2 - s_\theta^2)} \right]$
 $-ie \frac{s_\theta}{c_\theta} \frac{\gamma_\mu (1 + \gamma_5)}{2} \left[1 - \frac{\xi(c_T + 2g^2 c_1)}{c_\theta^2 - s_\theta^2} \right]$

(FR.32) 
$$-i \frac{s_Y}{\sqrt{2}} Y_{f,\alpha\beta} \left(1 - \frac{\xi_{CH}}{2} \right), \quad f = U, D, E$$

(FR.33) 
$$\frac{\sqrt{2} i g \xi}{v} \frac{\gamma_\mu (1 - \gamma_5)}{2} (V^\dagger)_{\alpha\beta} \left(\frac{a_T c_\theta^2 + 2e^2 a_1}{c_\theta^2 - s_\theta^2} - 2g^2 \xi a_{12} \right)$$

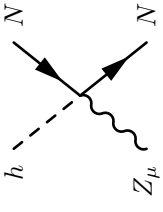
(FR.34) 
$$\frac{i g \xi c_\theta}{v} \left(\frac{s_\theta^2}{3c_\theta^2} - 1 \right) \frac{\gamma_\mu (1 - \gamma_5)}{2} \left[\frac{8e^2 a_1}{(c_\theta^2 - s_\theta^2)(1 + 2(c_\theta^2 - s_\theta^2))} + \frac{a_T}{c_\theta^2 - s_\theta^2} \frac{1 + 2c_\theta^2}{1 + 2(c_\theta^2 - s_\theta^2)} \right] + \frac{4ie\xi s_\theta}{3} \frac{\gamma_\mu (1 + \gamma_5)}{2} \left[\frac{a_T + 2g^2 a_1}{c_\theta^2 - s_\theta^2} \right]$$

(FR.35) 
$$\frac{i \xi g c_\theta}{v} \left(\frac{s_\theta^2}{3c_\theta^2} + 1 \right) \frac{\gamma_\mu (1 - \gamma_5)}{2} \left[\frac{4e^2 a_1}{(c_\theta^2 - s_\theta^2)(2 + (c_\theta^2 - s_\theta^2))} + \frac{a_T}{c_\theta^2 - s_\theta^2} \frac{4c_\theta^2 - 1}{2 + (c_\theta^2 - s_\theta^2)} \right] - \frac{2ie\xi s_\theta}{3} \frac{\gamma_\mu (1 + \gamma_5)}{2} \left[\frac{a_T + 2g^2 a_1}{c_\theta^2 - s_\theta^2} \right]$$



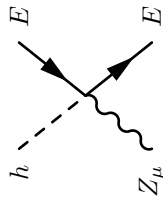
(FR.36)

$$\frac{\sqrt{2}ig\xi}{v} \frac{\gamma_\mu(1-\gamma_5)}{2} \left(\frac{a_T c_\theta^2 + 2e^2 a_1}{c_\theta^2 - s_\theta^2} - 2g^2 \xi a_{12} \right)$$



(FR.37)

$$-\frac{ig\xi}{vc_\theta} \frac{\gamma_\mu(1-\gamma_5)}{2} \left[\frac{8e^2 a_1}{(c_\theta^2 - s_\theta^2)(1+2(c_\theta^2 - s_\theta^2))} + \frac{a_T}{c_\theta^2 - s_\theta^2} \frac{1+2c_\theta^2}{1+2(c_\theta^2 - s_\theta^2)} \right]$$



(FR.38)

$$\frac{i\xi g(c_\theta^2 - s_\theta^2)}{vc_\theta} \frac{\gamma_\mu(1-\gamma_5)}{2} \left[\frac{4e^2 a_1}{(c_\theta^2 - s_\theta^2)(2+(c_\theta^2 - s_\theta^2))} + \frac{a_T}{c_\theta^2 - s_\theta^2} \frac{4c_\theta^2 - 1}{c_\theta^2 - s_\theta^2} \right] - \frac{i\xi e s_\theta}{v c_\theta} \frac{\gamma_\mu(1+\gamma_5)}{2} \left[\frac{a_T + 2g^2 a_1}{c_\theta^2 - s_\theta^2} \right]$$

References

- [1] F. Englert and R. Brout, *Broken Symmetry and the Mass of Gauge Vector Mesons*, Phys.Rev.Lett. **13** (1964) 321–323.
- [2] P. W. Higgs, *Broken Symmetries, Massless Particles and Gauge Fields*, Phys.Lett. **12** (1964) 132–133.
- [3] P. W. Higgs, *Broken Symmetries and the Masses of Gauge Bosons*, Phys.Rev.Lett. **13** (1964) 508–509.
- [4] K. Hagiwara, R. Peccei, D. Zeppenfeld, and K. Hikasa, *Probing the Weak Boson Sector in $e^+e^- \rightarrow W^+W^-$* , Nucl.Phys. **B282** (1987) 253.
- [5] W. Buchmuller and D. Wyler, *Effective Lagrangian Analysis of New Interactions and Flavor Conservation*, Nucl.Phys. **B268** (1986) 621.
- [6] B. Grzadkowski, M. Iskrzynski, M. Misiak, and J. Rosiek, *Dimension-Six Terms in the Standard Model Lagrangian*, JHEP **1010** (2010) 085, [[arXiv:1008.4884](#)].
- [7] K. Hagiwara, R. Szalapski, and D. Zeppenfeld, *Anomalous Higgs boson production and decay*, Phys.Lett. **B318** (1993) 155–162, [[hep-ph/9308347](#)].
- [8] M. Gonzalez-Garcia, *Anomalous Higgs couplings*, Int.J.Mod.Phys. **A14** (1999) 3121–3156, [[hep-ph/9902321](#)].
- [9] T. Corbett, O. Eboli, J. Gonzalez-Fraile, and M. Gonzalez-Garcia, *Constraining anomalous Higgs interactions*, Phys.Rev. **D86** (2012) 075013, [[arXiv:1207.1344](#)].
- [10] T. Corbett, O. Eboli, J. Gonzalez-Fraile, and M. Gonzalez-Garcia, *Robust Determination of the Higgs Couplings: Power to the Data*, Phys.Rev. **D87** (2013) 015022, [[arXiv:1211.4580](#)].
- [11] **ATLAS** Collaboration, G. Aad *et. al.*, *Observation of a New Particle in the Search for the Standard Model Higgs Boson with the Atlas Detector at the LHC*, Phys.Lett. **B716** (2012) 1–29, [[arXiv:1207.7214](#)].
- [12] **CMS** Collaboration, S. Chatrchyan *et. al.*, *Observation of a New Boson at a Mass of 125 GeV with the Cms Experiment at the LHC*, Phys.Lett. **B716** (2012) 30–61, [[arXiv:1207.7235](#)].
- [13] I. Low, J. Lykken, and G. Shaughnessy, *Have We Observed the Higgs (Imposter)?*, Phys.Rev. **D86** (2012) 093012, [[arXiv:1207.1093](#)].
- [14] J. Ellis and T. You, *Global Analysis of the Higgs Candidate with Mass 125 GeV*, JHEP **1209** (2012) 123, [[arXiv:1207.1693](#)].
- [15] P. P. Giardino, K. Kannike, M. Raidal, and A. Strumia, *Is the Resonance at 125 GeV the Higgs Boson?*, Phys.Lett. **B718** (2012) 469–474, [[arXiv:1207.1347](#)].

- [16] M. Montull and F. Riva, *Higgs Discovery: the Beginning Or the End of Natural Ewsb?*, JHEP **1211** (2012) 018, [[arXiv:1207.1716](#)].
- [17] J. Espinosa, C. Grojean, M. Muhlleitner, and M. Trott, *First Glimpses at Higgs' Face*, JHEP **1212** (2012) 045, [[arXiv:1207.1717](#)].
- [18] D. Carmi, A. Falkowski, E. Kuflik, T. Volansky, and J. Zupan, *Higgs After the Discovery: a Status Report*, JHEP **1210** (2012) 196, [[arXiv:1207.1718](#)].
- [19] S. Banerjee, S. Mukhopadhyay, and B. Mukhopadhyaya, *New Higgs Interactions and Recent Data from the LHC and the Tevatron*, JHEP **1210** (2012) 062, [[arXiv:1207.3588](#)].
- [20] F. Bonnet, T. Ota, M. Rauch, and W. Winter, *Interpretation of Precision Tests in the Higgs Sector in Terms of Physics Beyond the Standard Model*, Phys.Rev. **D86** (2012) 093014, [[arXiv:1207.4599](#)].
- [21] T. Plehn and M. Rauch, *Higgs Couplings After the Discovery*, Europhys.Lett. **100** (2012) 11002, [[arXiv:1207.6108](#)].
- [22] A. Djouadi, *Precision Higgs Coupling Measurements at the LHC Through Ratios of Production Cross Sections*, [arXiv:1208.3436](#).
- [23] B. Batell, S. Gori, and L.-T. Wang, *Higgs Couplings and Precision Electroweak Data*, JHEP **1301** (2013) 139, [[arXiv:1209.6382](#)].
- [24] G. Moreau, *Constraining Extra-Fermion(S) from the Higgs Boson Data*, Phys.Rev. **D87** (2013) 015027, [[arXiv:1210.3977](#)].
- [25] G. Cacciapaglia, A. Deandrea, G. D. La Rochelle, and J.-B. Flament, *Higgs Couplings Beyond the Standard Model*, JHEP **1303** (2013) 029, [[arXiv:1210.8120](#)].
- [26] A. Azatov and J. Galloway, *Electroweak Symmetry Breaking and the Higgs Boson: Confronting Theories at Colliders*, Int.J.Mod.Phys. **A28** (2013) 1330004, [[arXiv:1212.1380](#)].
- [27] E. Masso and V. Sanz, *Limits on Anomalous Couplings of the Higgs to Electroweak Gauge Bosons from LEP and LHC*, Phys.Rev. **D87** (2013), no. 3 033001, [[arXiv:1211.1320](#)].
- [28] G. Passarino, *NLO Inspired Effective Lagrangians for Higgs Physics*, Nucl.Phys. **B868** (2013) 416–458, [[arXiv:1209.5538](#)].
- [29] A. Falkowski, F. Riva, and A. Urbano, *Higgs at Last*, [arXiv:1303.1812](#).
- [30] P. P. Giardino, K. Kannike, I. Masina, M. Raidal, and A. Strumia, *The Universal Higgs Fit*, [arXiv:1303.3570](#).
- [31] J. Ellis and T. You, *Updated Global Analysis of Higgs Couplings*, JHEP **1306** (2013) 103, [[arXiv:1303.3879](#)].

- [32] A. Djouadi and G. Moreau, *The Couplings of the Higgs Boson and Its CP Properties from Fits of the Signal Strengths and Their Ratios at the 7+8 TeV LHC*, [arXiv:1303.6591](#).
- [33] R. Contino, M. Ghezzi, C. Grojean, M. Muhlleitner, and M. Spira, *Effective Lagrangian for a Light Higgs-Like Scalar*, JHEP **1307** (2013) 035, [[arXiv:1303.3876](#)].
- [34] B. Dumont, S. Fichet, and G. von Gersdorff, *A Bayesian view of the Higgs sector with higher dimensional operators*, JHEP **1307** (2013) 065, [[arXiv:1304.3369](#)].
- [35] J. Elias-Miro, J. Espinosa, E. Masso, and A. Pomarol, *Higgs Windows to New Physics Through $D = 6$ Operators: Constraints and One-Loop Anomalous Dimensions*, [arXiv:1308.1879](#).
- [36] D. Lopez-Val, T. Plehn, and M. Rauch, *Measuring Extended Higgs Sectors as a Consistent Free Couplings Model*, JHEP **1310** (2013) 134, [[arXiv:1308.1979](#)].
- [37] E. E. Jenkins, A. V. Manohar, and M. Trott, *Renormalization Group Evolution of the Standard Model Dimension Six Operators I: Formalism and λ Dependence*, JHEP **1310** (2013) 087, [[arXiv:1308.2627](#)].
- [38] A. Pomarol and F. Riva, *Towards the Ultimate S_m Fit to Close in on Higgs Physics*, [arXiv:1308.2803](#).
- [39] S. Banerjee, S. Mukhopadhyay, and B. Mukhopadhyaya, *Higher dimensional operators and LHC Higgs data : the role of modified kinematics*, [arXiv:1308.4860](#).
- [40] A. Alloul, B. Fuks, and V. Sanz, *Phenomenology of the Higgs Effective Lagrangian via FeynRules*, [arXiv:1310.5150](#).
- [41] D. B. Kaplan and H. Georgi, *$SU(2) \times U(1)$ Breaking by Vacuum Misalignment*, Phys.Lett. **B136** (1984) 183.
- [42] D. B. Kaplan, H. Georgi, and S. Dimopoulos, *Composite Higgs Scalars*, Phys. Lett. **B136** (1984) 187.
- [43] T. Banks, *Constraints on $SU(2) \times U(1)$ Breaking by Vacuum Misalignment*, Nucl.Phys. **B243** (1984) 125.
- [44] H. Georgi, D. B. Kaplan, and P. Galison, *Calculation of the Composite Higgs Mass*, Phys.Lett. **B143** (1984) 152.
- [45] H. Georgi and D. B. Kaplan, *Composite Higgs and Custodial $SU(2)$* , Phys.Lett. **B145** (1984) 216.
- [46] M. J. Dugan, H. Georgi, and D. B. Kaplan, *Anatomy of a Composite Higgs Model*, Nucl.Phys. **B254** (1985) 299.

- [47] K. Agashe, R. Contino, and A. Pomarol, *The Minimal Composite Higgs Model*, Nucl.Phys. **B719** (2005) 165–187, [[hep-ph/0412089](#)].
- [48] R. Contino, L. Da Rold, and A. Pomarol, *Light Custodians in Natural Composite Higgs Models*, Phys.Rev. **D75** (2007) 055014, [[hep-ph/0612048](#)].
- [49] B. Gripaios, A. Pomarol, F. Riva, and J. Serra, *Beyond the Minimal Composite Higgs Model*, JHEP **0904** (2009) 070, [[arXiv:0902.1483](#)].
- [50] D. Marzocca, M. Serone, and J. Shu, *General Composite Higgs Models*, JHEP **1208** (2012) 013, [[arXiv:1205.0770](#)].
- [51] N. Arkani-Hamed, A. G. Cohen, and H. Georgi, *Electroweak Symmetry Breaking from Dimensional Deconstruction*, Phys.Lett. **B513** (2001) 232–240, [[hep-ph/0105239](#)].
- [52] M. Schmaltz and D. Tucker-Smith, *Little Higgs Review*, Ann.Rev.Nucl.Part.Sci. **55** (2005) 229–270, [[hep-ph/0502182](#)].
- [53] C. G. Callan, S. Coleman, J. Wess, and B. Zumino, *Structure of Phenomenological Lagrangians. II*, Phys. Rev. **177** (Jan, 1969) 2247–2250.
- [54] L. Susskind, *Dynamics of Spontaneous Symmetry Breaking in the Weinberg- Salam Theory*, Phys. Rev. **D20** (1979) 2619–2625.
- [55] S. Dimopoulos and L. Susskind, *Mass without Scalars*, Nucl. Phys. **B155** (1979) 237–252.
- [56] S. Dimopoulos and J. Preskill, *Massless Composites with Massive Constituents*, Nucl.Phys. **B199** (1982) 206.
- [57] B. Grinstein and M. Trott, *A Higgs-Higgs Bound State Due to New Physics at a TeV*, Phys.Rev. **D76** (2007) 073002, [[arXiv:0704.1505](#)].
- [58] R. Contino, C. Grojean, M. Moretti, F. Piccinini, and R. Rattazzi, *Strong Double Higgs Production at the LHC*, JHEP **1005** (2010) 089, [[arXiv:1002.1011](#)].
- [59] J. Bagger, V. D. Barger, K.-m. Cheung, J. F. Gunion, T. Han, *et. al.*, *The Strongly Interacting $W W$ System: Gold Plated Modes*, Phys.Rev. **D49** (1994) 1246–1264, [[hep-ph/9306256](#)].
- [60] V. Koulovassilopoulos and R. S. Chivukula, *The Phenomenology of a Nonstandard Higgs Boson in $W_L W_L$ Scattering*, Phys.Rev. **D50** (1994) 3218–3234, [[hep-ph/9312317](#)].
- [61] C. Burgess, J. Matias, and M. Pospelov, *A Higgs Or Not a Higgs? What to Do If You Discover a New Scalar Particle*, Int.J.Mod.Phys. **A17** (2002) 1841–1918, [[hep-ph/9912459](#)].

- [62] A. Azatov, R. Contino, and J. Galloway, *Model-Independent Bounds on a Light Higgs*, JHEP **1204** (2012) 127, [[arXiv:1202.3415](#)].
- [63] R. Alonso, M. Gavela, L. Merlo, S. Rigolin, and J. Yepes, *The Effective Chiral Lagrangian for a Light Dynamical ‘Higgs’*, Phys.Lett. **B722** (2013) 330–335, [[arXiv:1212.3305](#)].
- [64] G. Buchalla, O. Cata, and C. Krause, *Complete Electroweak Chiral Lagrangian with a Light Higgs at NLO*, [arXiv:1307.5017](#).
- [65] R. Contino, D. Marzocca, D. Pappadopulo, and R. Rattazzi, *On the Effect of Resonances in Composite Higgs Phenomenology*, JHEP **1110** (2011) 081, [[arXiv:1109.1570](#)].
- [66] A. Manohar and H. Georgi, *Chiral Quarks and the Nonrelativistic Quark Model*, Nucl.Phys. **B234** (1984) 189.
- [67] E. E. Jenkins, A. V. Manohar, and M. Trott, *Naive Dimensional Analysis Counting of Gauge Theory Amplitudes and Anomalous Dimensions*, Phys. Lett. **B726** (2013) 697–702, [[arXiv:1309.0819](#)].
- [68] I. Brivio et al., *Composite-Higgs Models and Dynamical Higgs Effective Lagrangian*. In preparation.
- [69] M. S. Chanowitz, M. Golden, and H. Georgi, *Low-Energy Theorems for Strongly Interacting W’s and Z’s*, Phys.Rev. **D36** (1987) 1490.
- [70] C. Burgess and D. London, *On Anomalous Gauge Boson Couplings and Loop Calculations*, Phys.Rev.Lett. **69** (1992) 3428–3431.
- [71] C. Burgess and D. London, *Uses and Abuses of Effective Lagrangians*, Phys.Rev. **D48** (1993) 4337–4351, [[hep-ph/9203216](#)].
- [72] R. Alonso, M. Gavela, L. Merlo, S. Rigolin, and J. Yepes, *Minimal Flavour Violation with Strong Higgs Dynamics*, JHEP **1206** (2012) 076, [[arXiv:1201.1511](#)].
- [73] R. Alonso, M. Gavela, L. Merlo, S. Rigolin, and J. Yepes, *Flavor with a Light Dynamical “Higgs Particle”*, Phys.Rev. **D87** (2013) 055019, [[arXiv:1212.3307](#)].
- [74] G. Isidori and M. Trott, *Higgs Form Factors in Associated Production*, [arXiv:1307.4051](#).
- [75] G. Isidori, A. V. Manohar, and M. Trott, *Probing the nature of the Higgs-like Boson via $h \rightarrow VF$ decays*, [arXiv:1305.0663](#).
- [76] K. Hagiwara, S. Ishihara, R. Szalapski, and D. Zeppenfeld, *Low-Energy Effects of New Interactions in the Electroweak Boson Sector*, Phys.Rev. **D48** (1993) 2182–2203.

- [77] K. Hagiwara, T. Hatsukano, and S. S. R. Ishihara, *Probing nonstandard bosonic interactions via W boson pair production at lepton colliders*, Nucl.Phys. **B496** (1997) 66–102, [[hep-ph/9612268](#)].
- [78] T. Corbett, O. Eboli, J. Gonzalez-Fraile, and M. Gonzalez-Garcia, *Determining Triple Gauge Boson Couplings from Higgs Data*, Phys.Rev.Lett. **111** (2013) 011801, [[arXiv:1304.1151](#)].
- [79] A. Brunstein, O. J. Eboli, and M. Gonzalez-Garcia, *Constraints on quartic vector boson interactions from Z physics*, Phys.Lett. **B375** (1996) 233–239, [[hep-ph/9602264](#)].
- [80] A. Belyaev, O. J. Eboli, M. Gonzalez-Garcia, J. Mizukoshi, S. Novaes, *et. al.*, *Strongly interacting vector bosons at the CERN LHC: Quartic anomalous couplings*, Phys.Rev. **D59** (1999) 015022, [[hep-ph/9805229](#)].
- [81] O. J. Eboli, M. Gonzalez-Garcia, S. Lietti, and S. Novaes, *Anomalous quartic gauge boson couplings at hadron colliders*, Phys.Rev. **D63** (2001) 075008, [[hep-ph/0009262](#)].
- [82] O. Eboli, M. Gonzalez-Garcia, and S. Lietti, *Bosonic quartic couplings at CERN LHC*, Phys.Rev. **D69** (2004) 095005, [[hep-ph/0310141](#)].
- [83] O. Eboli, M. Gonzalez-Garcia, and J. Mizukoshi, *$pp \rightarrow jje^\pm\mu^\pm\nu\nu$ and $jje^\pm\mu^\pm\nu\nu$ at $\mathcal{O}(\alpha_{em}^6)$ and $\mathcal{O}(\alpha_{em}^4\alpha_s^2)$ for the study of the quartic electroweak gauge boson vertex at CERN LHC*, Phys.Rev. **D74** (2006) 073005, [[hep-ph/0606118](#)].
- [84] M. B. Gavela et al., *Bosonic Chiral Lagrangian for a light dynamical Higgs at next-to-leading order*. In preparation.
- [85] W. D. Goldberger, B. Grinstein, and W. Skiba, *Distinguishing the Higgs Boson from the Dilaton at the Large Hadron Collider*, Phys.Rev.Lett. **100** (2008) 111802, [[arXiv:0708.1463](#)].
- [86] G. Buchalla, O. Cata, and C. Krause, *On the Power Counting in Effective Field Theories*, [arXiv:1312.5624](#).
- [87] G. Giudice, C. Grojean, A. Pomarol, and R. Rattazzi, *The Strongly-Interacting Light Higgs*, JHEP **0706** (2007) 045, [[hep-ph/0703164](#)].
- [88] A. De Rujula, M. B. Gavela, P. Hernandez, and E. Masso, *The Selfcouplings of Vector Bosons: Does Lep-1 Obviate Lep-2?*, Nucl. Phys. **B384** (1992) 3–58.
- [89] E. Halyo, *Technidilaton Or Higgs?*, Mod.Phys.Lett. **A8** (1993) 275–284.
- [90] L. Vecchi, *Phenomenology of a Light Scalar: the Dilaton*, Phys.Rev. **D82** (2010) 076009, [[arXiv:1002.1721](#)].

- [91] B. A. Campbell, J. Ellis, and K. A. Olive, *Phenomenology and Cosmology of an Electroweak Pseudo-Dilaton and Electroweak Baryons*, JHEP **1203** (2012) 026, [[arXiv:1111.4495](#)].
- [92] S. Matsuzaki and K. Yamawaki, *Is 125 GeV Techni-Dilaton Found at LHC?*, [arXiv:1207.5911](#).
- [93] Z. Chacko, R. Franceschini, and R. K. Mishra, *Resonance at 125 GeV: Higgs Or Dilaton/Radion?*, [arXiv:1209.3259](#).
- [94] B. Bellazzini, C. Csaki, J. Hubisz, J. Serra, and J. Terning, *A Higgslike Dilaton*, [arXiv:1209.3299](#).
- [95] C. Grojean, O. Matsedonskyi, and G. Panico, *Light Top Partners and Precision Physics*, [arXiv:1306.4655](#).
- [96] D. Barducci, A. Belyaev, M. Brown, S. De Curtis, S. Moretti, *et. al.*, *The 4-Dimensional Composite Higgs Model (4DCHM) and the 125 GeV Higgs-Like Signals at the LHC*, JHEP **1309** (2013) 047, [[arXiv:1302.2371](#)].
- [97] J. Elias-Miro, J. Espinosa, E. Masso, and A. Pomarol, *Renormalization of Dimension-Six Operators Relevant for the Higgs Decays $H \rightarrow \gamma\gamma, \gamma Z$* , JHEP **1308** (2013) 033, [[arXiv:1302.5661](#)].
- [98] C. Grojean, E. E. Jenkins, A. V. Manohar, and M. Trott, *Renormalization Group Scaling of Higgs Operators and $\Gamma(H \rightarrow \gamma\gamma)$* , JHEP **1304** (2013) 016, [[arXiv:1301.2588](#)].
- [99] **Particle Data Group** Collaboration, J. Beringer *et. al.*, *Review of Particle Physics (Rpp)*, Phys.Rev. **D86** (2012) 010001.
- [100] M. E. Peskin and T. Takeuchi, *A New constraint on a strongly interacting Higgs sector*, Phys.Rev.Lett. **65** (1990) 964–967.
- [101] F. Feruglio and S. Rigolin, *Sum Rules for Asymptotic Form-Factors in $e^+e^- \rightarrow W^+W^-$ Scattering*, Phys.Lett. **B397** (1997) 245–254, [[hep-ph/9611414](#)].
- [102] K. Jansen, J. Kuti, and C. Liu, *The Higgs Model with a Complex Ghost Pair*, Phys.Lett. **B309** (1993) 119–126, [[hep-lat/9305003](#)].
- [103] K. Jansen, J. Kuti, and C. Liu, *Strongly Interacting Higgs Sector in the Minimal Standard Model?*, Phys.Lett. **B309** (1993) 127–132, [[hep-lat/9305004](#)].
- [104] B. Grinstein, D. O’Connell, and M. B. Wise, *The Lee-Wick Standard Model*, Phys.Rev. **D77** (2008) 025012, [[arXiv:0704.1845](#)].
- [105] I. Brivio *et al.*, *Impact of higher derivative operators on Higgs effective Lagrangians*. In preparation

- [106] K. Hagiwara, S. Matsumoto, and R. Szalapski, *Constraints on New Physics in the Electroweak Bosonic Sector from Current Data and Future Experiments*, Phys.Lett. **B357** (1995) 411–418, [[hep-ph/9505322](https://arxiv.org/abs/hep-ph/9505322)].
- [107] The **LEP** Collaborations and the LEP **TGC** Working group, *A combination of preliminary results on gauge boson couplings measured by the LEP experiments*, Tech. Rep. LEPEWWG/TGC/2003-01, 2003.
- [108] **D0 and CDF** Collaboration, B. Tuchming, *Tevatron Higgs results*, [arXiv:1307.4873](https://arxiv.org/abs/1307.4873).
- [109] **ATLAS** Collaboration, *Search for the Standard Model Higgs boson in $H \rightarrow \tau\tau$ decays in proton-proton collisions with the ATLAS detector*, Tech. Rep. ATLAS-CONF-2012-160, CERN, Geneva, Nov, 2012.
- [110] **ATLAS** Collaboration, *Search for the bb decay of the Standard Model Higgs boson in associated $(W/Z)H$ production with the ATLAS detector*, Tech. Rep. ATLAS-CONF-2013-079, CERN, Geneva, Jul, 2013.
- [111] **ATLAS** Collaboration, *Measurements of the properties of the Higgs-like boson in the four lepton decay channel with the ATLAS detector using 25 fb^{-1} of proton-proton collision data*, Tech. Rep. ATLAS-CONF-2013-013, CERN, Geneva, Mar, 2013.
- [112] **ATLAS** Collaboration, *Determination of the Top Quark Mass with a Template Method in the All-Hadronic Decay Channel using 2.04 fb^{-1} of ATLAS Data*, Tech. Rep. ATLAS-CONF-2012-030, CERN, Geneva, Mar, 2012.
- [113] **ATLAS** Collaboration, *Observation of an excess of events in the search for the Standard Model Higgs boson in the gamma-gamma channel with the ATLAS detector*, Tech. Rep. ATLAS-CONF-2012-091, CERN, Geneva, Mar, 2013.
- [114] **ATLAS** Collaboration, *Measurements of the properties of the Higgs-like boson in the two photon decay channel with the ATLAS detector using 25 fb^{-1} of proton-proton collision data*, Tech. Rep. ATLAS-CONF-2013-012, CERN, Geneva, Mar, 2013.
- [115] **CMS** Collaboration, *Search for the Standard-Model Higgs boson decaying to tau pairs in proton-proton collisions at $\sqrt{s} = 7$ and 8 TeV* , Tech. Rep. CMS-PAS-HIG-13-004, CERN, Geneva, 2013.
- [116] **CMS** Collaboration, *Search for the standard model Higgs boson produced in association with W or Z bosons, and decaying to bottom quarks for LHCp 2013*, Tech. Rep. CMS-PAS-HIG-13-012, CERN, Geneva, 2013.
- [117] **CMS** Collaboration, *Higgs to bb in the VBF channel*, Tech. Rep. CMS-PAS-HIG-13-011, CERN, Geneva, 2013.

- [118] **CMS** Collaboration, *Properties of the Higgs-like boson in the decay H to ZZ to $4l$ in pp collisions at $\sqrt{s} = 7$ and 8 TeV*, Tech. Rep. CMS-PAS-HIG-13-002, CERN, Geneva, 2013.
- [119] **CMS** Collaboration, *Evidence for a particle decaying to W^+W^- in the fully leptonic final state in a standard model Higgs boson search in pp collisions at the LHC*, Tech. Rep. CMS-PAS-HIG-13-003, CERN, Geneva, 2013.
- [120] **CMS** Collaboration, *Updated measurements of the Higgs boson at 125 GeV in the two photon decay channel*, Tech. Rep. CMS-PAS-HIG-13-001, CERN, Geneva, 2013.
- [121] **CMS** Collaboration, S. Chatrchyan *et. al.*, *Search for a Higgs boson decaying into a Z and a photon in pp collisions at $\sqrt{s} = 7$ and 8 TeV*, [arXiv:1307.5515](#).
- [122] **CMS** Collaboration, *Projected Performance of an Upgraded Cms Detector at the LHC and HL-LHC: Contribution to the Snowmass Process*, [arXiv:1307.7135](#).
- [123] **ATLAS** Collaboration, *Physics at a High-Luminosity LHC with Atlas*, [arXiv:1307.7292](#).
- [124] **OPAL** Collaboration, G. Abbiendi *et. al.*, *Measurement of charged current triple gauge boson couplings using W pairs at LEP*, Eur.Phys.J. **C33** (2004) 463–476, [[hep-ex/0308067](#)].
- [125] **L3** Collaboration, P. Achard *et. al.*, *Measurement of triple gauge boson couplings of the W boson at LEP*, Phys.Lett. **B586** (2004) 151–166, [[hep-ex/0402036](#)].
- [126] **ALEPH** Collaboration, S. Schael *et. al.*, *Improved measurement of the triple gauge-boson couplings $\gamma W W$ and $Z W W$ in e^+e^- collisions*, Phys.Lett. **B614** (2005) 7–26.
- [127] O. J. Eboli, S. Lietti, M. Gonzalez-Garcia, and S. Novaes, *ϵ_b constraints on selfcouplings of vector bosons*, Phys.Lett. **B339** (1994) 119–126, [[hep-ph/9406316](#)].
- [128] S. Dawson and G. Valencia, *Bounds on $g_5(Z)$ from precision LEP measurements*, Phys.Lett. **B333** (1994) 207–211, [[hep-ph/9406324](#)].
- [129] O. J. Eboli, M. Gonzalez-Garcia, and S. Novaes, *Indirect constraints on the triple gauge boson couplings from $Z \rightarrow b\bar{b}$ partial width: An Update*, Mod.Phys.Lett. **A15** (2000) 1–8, [[hep-ph/9811388](#)].
- [130] **ATLAS** Collaboration, G. Aad *et. al.*, *Measurement of WZ production in proton-proton collisions at $\sqrt{s} = 7$ TeV with the ATLAS detector*, Eur.Phys.J. **C72** (2012) 2173, [[arXiv:1208.1390](#)].
- [131] **ATLAS** Collaboration, G. Aad *et. al.*, *Measurement of the WW cross section in $\sqrt{s} = 7$ TeV pp collisions with the ATLAS detector and limits on anomalous gauge couplings*, Phys.Lett. **B712** (2012) 289–308, [[arXiv:1203.6232](#)].

- [132] V. Lombardo, on behalf the of **ATLAS** and **CMS** Collaborations, *Diboson production cross section at LHC*, [arXiv:1305.3773](#).
- [133] **CMS** Collaboration, S. Chatrchyan *et. al.*, *Measurement of the $W\gamma$ and $Z\gamma$ inclusive cross sections in pp collisions at $\sqrt{s} = 7$ TeV and limits on anomalous triple gauge boson couplings*, [arXiv:1308.6832](#).
- [134] **CMS** Collaboration, S. Chatrchyan *et. al.*, *Measurement of the sum of WW and WZ production with W + dijet events in pp collisions at $\sqrt{s} = 7$ TeV*, Eur.Phys.J. **C73** (2013) 2283, [[arXiv:1210.7544](#)].
- [135] O. Eboli, J. Gonzalez-Fraile, and M. Gonzalez-Garcia, *Scrutinizing the ZW^+W^- vertex at the Large Hadron Collider at 7 TeV*, Phys.Lett. **B692** (2010) 20–25, [[arXiv:1006.3562](#)].
- [136] N. D. Christensen and C. Duhr, *FeynRules - Feynman rules made easy*, Comput.Phys.Commun. **180** (2009) 1614–1641, [[arXiv:0806.4194](#)].
- [137] J. Alwall, M. Herquet, F. Maltoni, O. Mattelaer, and T. Stelzer, *MadGraph 5 : Going Beyond*, JHEP **1106** (2011) 128, [[arXiv:1106.0522](#)].
- [138] T. Sjostrand, S. Mrenna, and P. Z. Skands, *PYTHIA 6.4 Physics and Manual*, JHEP **0605** (2006) 026, [[hep-ph/0603175](#)].
- [139] J. Conway, “PGS 4.”
<http://physics.ucdavis.edu/~conway/research/software/pgs/pgs4-support.htm>
- [140] C. Degrande, J. Holzbauer, S. C. Hsu, A. Kotwal, S. Li, *et. al.*, *Studies of Vector Boson Scattering And Triboson Production with DELPHES Parametrized Fast Simulation for Snowmass 2013*, [arXiv:1309.7452](#).